Hywind Scotland Floating Offshore Wind Farm

Sound Source Characterisation of Operational Floating Turbines

JASCO Applied Sciences (UK) Ltd

17 March 2022

Submitted to:

Kari Mette Murvoll
Jürgen Weissenberger
Equinor Energy AS
Contract 4590220628

Authors:

Robin D.J. Burns, MSc
S. Bruce Martin, PhD
Michael A. Wood, PhD
Colleen C. Wilson, MSc
C. Eric Lumsden, MM
Federica Pace, PhD

P001562-001
Document 02521
Version 3.0 FINAL

JASCO APPLIED SCIENCES

Suggested citation:

Burns, R.D.J., S.B. Martin, M.A. Wood, C.C. Wilson, C.E. Lumsden, and F. Pace. 2022. *Hywind Scotland Floating Offshore Wind Farm: Sound Source Characterisation of Operational Floating Turbines*. Document 02521, Version 3.0 FINAL. Technical report by JASCO Applied Sciences for Equinor Energy AS.

Contents

Figures

Tables

Executive Summary

JASCO Applied Sciences conducted a sound source characterisation study of the Hywind Scotland floating offshore wind farm, involving in situ acoustic recording over three winter months (October 2020 to January 2021) at the Hywind site and at a Control site 14 km away. JASCO field engineers conducted the deployment and retrieval of the recording instrumentation from the Hywind support vessel, MCS *SWATH 1* (out of Peterhead) under the oversight of the Hywind Operations Room.

The recording instrument at the Hywind site employed a four-hydrophone tetrahedral array to provide bearing discrimination between sounds from different directions. The location of the recorder was selected to enable the acoustic isolation of one Hywind structure such that a noise signature from that unit could be extracted without contamination from the four other floating turbines in the farm. One further purpose of the directional array was to allow for an analysis of the location of transient noises from the Hywind mooring system. In a previous study of the Hywind prototype off Norway in 2011, occasional high amplitude mooring transients were detected but their precise origin was unknown. The recording program was completed successfully with recovery of a continuously recorded, 24-bit, acoustic data set (10 Hz to 32 kHz) from each site, a total of approximately 6.6 TB data.

Analysis of the recorded data was conducted to assess the spectral content of the sound signature from the Hywind structures. Continuous tonal noise, associated with rotating rotor and generator components below 500 Hz, was clearly evident and showed corelation with wind speed. Temporal variability in similar frequency tones was suggestive of different concurrent signature for individual Hywind turbines arriving simultaneously. The other key feature of the overall Hywind noise was the presence of frequent broadband transient sounds with a median duration of 1.5 s. These transients were audibly associated with strain and friction in the mooring system and showed a strong positive corelation in occurrence with wave height. Directional analysis of transient noise from three of the HYWIDND turbines indicates that the mooring noise is predominantly being generated in mooring components close to the floating spar and not from components farther down each mooring cable.

A quantitative analysis of the impulsiveness of the soundscape at Hywind was undertaken using an impulse detector as well as studying the distribution of the per-minute kurtosis. The SEL of each detected impulse was summed, which showed that the impulsive SEL was generally 6 dB below the daily total SEL. The mean duration of the impulses was on the order of 1.5 s, longer than the 1.0 s typically used to identify impulses for the purposes of assessing the effects of sound on hearing. The soundscape at Hywind had a greater kurtosis than at the Control site; however, the kurtosis was not high enough to be considered impulsive. Based on these three measures, it is recommended that the non-impulsive temporary threshold shift (TTS) sound exposure level (SEL) thresholds be applied to the wind farm sounds.

The total noise levels (tonal and transient) from HS1were extracted and back propagated to derive decidecade band source levels for a single Hywind Scotland system at five winds speeds between 5 and 25 kn. Unexpectedly, the total noise level from HS1 was higher in 5 kn of wind than at 10 kn of wind. The resulting median broadband source levels ranged from 162.5 to 167.2 dB re 1 μPa^2m^2 with the maximum 95th percentile at 25 kn of 172 dB re 1 μPa^2m^2. The HS1 source levels were used to model a basic noise footprint for the entire five turbine windfarm. The modelling shows that the distance to the averaged background SPL level (110 dB re1µPa) from the centre of the OWF (i.e., where the radiating noise decays to approximately the broadband ambient level) at the quietest state in 10 kn of wind, was approximately 4 km and in 25 kn of wind it was 13 km. A high-frequency cetacean (porpoise) would need to remain within 50 m of a turbine for 24 h before there would be a risk of temporary hearing threshold shift (15 kn wind).

1. Introduction

JASCO Applied Sciences (JASCO) was contracted by Equinor Energy AS (Equinor) to undertake a sound source characterisation (SSC) study for the Hywind floating wind turbine generators (WTG), located in the North Sea, 25 km to the East of Peterhead, Scotland (Figure 1). Hywind Scotland is the world's first operational floating Offshore Wind Farm (OWF) and comprises five WTGs, each mounted on a spar buoy/pillar that is moored to the seabed by an unballasted catenary system employing three mooring cables (Figure 2).

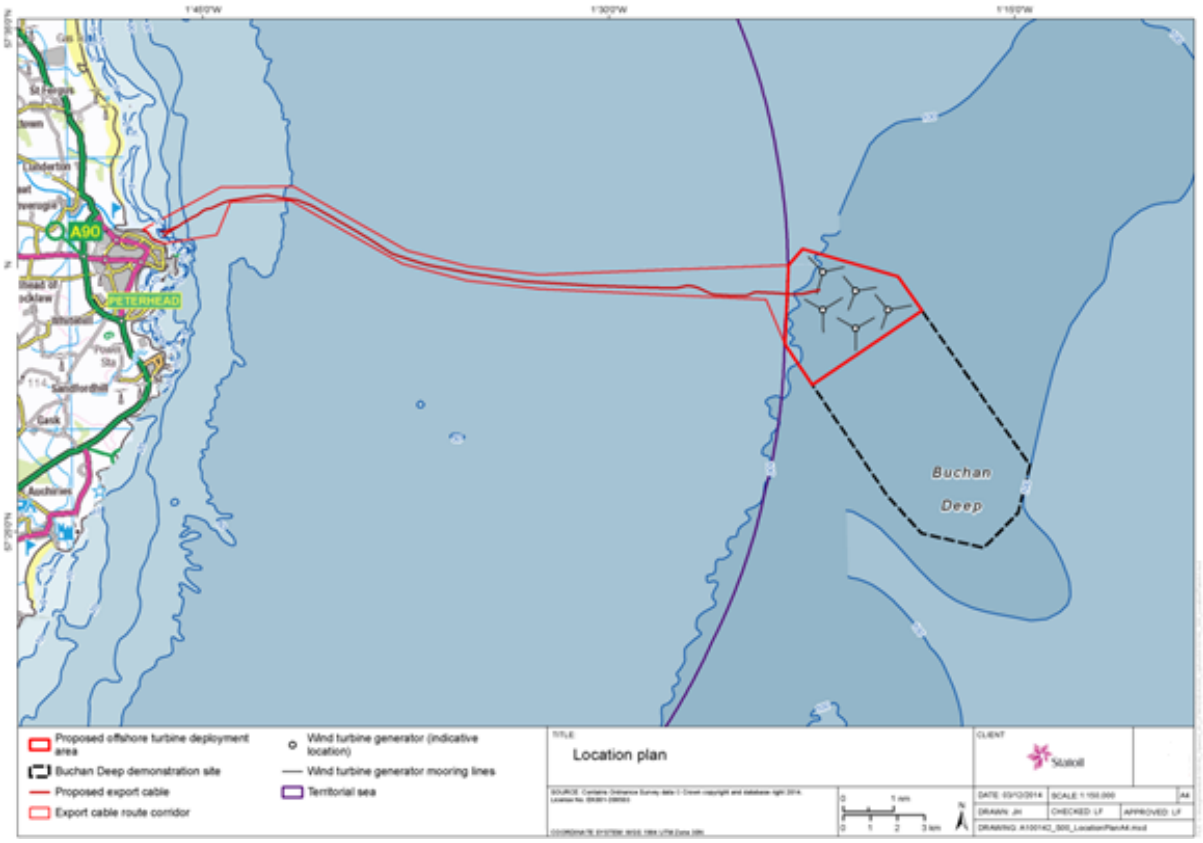

Figure 1. Location of the Hywind Scotland offshore floating wind farm.

The diameter of the spar at the water line is approximately 9–10 m, while the diameter of the submerged section is 14–15 m (Figure 2).

JASCO conducted a similar SSC study for Equinor (Statoil) in 2011 on the Hywind DEMO system off the coast of Stavanger, Norway. That study identified several tonal elements to the sound signature and an additional transient 'snapping/clicking' noise, potentially associated with the mooring system (Martin et al. 2011). The principal aim of this 2020 study was to record an operational noise profile for the larger Hywind Scotland system and back-propagate this data to extract a source spectrum for an individual Hywind unit. A secondary aim was to determine whether the broadband mooring transients that were detected from the Hywind DEMO system, were still present.

Figure 2. Image of the Hywind floating wind turbine, mooring and power transfer cables.

This SSC study employed two JASCO recording instruments on the seabed for three months over autumn to winter 2020–2021 to continuously capture noise from the windfarm site and a control site remote to the wind farm. The recorder located in the wind farm was fitted with a directional array of four hydrophones to provide acoustic discrimination in bearing and elevation between the considerable number and spatial distribution of possible noise sources.

The control recorder was retrieved in January 2021 and the Hywind mooring in July 2021. A detailed analysis of the data was carried out in autumn that year. A bespoke automated code, tailored to the frequency range and environmental conditions at the wind farm, was developed to process the directional data because the wide distribution of potential noise sources within the wind farm was considerable (notably the spread of each mooring system).

2. Methods

2.1. Acoustic Data Acquisition

Underwater sound was recorded with two JASCO Autonomous Multichannel Acoustic Recorders (AMAR) mounted on simple baseplate moorings. A single AMAR G4 with a quad-hydrophone directional array on a static frame, was deployed within the Hywind site and a second AMAR G3 with a single omni-directional hydrophone was deployed at a remote location to gather 'control' ambient noise.

2.1.1. Deployment

Both moorings were lowered to the seabed from the Hywind service vessel (MCS *SWATH 1*), and the lowering line was disconnected from the mooring's lifting ring by activation of an acoustic release. The omni-directional control site recorder did not require any specific orientation, but the Hywind site recorder, with its four-hydrophone array, did require orientation to enable bearing alignment and accuracy. The orientation process was applied retrospectively during post-processing of the data by aligning known positions from the AIS track of the *SWATH 1* with the directional vessel noise as well as corroborating the alignment with the known positions of the Hywind turbines

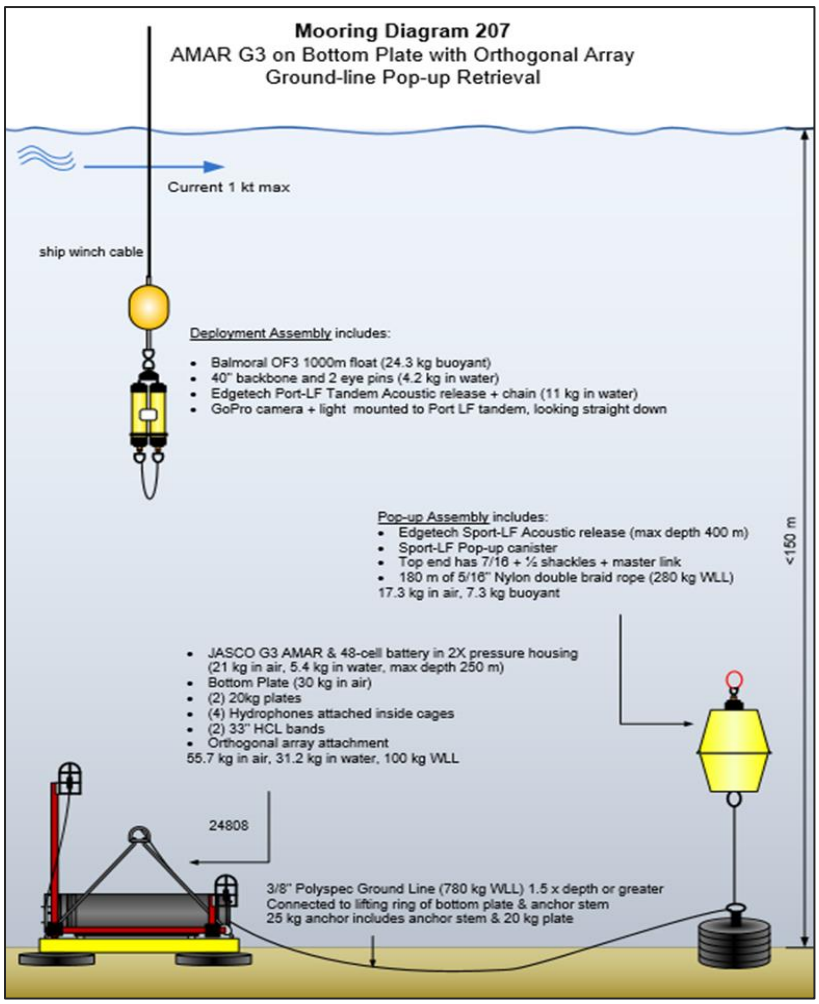

Figure 3. Baseplate mooring design with the deployment assembly shown.

The Control site was selected to be sufficiently distant from the Hywind OWF (~13 km to the northeast) to exclude significant levels of noise from the turbines and moorings but close enough to provide representative ambient noise levels for that depth and region of the North Sea. The control location was also close to the intersection of two seabed pipelines to reduce the risk of trawling loss of the instrument (Figure 4).

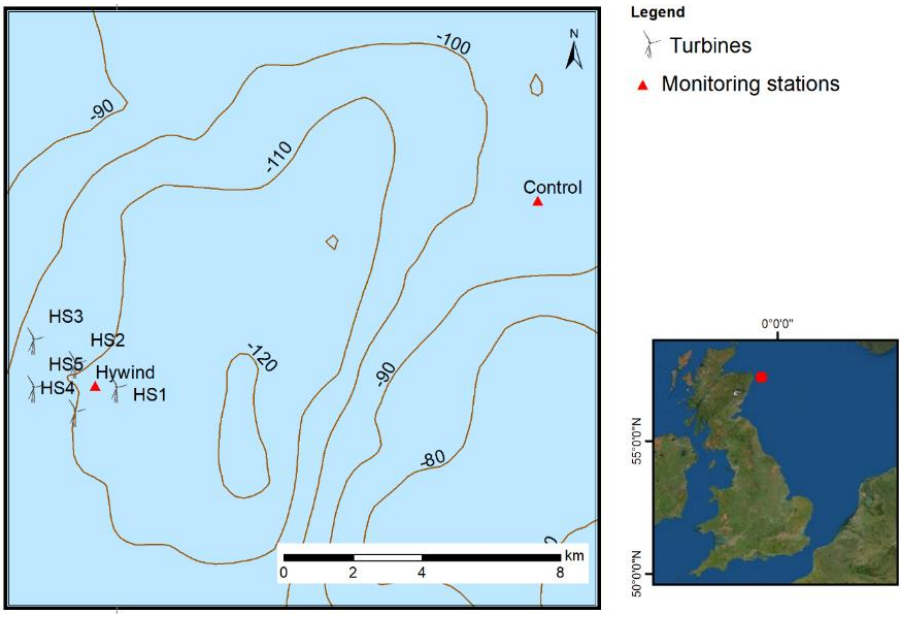

Figure 4. Map showing the Hywind and Control site locations.

The Hywind site recording location was selected specifically to isolate one Hywind turbine east of the recording instrument such that the array's directional properties could be used to extract the noise signature from a single Hywind system without contamination from the other turbines in the farm. The isolated system selected was HS1 and the mooring was deployed to the west northwest at a 642 m distance (Figure 5). The exact distance between the AMAR and HS1 did not have to be pre-defined for back-propagation purposes, as long as it was known. This simplified the deployment process for the mooring.

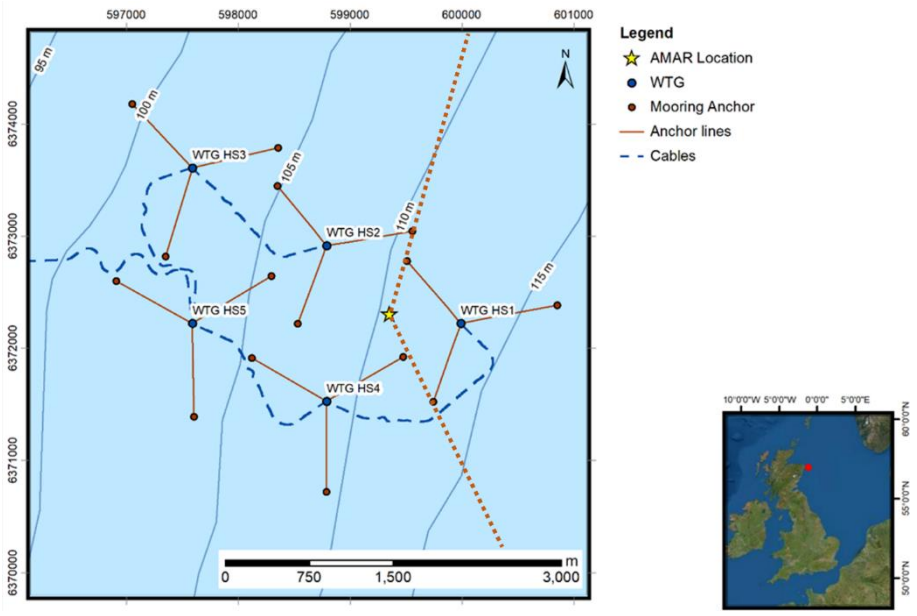

Figure 5. AMAR position within the Hywind OWF. Red dashed lines identify the bearing isolation of HS1 and its mooring system to the East

2.1.2. Recording Parameters

Both AMARs were fitted with M36-V35-100 omni-directional hydrophones (with a nominal sensitivity of −165 dBV with preamp) from GeoSpectrum Technologies Inc. (GTI). Each hydrophone was protected by a cage covered with a shroud to minimize any flow noise. For the Hywind station, the four hydrophones were fixed in a tetrahedral arrangement to allow determination of the time of arrivals from different directions (Figure 6). The relative distance of each hydrophone on the support structure was calculated and precisely set to support post-processing directional calculations (Table 1).

Table 1. Relative distances of the four hydrophones (as labelled in Figure 6) mounted on the Hywind monitoring station.

Hydrophone ID	Length (mm)
A-B	481
A-D	724
B-D	595
B-C	482
C-A	647
C-D	717

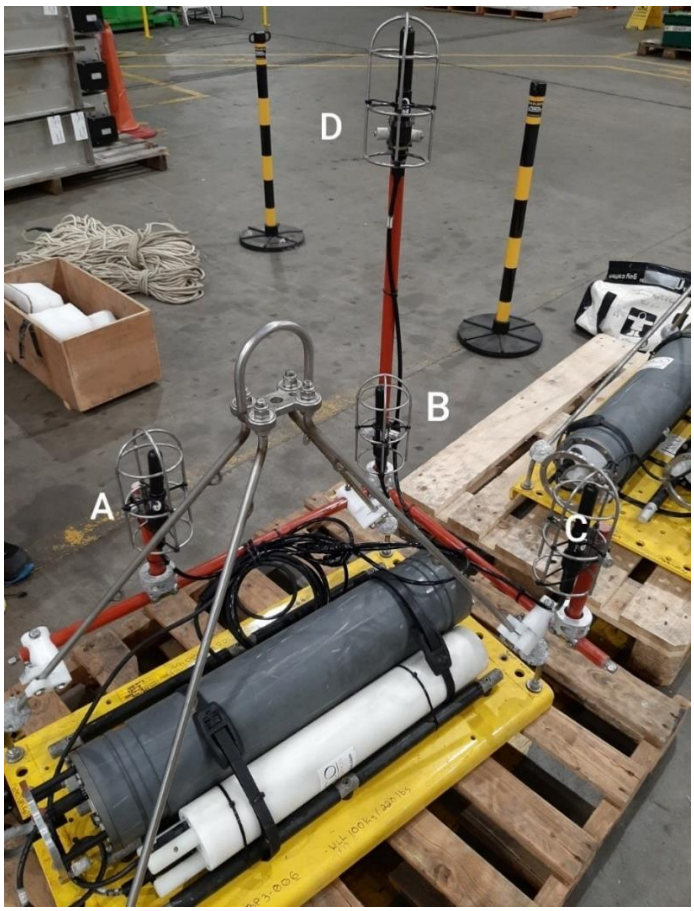

Figure 6. Photo of the Hywind baseplate before deployment with fitted AMAR G4 (white tube), battery back (grey tube) and tetrahedral hydrophone array mounted on a static frame (red tubes).

The AMARs recorded continuously at a sample rate of 64,000 Hz to return a recorded bandwidth of 10 to 32,000 Hz. The recording channel had 24-bit resolution with a spectral noise floor of 20 dB re 1 $\mu Pa^2/Hz$ and a nominal ceiling of 165 dB re 1 µPa. Acoustic data were stored on 512 GB of internal solid-state flash memory.

Each AMAR was calibrated before deployment and after retrieval with a pistonphone type 42AC precision sound source (G.R.A.S. Sound & Vibration A/S) (Figure 7). The pistonphone calibrator produces a constant tone at 250 Hz at a fixed distance from the hydrophone sensor in an airtight space with known volume. The recorded level of the reference tone on the AMAR yields the system gain for the AMAR and hydrophone. To determine absolute sound pressure levels, this gain is applied during data analysis. Typical calibration variance using this method is less than 0.7 dB absolute pressure.

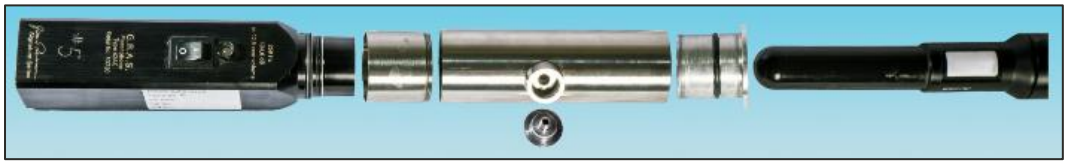

Figure 7. GRAS 42 AC Pistonphone, sleeve coupler and hydrophone

Data was recorded continuously (i.e., 24 h per day) from 21 Oct 2020 to 24 Jan 2021 at both sites, for the required monitoring duration of 96 days (Table 2) after which the solid-state memory in each system was full. The remaining power in the battery pack would have depleted slowly thereafter until exhausted. The total volume of data collected was approximately 6.6 TB.

Table 2. AMAR deployment and retrieval dates and locations. Retrieval time indicates the time at which the retrieval procedure was initiated.

Location	Deployment†	Retrieval†	Latitude	Longitude	Easting*	Northing*	Water depth (m)
Hywind	21 Oct 2020 13:44	15 Jul 2021 10.30	57° 29.109' N	001° 20.571' E	599348.894	6372604.308	112
Control	21 Oct 2020 11:43	24 Jan 2021 13:05	57° 31.801' N	001° 07.580' E	612189.991	6377935.635	95

† Time in UTC
* UTM 30N (WGS84)

2.1.3. Retrieval

Retrieval of this mooring design is typically achieved through activation of the separate pop-up acoustic assembly, connected by ground line to the baseplate. The pop-up float is recovered on board the vessel and the secondary anchor lifted to access the ground line which, in turn, is used to lift the baseplate to the surface.

The Control site mooring was retrieved on 24 Jan 2021 (Table 2) by a JASCO field team aboard the *SWATH 1* exactly in line with this procedure. However, during retrieval of the Hywind site mooring on the same day the ground line became entangled in a hull fitting below the waterline of the *SWATH 1* as the baseplate was being winched to the surface and the vessel moved astern from the mooring position. When the line could not be freed, it had to be cut for vessel safety reasons and the baseplate mooring fell back to the seabed. The position was recorded at the time. Recovery of the mooring was finally achieved on 15 Jul 2021 by a Remotely Operated Vehicle (ROV) deployed from the *Havila Venus*, on task for Equinor. The mooring had remained upright and inert on the seabed, exactly where it had fallen from below the *SWATH 1*. The AMAR was undamaged, and the all the data were recovered from the on-board memory.

2.2. Acoustic Data Analysis

The acoustic data analysis methods for basic metrics are contained in Appendix A. Acoustic terminology and analysis are in accordance with ISO standard 18405 (ISO 2017).

Bearings and distances between the Hywind recording instrument and each of the turbines were calculated using mapping software Global Mapper (Table 3) and used as a reference to calculate the bearing angles of each of the four hydrophones deployed on the tetrahedral structure. Additionally, the acoustic signature of the *SWATH 1* was tracked on the Hywind array immediately after deployment and correlated with actual bearings derived from positions in the vessel's GPS track log. This provided additional directional confirmation of the orientation of the hydrophone array. A description of the directional analysis is contained in Appendix B.

Table 3. Distances and bearings of each of the Hywind wind turbine generators (WTGs) from the Autonomous Multichannel Acoustic Recorder (AMAR) deployed within the wind farm.

Location	Distance (m)	Bearing (°)
HS-1	605	095
HS-2	880	318
HS-3	2242	308
HS-4	951	1799
HS-5	1799	269

Impulses were detected in the data to quantify the number of impulses per hour for comparison to the mean hourly wind speed, as well as to quantify the impulsive daily SEL (with auditory frequency weighting). The analysis of continuous sounds from the floating turbines indicated that there were two strong tonal sounds below 100 Hz (see Section 4) whose energy would both affect the impulse detector's performance and should not be included with an analysis of impulsive energy. Therefore, the data were pre-filtered with a high-pass filter before impulse analysis. This finite impulse response filter was designed using MATLAB's filter designer application with the Kaiser Window method, a stop band frequency of 85 Hz, passband frequency of 100 Hz, and stopband attenuation of 80 dB. The impulse detector is based on a Teager-Kaiser energy detector. The filtered time-series were squared, summed over a 100 ms window, divided by the number of samples in the window to generate a 100 ms energy time series. The 100 ms time series was divided by its mean value for each 20 s buffer of data that is passed to the Teager-Kaiser operator (Kaiser 1990, Kandia and Stylianou 2006). Normalising the 20 s buffer by its mean value allows us to use a fixed threshold that is independent of the absolute magnitude of the raw time-series data. When the Teager-Kaiser operator exceeded the detector threshold, set empirically to 15, an impulse was detected. The processing then selected a 2.0 s window from the filtered time series centred on the impulse detection time and computed the decidecade sound exposure levels for the impulse. The detector was configured with a 'lock-out' of 1.0 s after a strike was identified to minimize false alarms on multipath arrivals.

Kurtosis is another approach used in this study to characterize impulsive sounds. Kurtosis (β) is defined as the ratio of the fourth moment to the squared second moment of the instantaneous sound pressure:

$$\beta = \frac{\frac{1}{N}\sum_N (p_i - \overline{p})^4}{\left[\frac{1}{N}\sum_N (p_i - \overline{p})^2\right]^2} \quad (1)$$

where p_i is the ith sample of instantaneous sound pressure, $\overline{p}$ is the arithmetic mean of sound pressure, and N is the number of data samples in the analysis window that affects resulting value for β. As suggested in Martin et al. (2020), 1 min analysis window was used for this project. Kurtosis of 3 represents random Gaussian noise, while kurtosis of 40 is used as a threshold for determining if a soundscape is impulsive for purposes of determining if an impulsive or non-impulsive hearing

threshold shift threshold is exceeded (NFMS 2018). Kurtosis for wind driven underwater ambient noise is also ~3.

3. Results

3.1. Total Sound Levels

This section presents the total sound levels (non-directional) from each of the sites to verify the quality of the recordings and as a summary of the received sound levels. We present the results in four ways:

1. **Band-level plots**: These strip charts show the averaged received sound levels as a function of time within a given frequency band. We show the total sound level (10–32000 Hz) and the decade bands for 8.9–89.1, 89–891, 891–8913, and 8913–32000 Hz. The 8.9–89.1 Hz band is associated with fin, sei, and blue whales, large shipping vessels, seismic surveys, and mooring noise. The 89–891 Hz band is generally associated with wind and wave noise, but can also include sounds from minke, right, and humpback whales, nearby vessels, and seismic surveys. Sounds above 1000 Hz include humpback whales, pilot whale and dolphin whistles, and wind and wave noise.
2. **Long-term Spectral Averages (LTSAs)**: LTSAs use colour to show power spectral density levels as a function of time (*x*-axis) and frequency (*y*-axis). The LTSAs are excellent summaries of the temporal and frequency variability in the data.
3. **Distribution of decidecade band SPL**: These box-and-whisker plots shows the average and extreme sound levels in each decidecade-band. As discussed in Appendix A, decidecade-bands are representative of the hearing bands of many mammals. They are often used as the bandwidths for expressing the source level of broadband sounds like shipping and seismic surveys. The distribution of decidecade noise levels can be used as the noise floor for modelling the detection of vessels or marine mammal calls.
4. **Power Spectral Densities (PSDs)**: PSDs show the statistical sound levels in 1 Hz frequency bins. These levels can be directly compared to the Wenz curves. We also plot the spectral probability density (Merchant et al. 2013) to assess whether the distribution is multi-modal.

Figures for the Hywind site are presented for one of the four hydrophone channels in this section (i.e., omni-directional) for ease of comparison with the control site. The data recorded on all four channels of the Hywind station produced very similar results. Individual results for all channels are presented in Appendix B.1.

Figure 8 presents band levels and LTSAs for each site. The control site's LTSA shows lower levels across the full frequency spectrum and, in particular, below 1kHz. At the Hywind site, sound levels between 100–120 dB are noticeable throughout the deployment between 8.9–300 Hz.

Transient broadband increases in energy, associated with marine vessels are noticeable at both the control and the Hywind site. The two obvious horizontal bands (at 25 and 79 Hz) present for almost the entire deployment at the Hywind site are also noticeable characteristics.

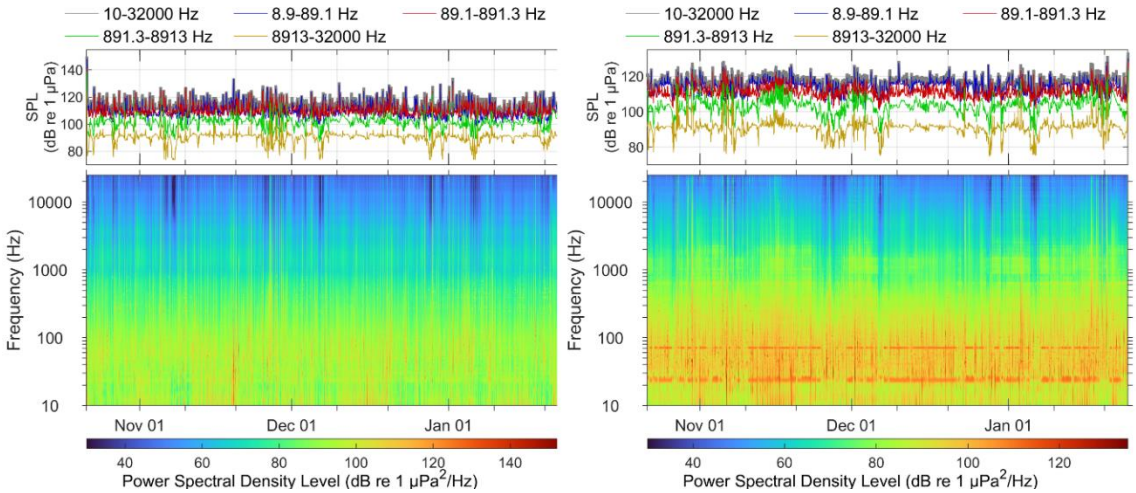

Figure 8. Acoustic summary at the control (left) and Hywind (right, channel 0) monitoring stations.

The most obvious differentiating feature of the PSD and decidecade-band analysis (Figure 9) are the two large peaks at 25 and 75 Hz seen at the Hywind site but mostly absent at the Control site. Median PSD levels in these two bands were 10–20 dB higher than at the adjacent frequencies, indicating a very significant increase in sound pressure levels. These noises are therefore important contributors and features of the soundscape, and they are most likely related to Hywind turbine and electricity transmission system noise (Figure 10) in combination with the relatively regular mooring noise. A small peak at 25 Hz is visible in the PSD of the control site, which may indicate a degree of residual audibility of this component of the Hywind noise at that distance.

At the Hywind site, several additional peaks can be seen between 100–400 Hz. These are believed to be associated with regular but transient sounds described as ‘creaks’, ‘snaps’ and ‘rattles’ thought to be associated with components of the Hywind mooring system. The occurrence of these generally broadband transients is irregular, and their duration also shows some variability with typical durations between 0.2 and 1.0 s.

Several distinct peaks are noticeable at both sites between 20–32 kHz. These sounds were manually investigated by generating spectrograms for selected recordings and were confirmed as matching the frequency peaks seen in the PSD, as shown in Appendix B.1. Given both the high-frequency, regular transmission characteristics and equal presence at both sites, in addition to evidence of concurrent vessel noise, it is thought that they are unrelated specifically to Hywind operational noise and are most likely to be some form of vessel mounted echo sounder or similar transmitting device.

Generally, the shape of the PSD percentiles was similar at both stations, except for those identified peaks, and below 20 Hz where the control site has a wider statistical spread of levels, visible in the spectral probability density shading. This is most likely due to the proximity of passing vessels that would navigate around the Hywind site but were able to transit directly over the control site recorder.

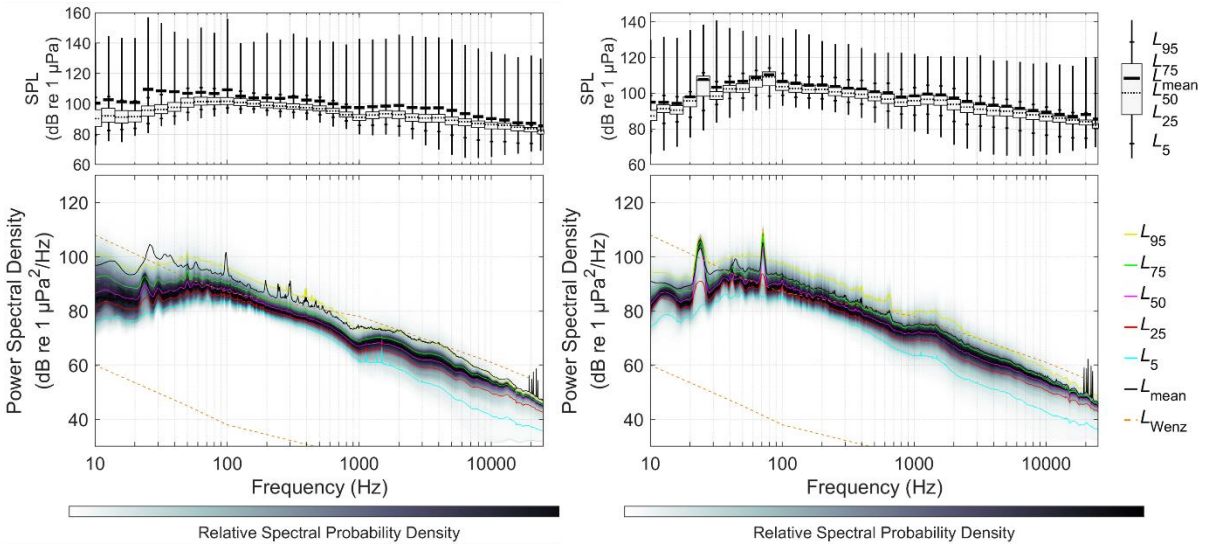

Figure 9. (Bottom) Power spectral density levels and (top) decidecade-octave-band sound pressure level (SPL) (left) at the control (left) and Hywind (right) monitoring stations. Values for each percentile appear in Tables F-1 and F-2.

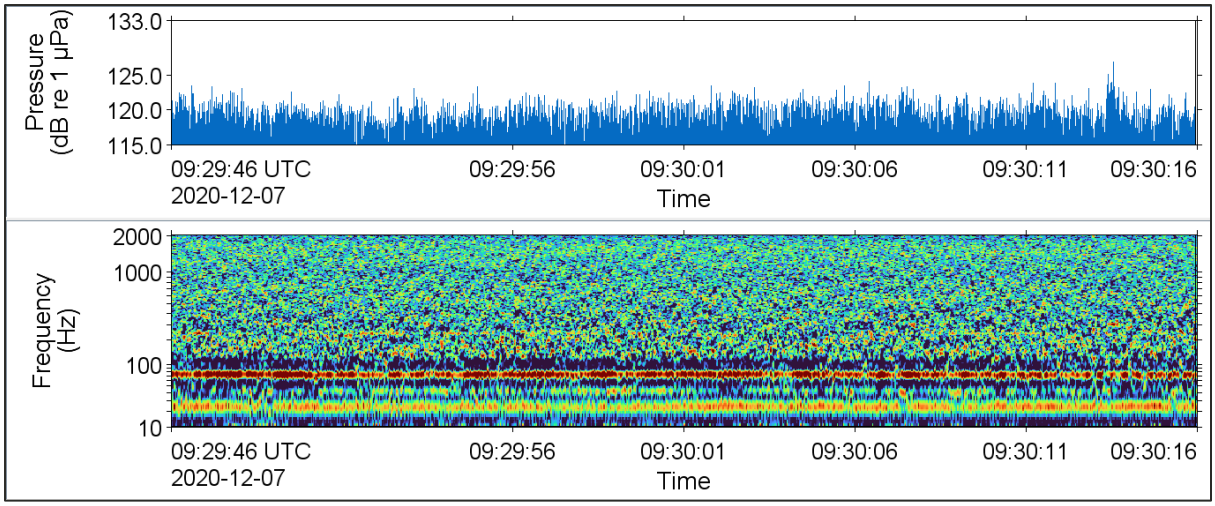

Figure 10. Amplitude (top) and spectrogram (bottom) of a 30 s section of a recording from the Hywind site from 7 Dec 2020 showing the dominant 25 and 75 Hz tones. A fainter harmonic is also visible between these two primary frequencies.

3.2. Comparison with Environmental Conditions

Sound levels in representative decidecade bands (Ddec) from the Control and Hywind stations were compared to NORA10 (operated by the Norwegian Meteorological Institute) environmental conditions at the P2 location (Figure 12), including wind speed, wind direction, and significant wave height (Hs) to assess for compliance with averaged ocean conditions. From the environmental parameters, the wind speed and wave height have a strong positive correlation, which reflect natural conditions of wind generated waves. For the Control site, the strongest positive relationships are at the highest two decidecade bands, when compared to either the wind speed or wave height. These correspond with the frequencies impacted by sea state, as per the Wenz curves (Figure 13). There is also a moderate positive correlation with the lowest frequency band, which is within the range impacted by surface waves. At the Hywind station, there are strong-moderate positive correlations with all frequency bands. The most substantial changes are the increase in correlation between wind speed and the lowest two decidecade bands. These increases are attributed to the finding that turbine and mooring noise increases with wind speed. There are slight decreases at Hywind in correlation strength of either wind speed or wave height at the highest two decidecade bands compared to the Control, for which a possible explanation could be a difference in sea state at the two stations, but the difference is small and there is unlikely to be a significant increase in sea state at the control site, despite the slightly longer fetch for the prevailing wind to the control site.

The correlograms below present a corelation analysis for each of the environmental factors and noise bands shown. The variable names on the diagonal become the vertical and horizontal axis labels for each grid panel. The scatter plots in the upper right compare each variable. The circles in the bottom left show the strength of the correlation of variable pairs simultaneously by amount of circle filled (clockwise from top if positive, anti-clockwise if negative), and darkness of colour (pale-to-dark blue/red). Blue indicates a positive correlation, and red a negative. For example, wind speed and wave height have a strong positive correlation represented by the dark blue colour and ~80% fill. The darker the blue colour, the greater the positive correlation, based on an automated colour scale set by the range of data. Wind direction and the 80 Hz decidecade have a weakly negative correlation exemplified by the small fraction of pale red fill.

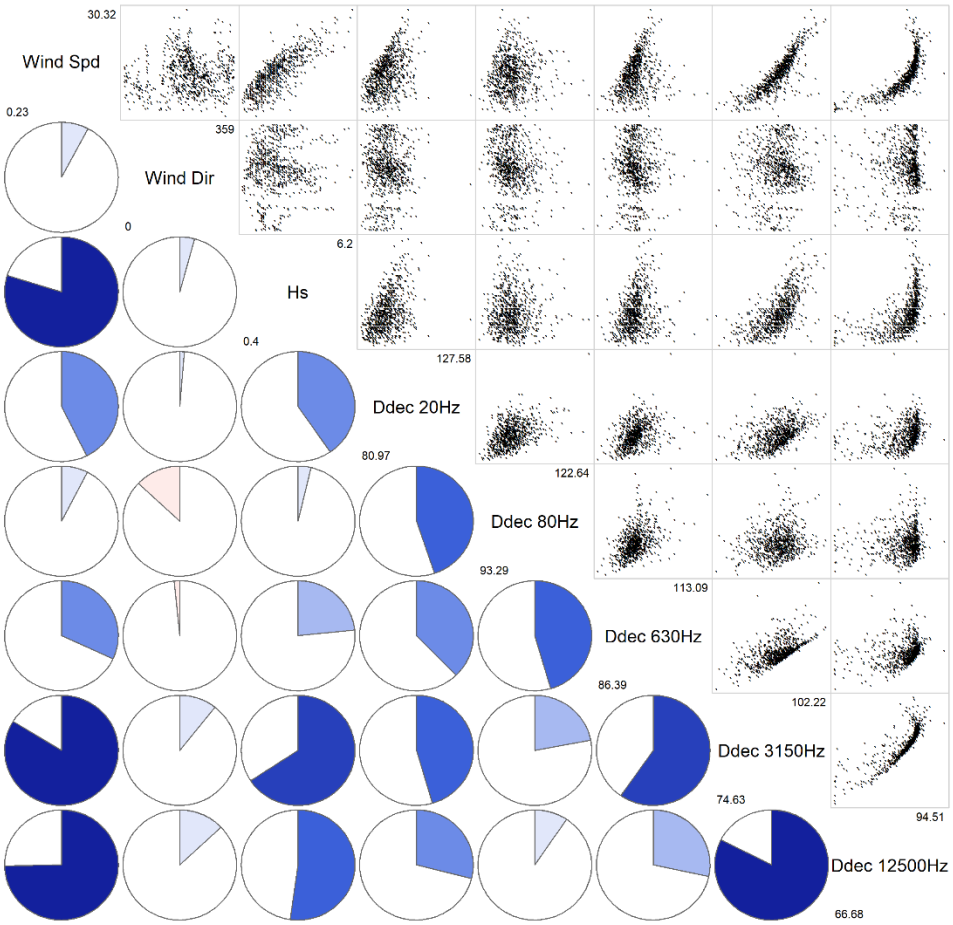

Figure 11. Correlograms comparing decidecade sound levels with environmental parameters for the Control site.

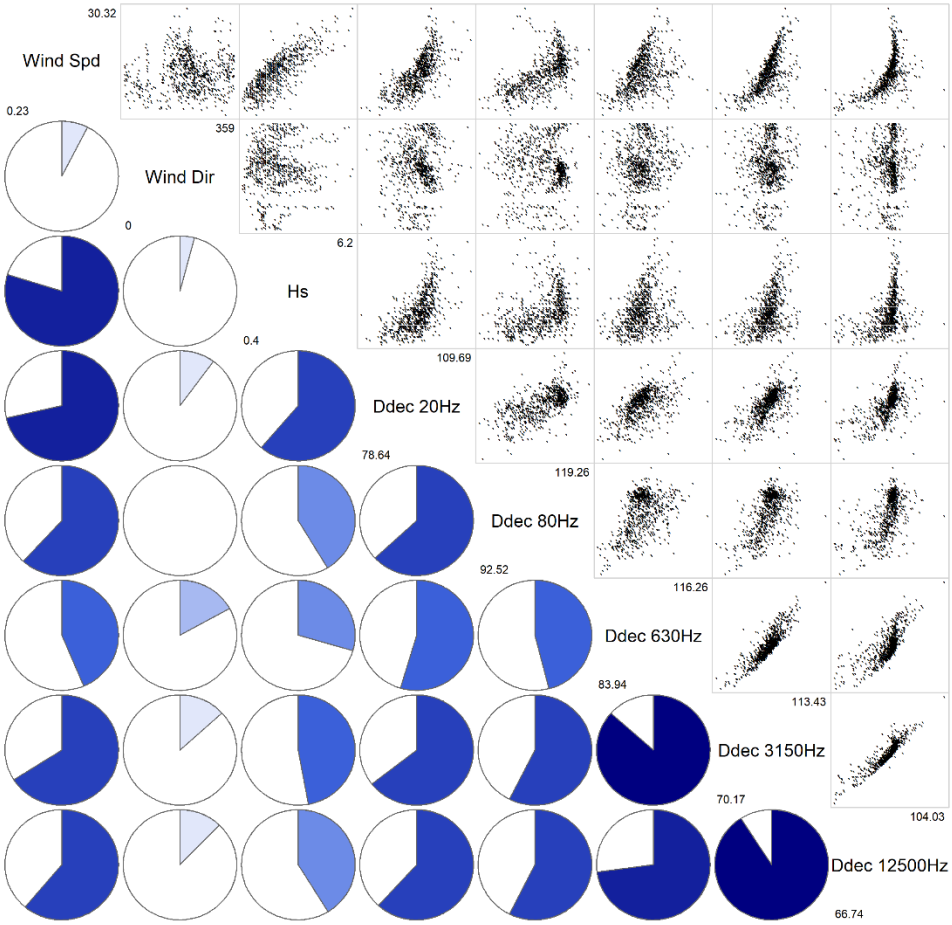

Figure 12. Correlograms comparing decidecade sound levels with environmental parameters for the Hywind stations.

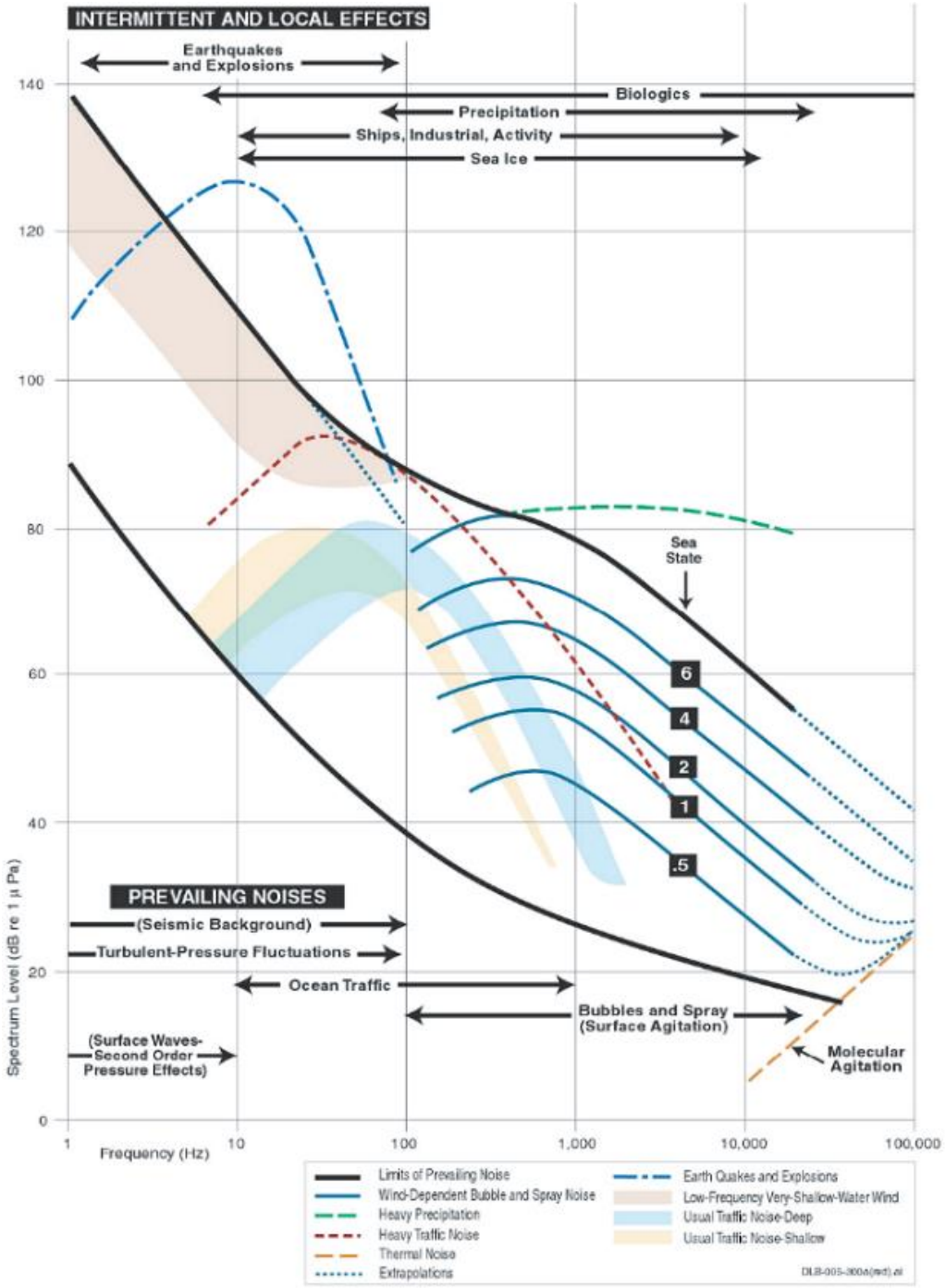

Figure 13. Wenz curves describing pressure spectral density levels of marine ambient sound from weather, wind, geologic activity, and commercial shipping. Thick lines indicate limits of prevailing noise. Figure reproduced from National Research Council (2003) and Wenz (1962).

3.3. Acoustic Analysis of Recorded Noise

Acoustic analysis of the recorded data was carried out using a combination of auto-processed event detection, manual spectral analysis of events, and Passive Aural Listening. Operational logs for the Hywind turbines were received towards the end of this analysis work, which provided some context regarding operating modes for the turbines.

Three separate categories of noise were determined from the analysis—firstly mechanical and electrical noise from the turbines, secondly 'mooring' noise and thirdly, noise which could not be definitively attributed to either category. More detailed directional analysis was conducted following directional processing of the four array channels, and this is presented separately in Section 3.4.

3.3.1. Turbine Related Noise – Spectral Content

The dominant operational noise from the Hywind turbine system appears to be distinct tonal sounds (i.e., relatively narrowband, continuous sounds typically associated with running machinery). Two dominant tones were evident below 100 Hz, and a further set of tones was evident between approximately 350 and 460 Hz. These tones were moderately stable in frequency, but, at times, displayed significant instability that is likely to reflect the variability in the RPM of the rotating turbine as the wind speed fluctuates.

The Hywind generator is understood to be directly linked (i.e., not geared) to the rotating hub of the turbine blades and that operational rotation speeds are typically in the region of 10 to 15 RPM. Interestingly, no corresponding fundamental tonal or harmonically related tones, at the converted cycles per second frequency, is visible in the data, and it remains unclear exactly which rotating component of the generator, or other system component, is creating this noise. Unsurprisingly, there was no evidence of any relatable gearing tones in the recordings.

Figure 14 shows two pairs of the dominant lower-frequency tones (below 100 Hz) indicating that there are at least two audible Hywind turbines at this time, although there is a potentially third but considerably weaker tone visible at one or two very short time periods. The analysis comb (at set of harmonically related lines, in this case separate by 23.84 Hz) is suggestive of a harmonic relationship between the ~24 and ~74 Hz primary tones (as well as a weaker tone close to 50 Hz), but the symmetry in oscillation is poor and the significant difference in intensity between what would be the second harmonic (close to 50 Hz) and the third harmonic (close to 74 Hz) is so significant that this serves to undermine the harmonic association theory, and it is concluded that these two dominant tones have separate but closely related origins.

Weaker secondary tonals are evident in Figure 14 between 30 and 50 Hz, and these are explored further below. Precise correlation of specific tonal features with a specific turbine operational mode was complicated by the presence of five turbines in the wind farm and the potential for several modes to be in operation at any one time. Additionally, occasional low-frequency tones from passing vessels were also routinely seen and had to be identified and excluded. Analysis below was conducted as far as possible when all five turbines were operating in the same mode.

Directional frequency analysis from the array data indicates that there is often quite a difference between the acoustic signature for each Hywind system, despite functioning in close proximity to each other. Significantly, different rotation rates are seen in the analysis that may be due to either small-scale variability in the wind pressure field, different loading on each generator or different blade pitch settings (if indeed the blades are controlled), or a combination of these and other factors. Therefore, no single Hywind noise signature would be representative of all turbines at any one time, and an overall aggregate noise assessment is necessary to determine the total radiated noise field for the whole site. This is the approach taken in Section 4 to determine source levels.

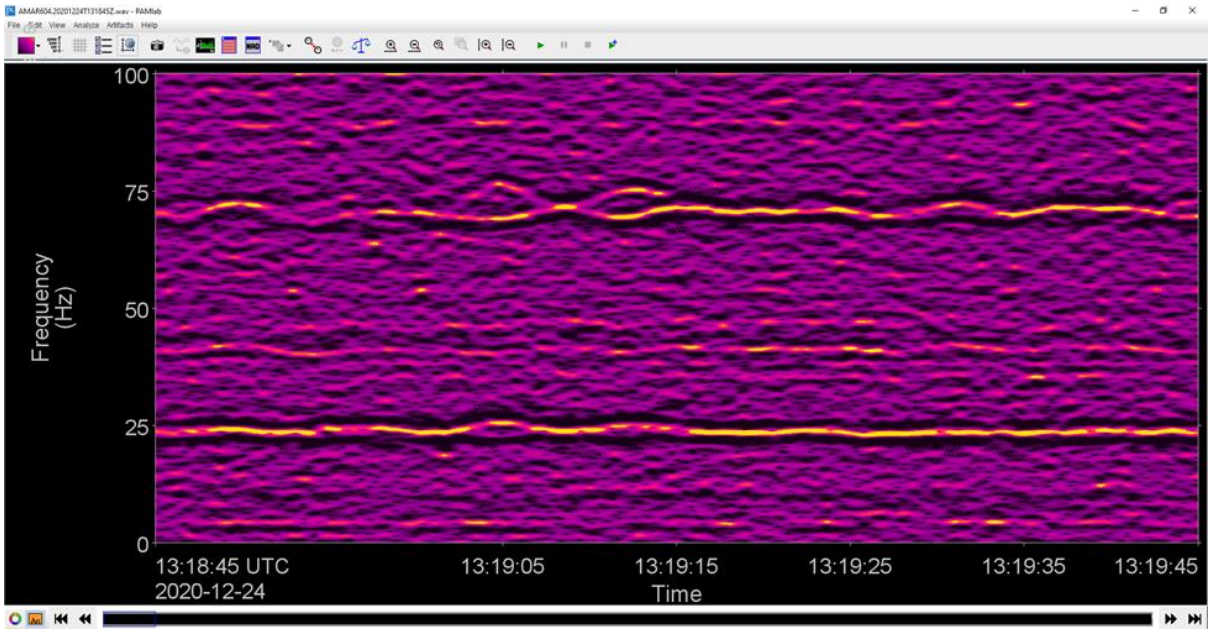

Figure 14. Primary tonal noise features below 100 Hz of the Hywind site showing overlap of the 25 and 74 Hz sources from at least two (possibly three) different Hywind turbines.

Figure 15 shows a narrowband analysis over a 2.8 s window of the low-frequency tone at ~74 Hz. The marked intensity of these tones against the background highlights their dominance in the overall soundscape.

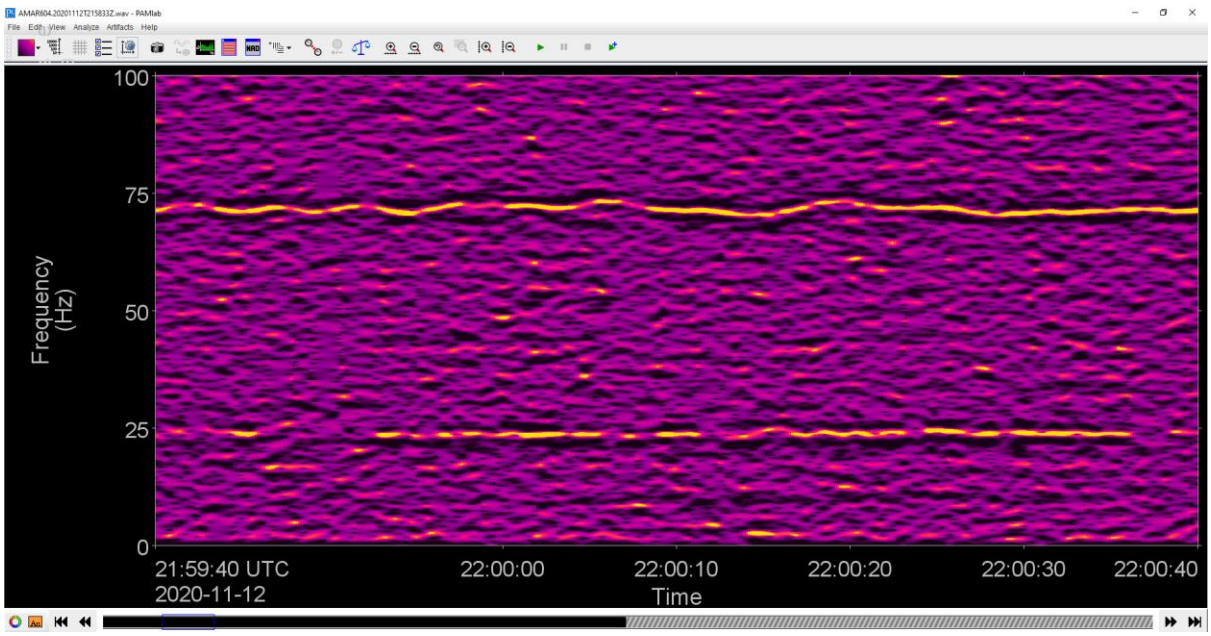

Figure 15. Narrowband analysis of the meandering tone at ~71 Hz.

Farther up in the acoustic spectrum, between ~350 Hz and 460 Hz, are several additional pronounced tonal sounds that are also evident in the long-term PSD values for the Hywind site (Figure 9). These tones are clearly visible in Figure 16 along with the primary tones below 100 Hz but showing little direct association with them. There is a temporal oscillation in intensity that is not mirrored with the lower frequency tones and no direct harmonic association again suggesting a different but still related origin. It is unknown if there is additional machinery on the Hywind structure, such as a bilge pump or

any other rotational machinery but given that there is no gearing in the turbine drive train, it is thought that these higher frequency tones are either related to another mechanical system in the Hywind structure or peripherally related elements of the generator. A fuller understanding of the rotation speed of all the components within the turbine may allow for a closer understanding of the precise source of each noise.

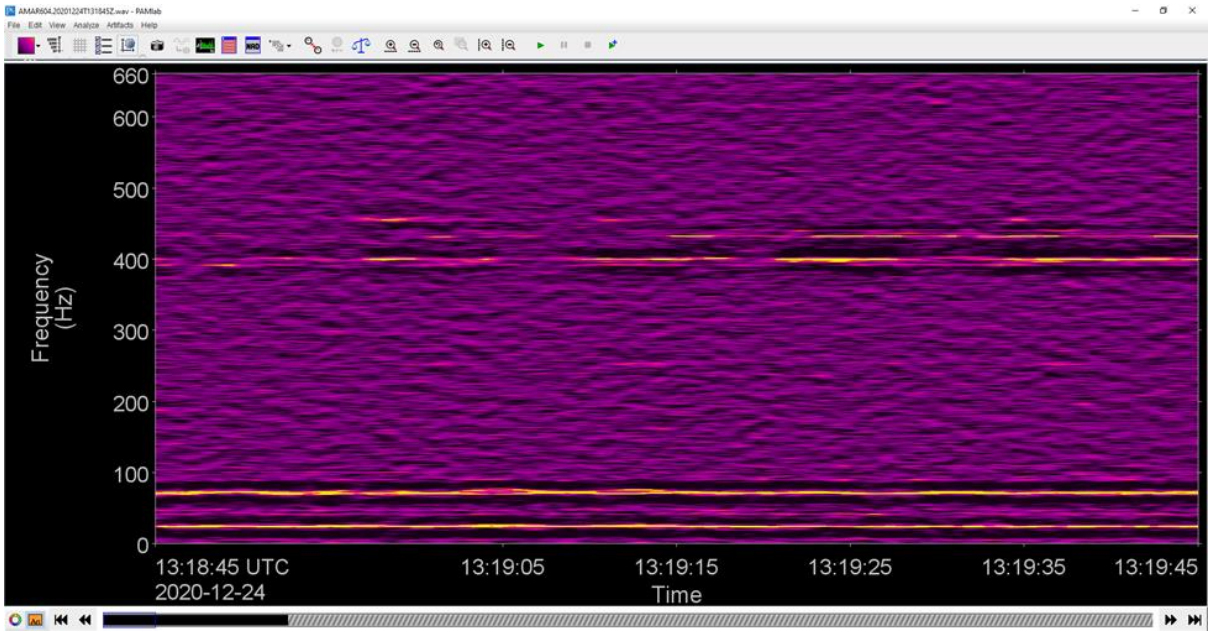

Figure 16. Additional higher frequency tones displaying a regular oscillation in intensity over a 1 min period.

Weaker, but still relatively persistent, tones within the noise field have also been identified but appear to be unrelated directly to the primary rotational tones that dominate the signature and are not always visible even when the sets of primary dominant tones are. These additional elements are possibly associated with the power generation mode, as they are not continuously present but do display a degree of intensity correlation with wind speed (Figure 17). They have no obvious harmonic relationship with the rotational primary tones and could be more related to electrical transformer or other power handling equipment. This additional noise is sufficiently loud in the measured band levels at different wind speeds to be a significant contributor to the overall radiated noise field and features again in the source level derivation work in Section 4.

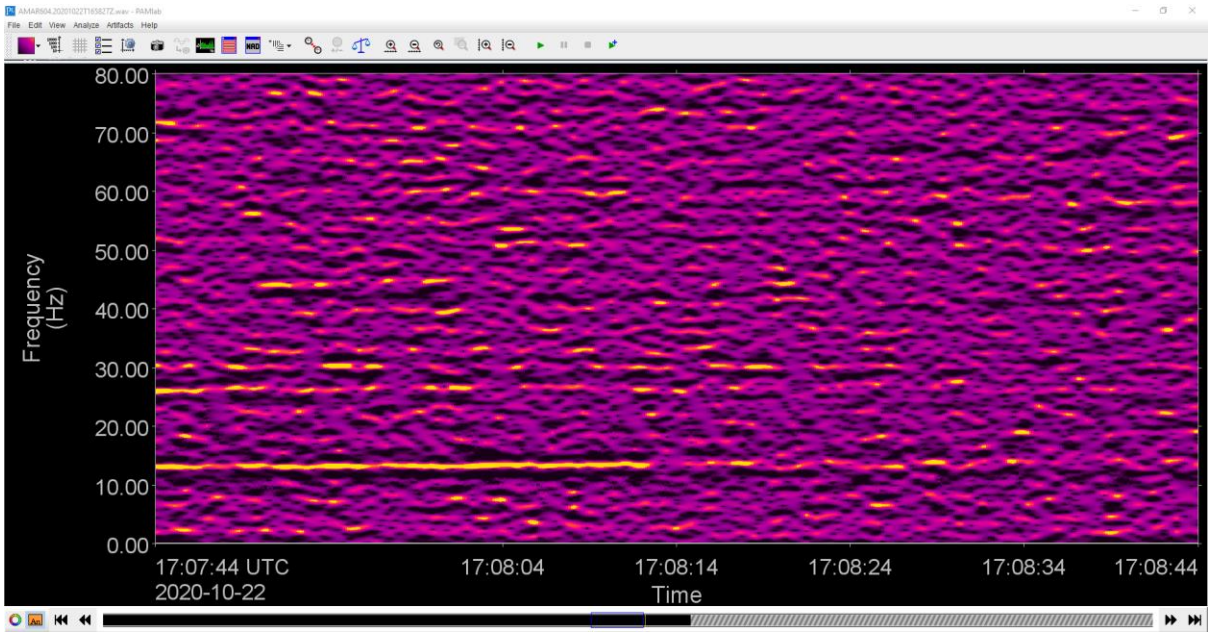

Figure 17. Additional tonal content evident during power generation mode. Centroid frequency 13.46 Hz. Emissions are strong with harmonic structure

A longer time series over 20 minutes (Figure 18) in power generation mode, shows the relative stability of the dominant tonal noise and also highlights what is likely to be a small degree of variability in frequency between two different turbines in the higher frequency tones (~380–460 Hz). At this relatively low wind speed, evidence of the weaker power generation tones, seen mostly below 100 Hz, is somewhat masked due to significant shading from the very strong ~24 and ~75 Hz primary tones. As wind speed increases, these secondary, low-frequency tones start to become more apparent.

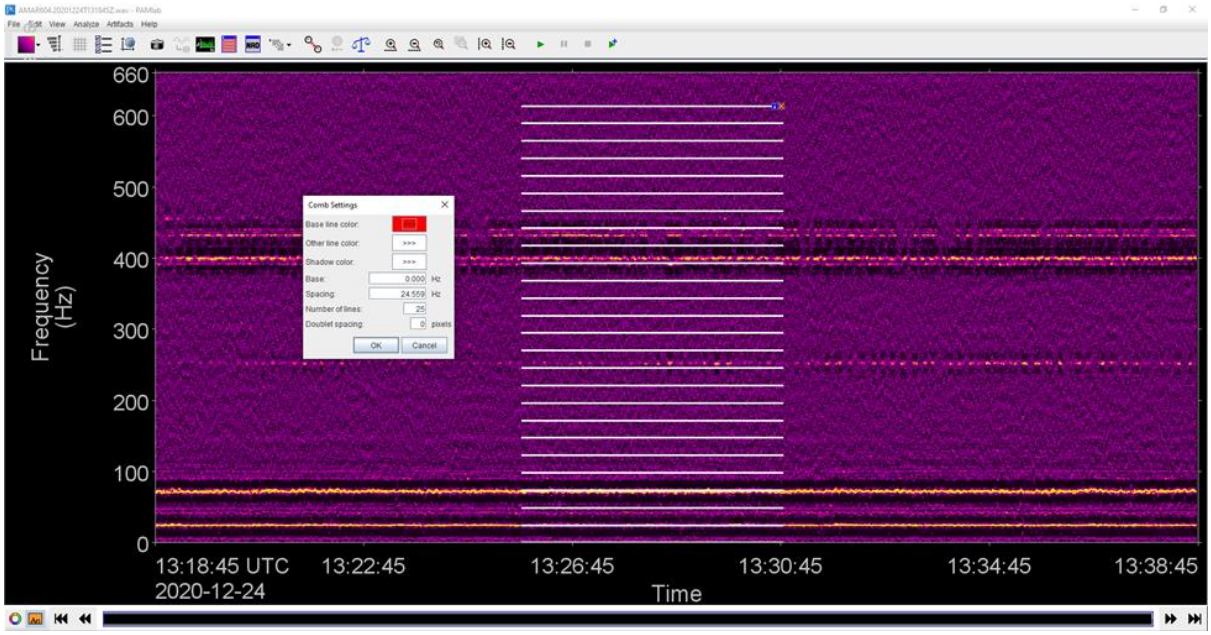

Figure 18. A 20 min time series in power generation mode showing the dominant tonal noise elements of the overall wind farm signature.

3.3.2. Mooring System Noise

One of the aims of the project was to understand whether the ‘snapping’ transients, believed to be caused by the prototype mooring system, were still present. Analysis of the acoustic data revealed a significant amount of mooring noise, but there was very little evidence of the intense, very sharp, impulsive ‘snap’ sound that was previously detected.

However, there was considerably more mooring-related noise than had been found in the Hywind Demo recordings, notwithstanding the fact that there are five Hywind systems at the site rather than just one. The new mooring transients are typically broadband, repetitive, and considerably less impulsive and fall into three distinct types, described from aural analysis as ‘creaks’, ‘bangs’, and ‘rattles’. Figure 19 shows an example of four ‘bang’ transients of varying duration from 0.3 to 1.0 s. There is a sense from audio analysis of tension release in many of these noises, supported by the rapid onset and significant intensity of the sound seen in the spectrograms. Figure 20 shows an example of a ‘creak’ transient.

Further detailed directional analysis was conducted on the transient noises resulting in characterisation and assignment of specific noise types to individual Hywind systems within the wind farm. The directional noise analysis provides an additional insight into the nature and source of mooring noise and is presented in Section 3.4. An analysis of the impulsiveness of the sounds is presented in Section 3.7.

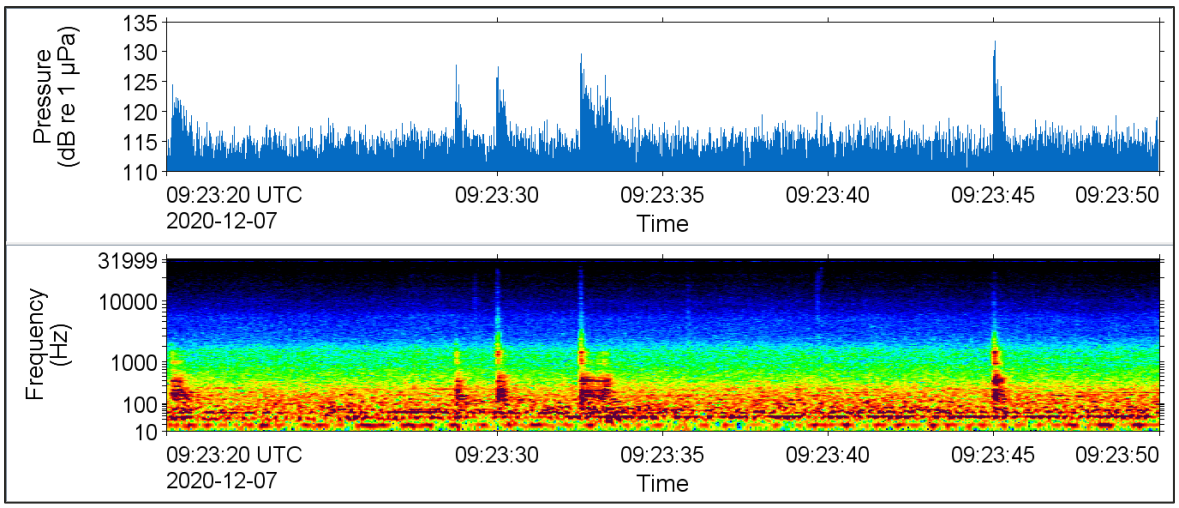

Figure 19. Amplitude (top) and spectrogram (bottom) of a 30 s section of a recording from the Hywind site from 7 Dec 2020 showing four impulsive mooring transients.

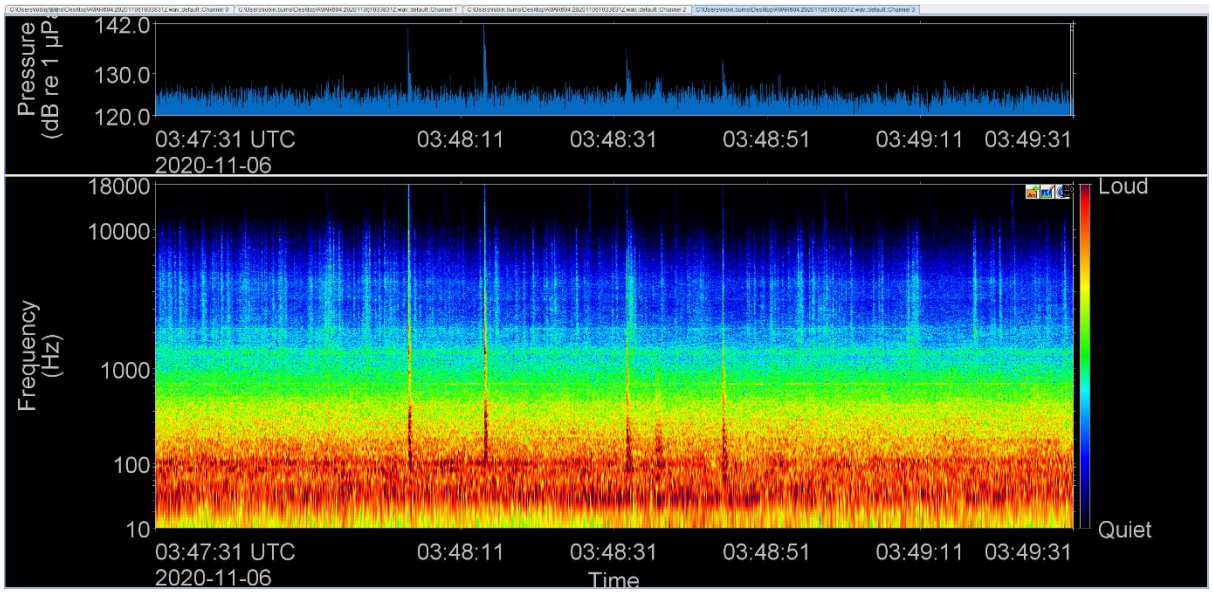

Figure 20. Example of a repetitive broadband ‘creak’ transient with a temporal period of between 0.8 and 1.0 s.

One feature of the mooring transients is that their occurrence showed a degree of positive correlation with wind speed, but it was a relatively weak relationship. The auto-processed impulse detection results for the entire recording period confirmed a progressive onset of transient noises which increasing markedly as wind speed reached 25 kn. Further analysis was conducted of transient occurrence against significant wave height which revealed a somewhat stronger correlation. This positive relationship is speculated to relate to the greater influence of waves, rather than wind speed, on the heave motion of the structure which results in a dynamic response of the mooring system. More detailed analysis of the phenomenon over shorter time periods may reveal a more precise association between these two parameters. Further discussion of this finding is presented in Section 3.7

Figure 21 shows an example of repetitive, relatively low intensity mooring transients in a moderate wind speed. At higher wind speeds the amount of mooring noise can be seen to increase and it becomes an important additional contributor to the overall noise signature of the wind farm. This is evident in analysed received band levels presented in Section 4.5. The different mooring transient sounds were not mutually exclusive and combinations of different types of noise were routinely seen in the data (Figure 22), and this is consistent with the finding that each Hywind system appeared to generate its own mooring noise.

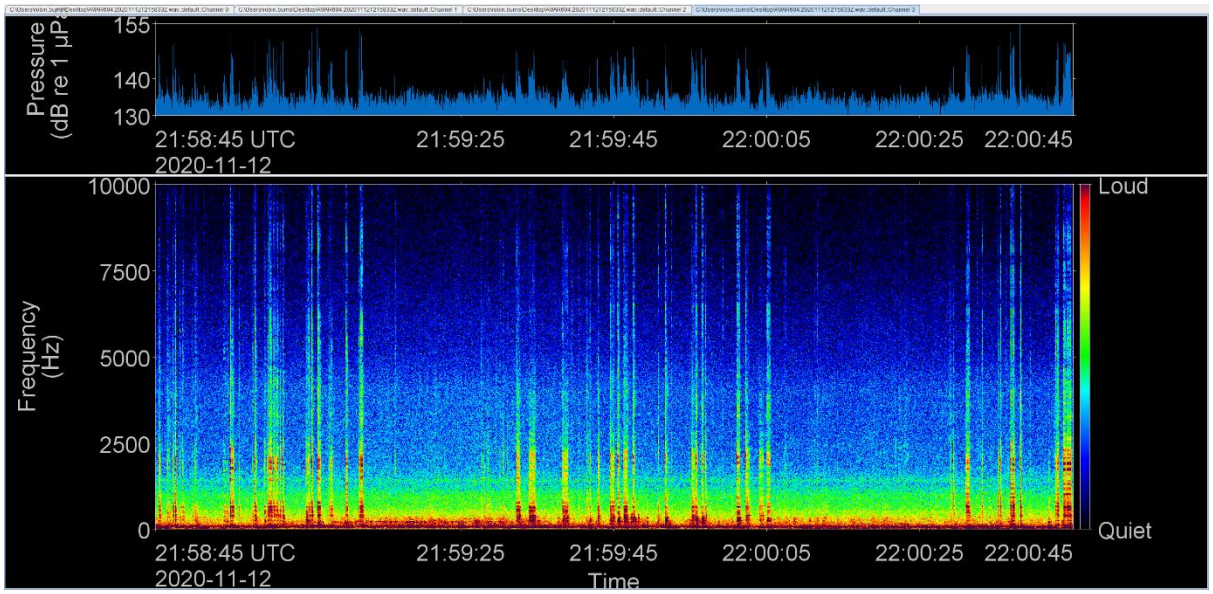

Figure 21. Repetitive broadband mooring transients in moderate wind conditions. Turbine tonals can be seen at the bottom of the displayed spectrum.

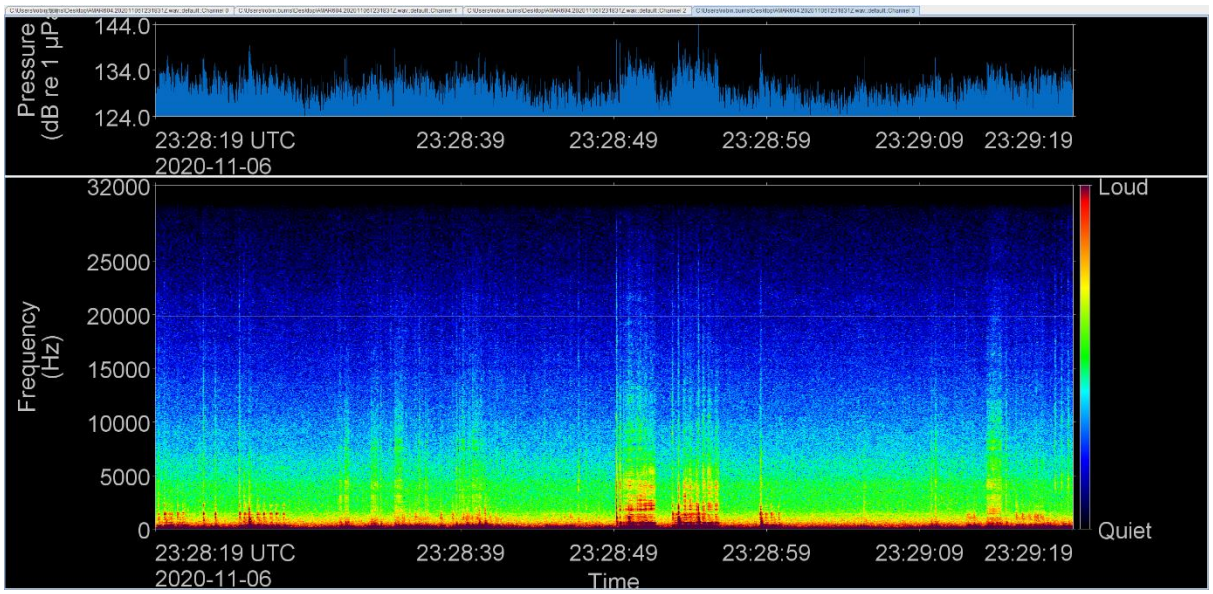

Figure 22. Two, loud, protracted-broadband, rattle transients detected amongst a series of repetitive lower intensity creaks.

3.3.3. Unattributed Noise

Several acoustic features were identified within the data that remain unattributed due to an incomplete understanding of all possible noise sources within each Hywind system. Figure 23 shows a 20 min period populated by several unstable Hywind tones and several mooring transients. The multiple tones are likely to be representative of several RPM rates at each audible turbine. However, in addition, there are a number of ‘saw-tooth’ patterns in the data, of varying intensities and frequencies, potentially from different Hywind systems at different distances from the recorder. These remain unknown in origin, but speculation suggests this may be some form of motor or pump associated with a rotational speed regulation system possibly adjusting blade angle of attack. However, this remains purely a theory and cannot be corroborated from the acoustic data alone.

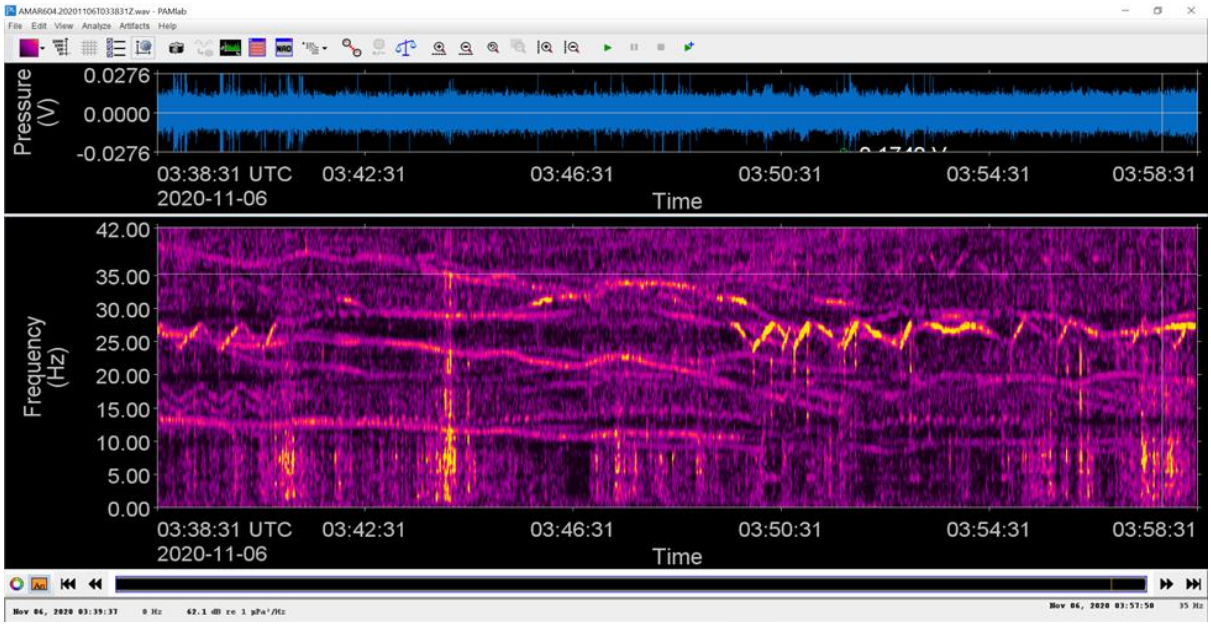

Figure 23. A 20 min spectrogram showing several unstable rotational tonals and several unidentified narrowband ‘saw-tooth’ features.

Finally, active sonar transmissions from vessels were detected relatively often during the recording period. These are possibly unrelated to the Hywind operation, and Figure 24 shows active transmissions from a positioning system and a survey/echo-sounder or sub-bottom profiler (or similar). This type of noise was frequent enough to feature in the overall PSD values for the entire recording period and makes a significant contribution to the higher frequency daily sound exposure levels for that part of the North Sea.

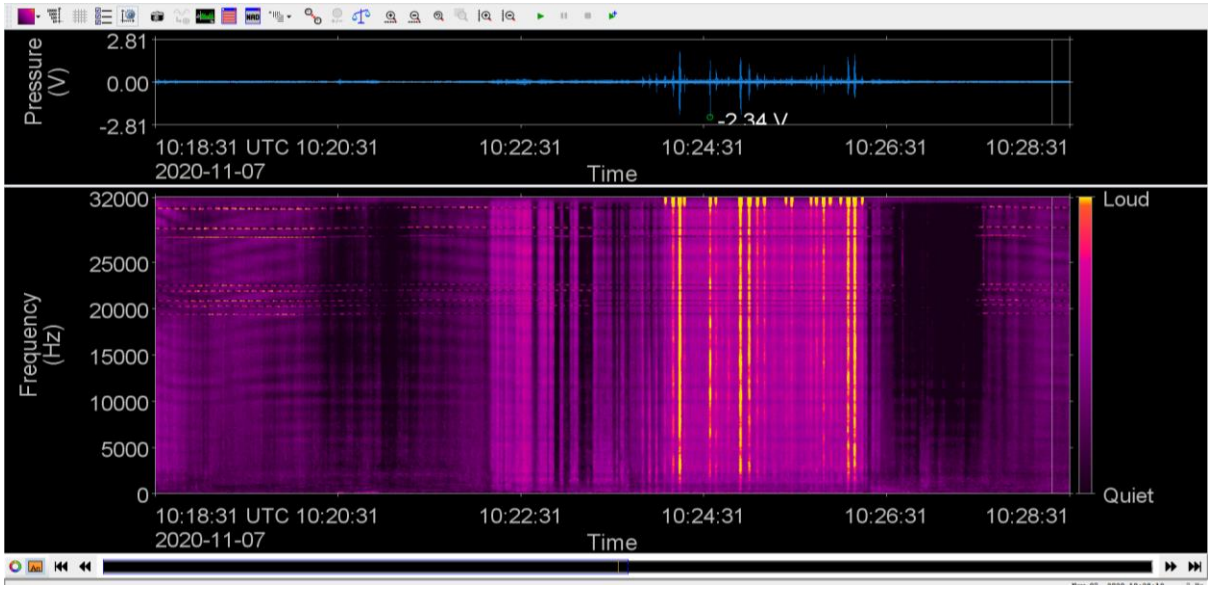

Figure 24. A 10 min spectrogram showing probably active acoustic transmissions from a vessel-mounted echo-sounder, sub-bottom profiler or similar active system and separate positioning system 'ticks'.

3.4. Directional Detection Hywind Noise

3.4.1. Methodology and Presentation of Directional Data

The tetrahedral hydrophone array employed on the Hywind-site AMAR allows for the spatial discrimination of bearing and elevation of detected sound, as outlined in Appendix B. The directional information is stored within the auto-processing detection of individual events, and the relationship between each sound and relative direction to the array can be discerned by applying the appropriate directional sector colour to the displayed noise from that sector. In the directogram figures in this section, bearing sector is presented in the colour wheel in the top right corner. The fidelity of the array determines the radial width of each sector, in this case 22.5 degrees. Noise originating from different sectors in the wheel are therefore rendered in the directogram in different colours. The orientation of the colour wheel is shown in Figure 25 with the AMAR position assumed to be at the centre of the wheel. As an example of how to interpret the directionality, noise from the southeast of the AMAR would be presented in one of the three green shades whereas noise from the southwest would be coloured in one of the blue sector colours.

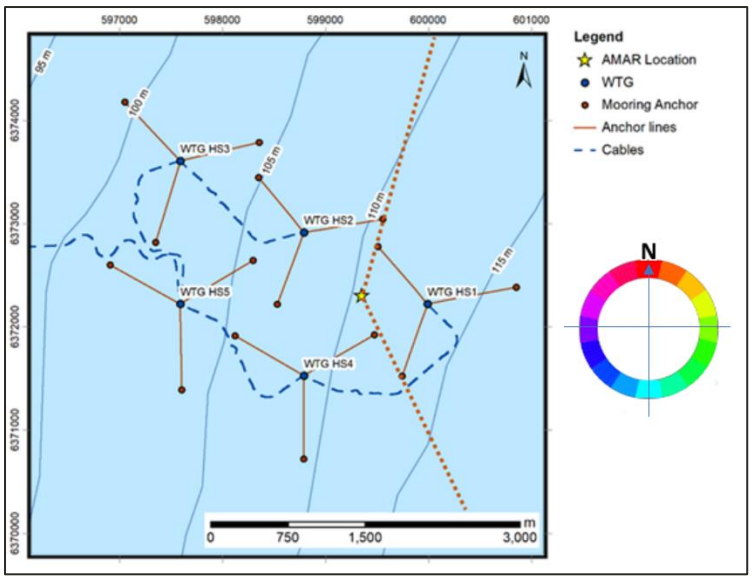

Figure 25. Colour wheel orientation relative to North and the layout of the Hywind structures.

Figure 26 is an example of a directogram from 1 Jan 2021 showing broadband transient noise from three different directions.

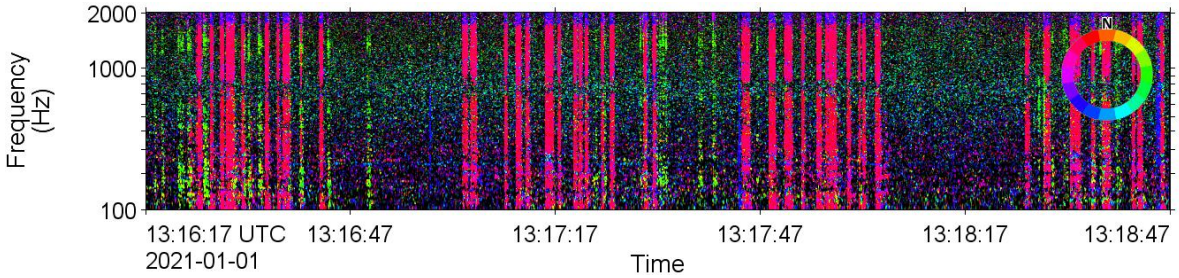

Figure 26. A 2 min directogram from 1 Jan 2021 showing audible mooring transients during a period of high winds.

This file was then manually annotated (Figure 27) by establishing analysis boxes around distinct sound events in the directogram (using JASCO's PAMlab software). The boxes encompass the start and end times of teach event and generate both acoustic and temporal metrics for each one. PAMlab then saves data from each annotation, including SPL, directional bearing, and elevation bearing which was used to compare sound sources.

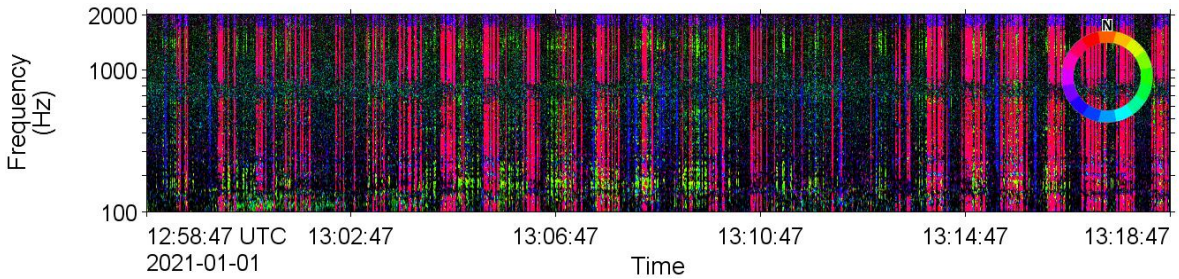

Figure 27. Manually annotated directogram identifying mooring transients for a 2 min window on 1 Jan 2021.

3.4.2. Mooring Noise Directional Analysis

During periods of higher wind speed (and by association wave height), there was a noticeable increase in detections of repetitive mooring noise at the Hywind station. Over 300 detections were manually annotated over a 20 min segment on 1 Jan 2021 (Figure 28). The audible broadband mooring transients on the directogram are consistently either pink, blue, or green, indicating three discrete and separate sources. The direction of the three colour sectors from the colour wheel relates exactly to the direction of HS-1 (to the east), HS-4 (to the southwest) and HS-2 (to the northwest). It is noticeable that HS-2 appears to be generating more mooring noise than either HS-1 or HS-4.

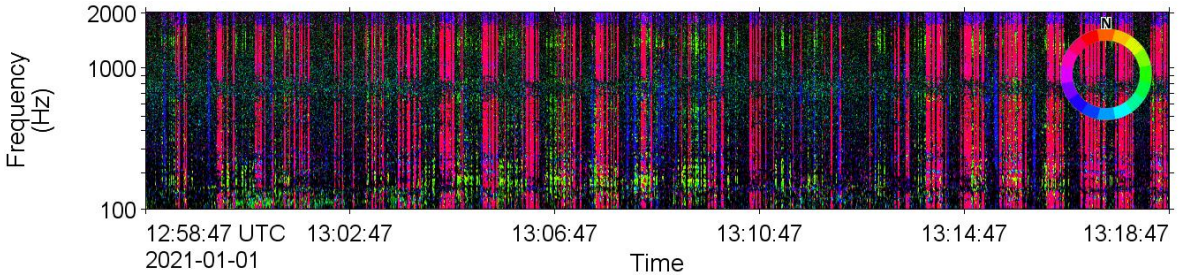

Figure 28. Directogram of 20 min of data during winds greater than 20 kn on 1 Jan 2021.

The transients originating from relatively small bearing clusters, aligned with HS-1, HS-2, and HS-4, were acoustically different and distinct from each other. Each cluster also had similar sound pressure levels indicating a consistency in source generation and distance. The sounds are thought to be generated by the same type of mooring movement such as the rubbing of surfaces under tension. Most of the transients are a series of staccato sounds, but each turbine's mooring noise appears to have a unique spectral and temporal identities:

Each of the three transient 'types' is analysed further below.

3.4.2.1. HS-1

HS-1 was associated with a low 'bang' (green) (Figure 29). This was the quietest of the three sounds and is dominated by the lowest frequencies (<250 Hz). They tend to be the shortest duration sounds but can last over 2.5 s, with occasional prolonged reverberation. This sound is sometimes inaudible due to masking from one of the other sounds or potentially other ambient sounds. Figure 30 shows a shorter, fine, temporal-scale directogram of a transient from HS-1

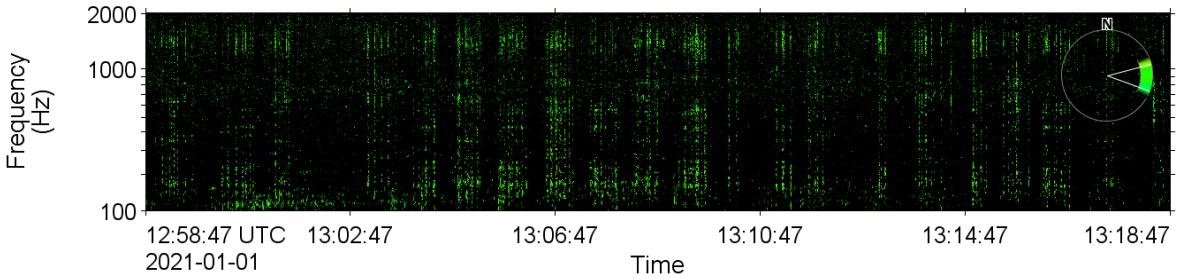

Figure 29. Directogram showing only transients received from the direction of HS-1.

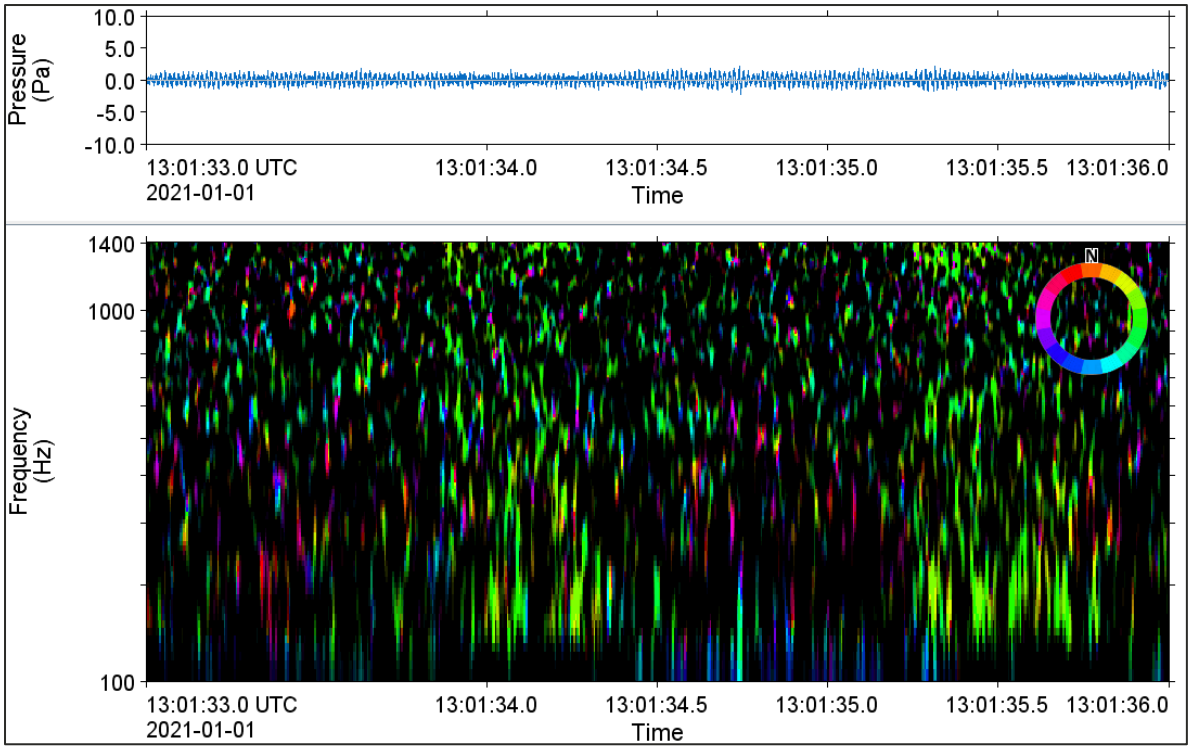

Figure 30. Fine temporal scale view of a transient from HS-1.

3.4.2.2. HS-2

HS-2 generated a ‘creak’ (red) transient (Figure 31). This had the highest SPL and masked the other two sounds when occurrence overlapped. The duration of individual sounds is around 0.4 s, with some up to 1.5 s. This sound often has frequencies absent in the band of 700–900 Hz. Figure 32 shows a zoomed-in view of an HS-2 transient with pressure variance over 3 s.

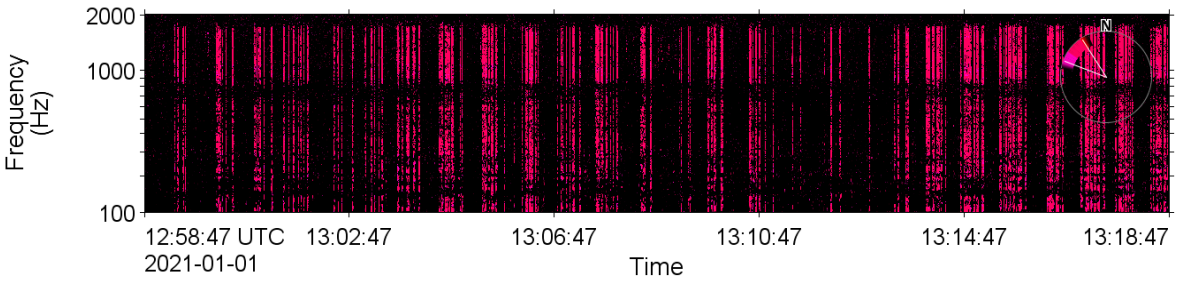

Figure 31. Directogram showing only transients received from the direction of HS-2.

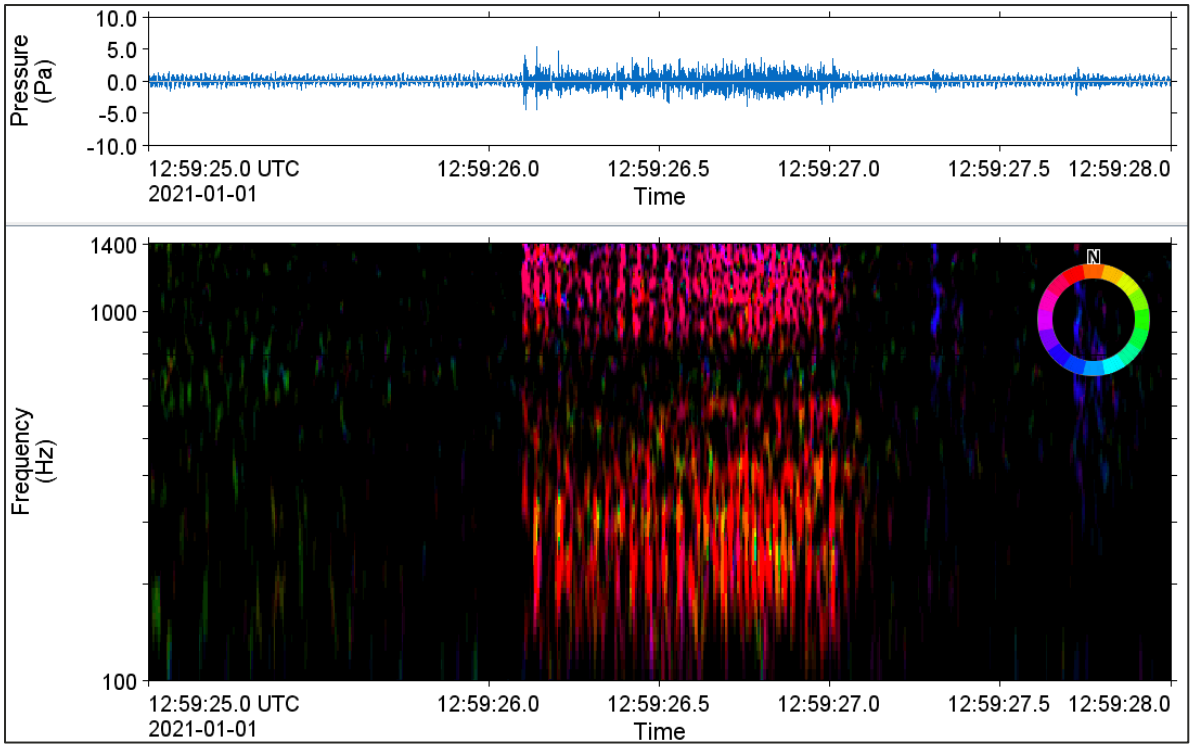

Figure 32. Fine temporal-scale view of a transient from HS-2.

3.4.2.3. HS-4

HS-4 was associated with a ‘rattle’ (blue) type sound (Figure 33). There is variation in duration from approximately 0.5–1.0 s for an individual event. It sounds like a repeated tapping noise, with variability in number of taps. The blue sounds have most of their energy in the band of 200–800 Hz. Figure 34 shows a 3 s directogram of the HS-4 transient.

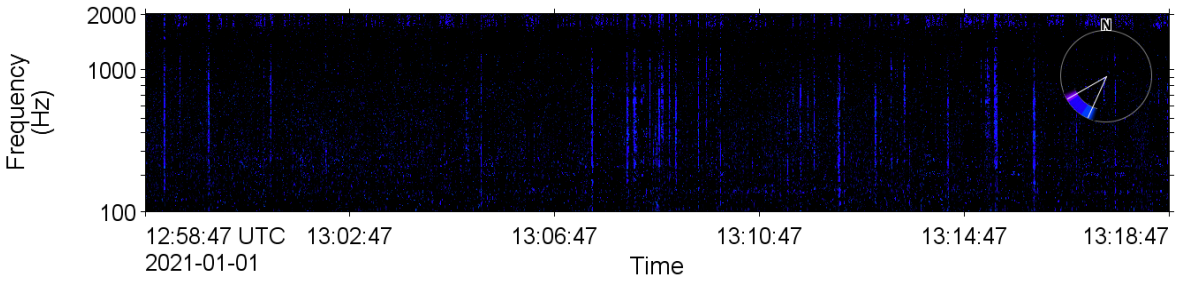

Figure 33. Directogram showing only transients received from HS-4 turbine.

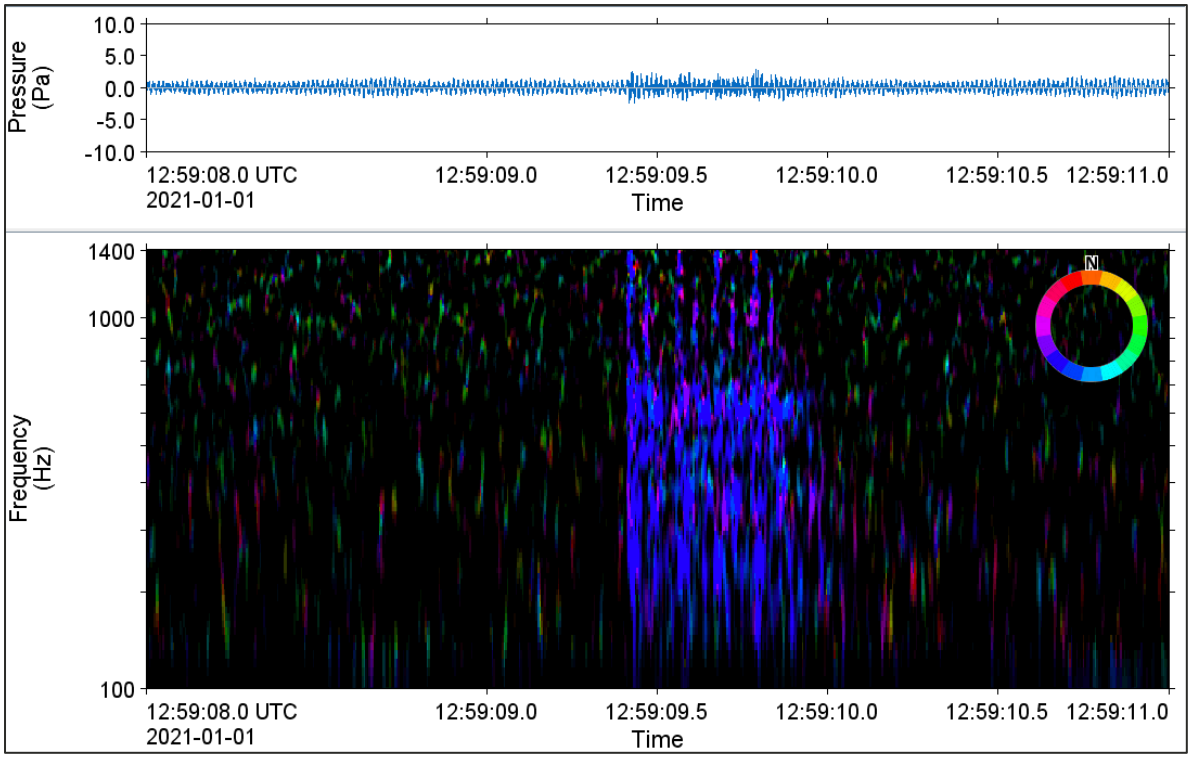

Figure 34. Finer temporal-scale view of a transient from HS-4.

Bearings for each transient type were plotted together against received SPL to identify the variability in both parameters (Figure 35). A strong relationship was observed indicating that the mooring noise levels were different for each Hywind system (given their relatively equal distance from the AMAR) and that the source of the transient was close to the bearing of the pillar. This suggests that the movement in the mooring system components causing the noise is restricted to the mooring components close to or at the pillar, rather than farther down the mooring chains, away from the pillar towards the anchors. It also raises the question why one mooring might be making more noise than another when both are subject to the same dynamic stresses.

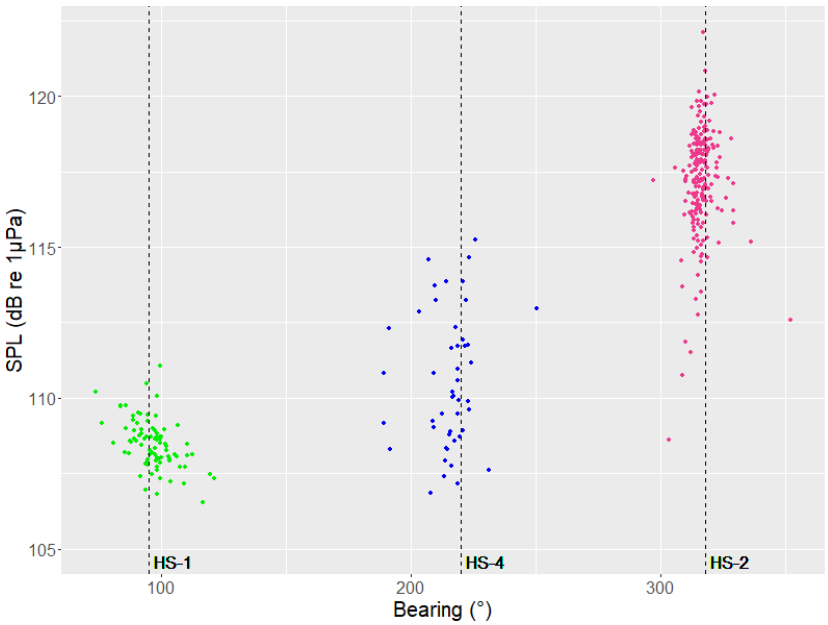

Figure 35. Plot of transient bearing from the AMAR against sound pressure level (SPL) for a 20 min period on 1 Jan 2021. HS-1 ‘bang’ transients (green), HS-2 ‘creak’ transients (pink), and HS-4 ‘rattle’ transients (blue).

Directional analysis was also applied to the tonal noise radiating from the turbines. Earlier analysis indicated that tonal noise was not consistent between different turbines and there was occasionally a significant difference in the tonal signatures, suggesting different operating RPMs under the same wind conditions. Figure 36 shows a 1 min directogram which identifies significantly different tones from the HS-1 turbine (green) to HS-4 (blue). Embedded within the directogram are some mooring transients from HS-2 (pink).

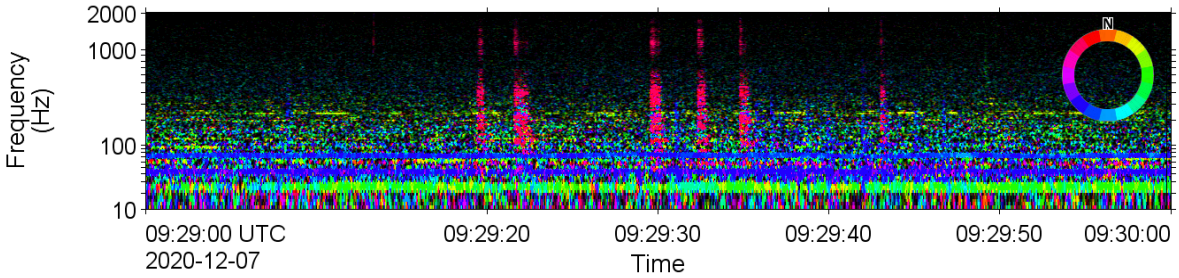

Figure 36. Directogram showing turbine related tonals from two different Hywind systems, predominantly HS1 and HS4 and several mooring transients from HS2.

Transient occurrence was initially assessed against wind speed over four different and short time periods to confirm the anticipated relationship. Figures 37 to 40 show directograms of periods with wind speed from 5, 10, 15, and 20 kn, respectively. These times were selected for having sustained wind speeds with a range ±1 kn for at least 3 h. The figures support the assertion that there is a positive relationship between transient occurrence and wind speed.

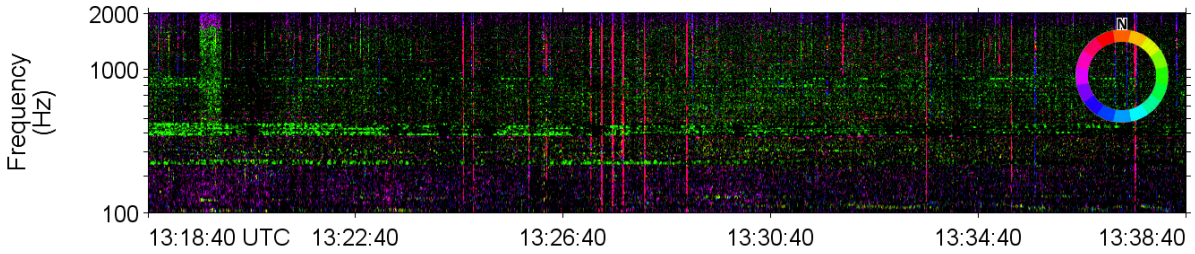

Figure 37. Directogram of a period with a 5 kn wind speed.

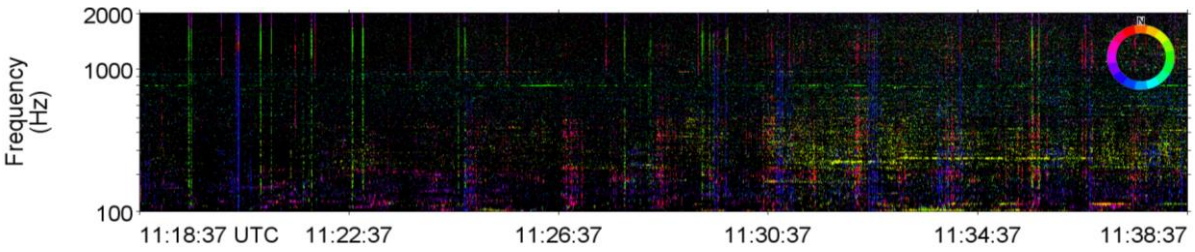

Figure 38. Directogram of a period with a 10 kn wind speed.

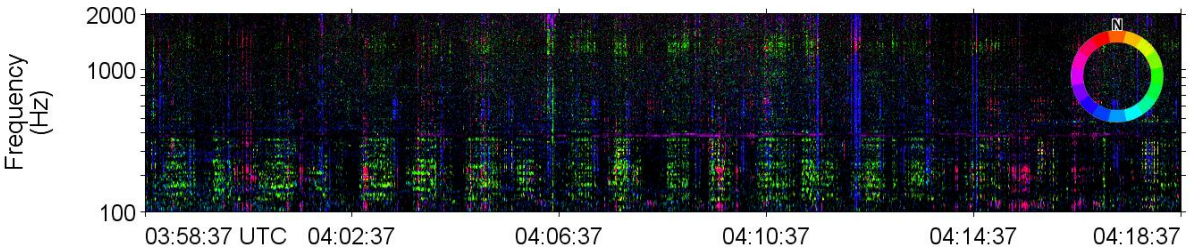

Figure 39. Directogram of a period with 15 kn wind speed.

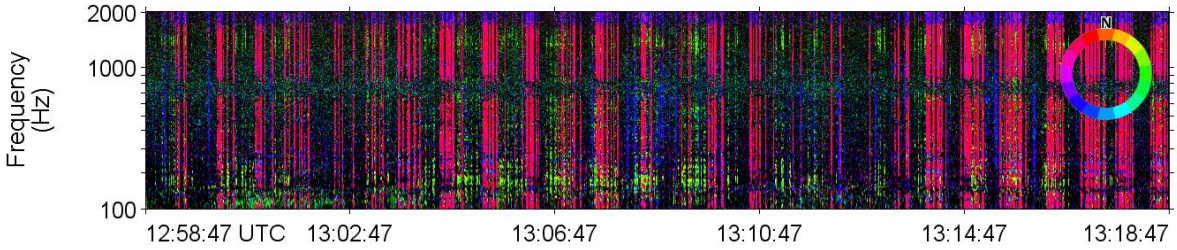

Figure 40. Directogram of a period with 20 kn wind speed.

The detections made in PAMlab also determine an elevation angle from the recorder to the source of the sound. While the elevations determined remained consistent for each of the three sounds, the angles were higher than the actual estimated angles between the recorder and the turbine floats. The sound speed profiles of the area were obtained (Figure 48) to see if propagation effects would influence the perceived elevation; however, profiles are consistent with depth and would not impact the angle. The nearly constant sound speed also indicates that the different amplitudes received for the sounds from each turbine are not due to propagation effects. The elevation of detected sound remains an area for further work.

3.5. Marine Strategy Framework Directive Descriptor 11 (MSFD D11)

The Marine Framework Strategy Directive (MFSD) of the European Union employs the mean sound pressure level in the 63 and 125 Hz decidecade bands as indicators of good environmental status. The objective of reporting the distribution of sound pressure levels in these bands is to build an understanding of ocean sound levels; however, there are no thresholds or limits that must be achieved. The Control and Hywind data were analysed in decidecade frequency bands using 1 min analysis windows. Figure 41 shows the distribution of sound pressure levels for the two decidecade bands for the two sites. The median levels at the Hywind site were 5.5 dB higher than sound levels at the Control site at 63 Hz, and 2 dB higher at 125 Hz. The greater range of outlier values at the Control site brought the mean levels closer together with the Hywind site 1 dB higher than Control at 63 Hz and only 0.6 dB higher at 125 Hz.

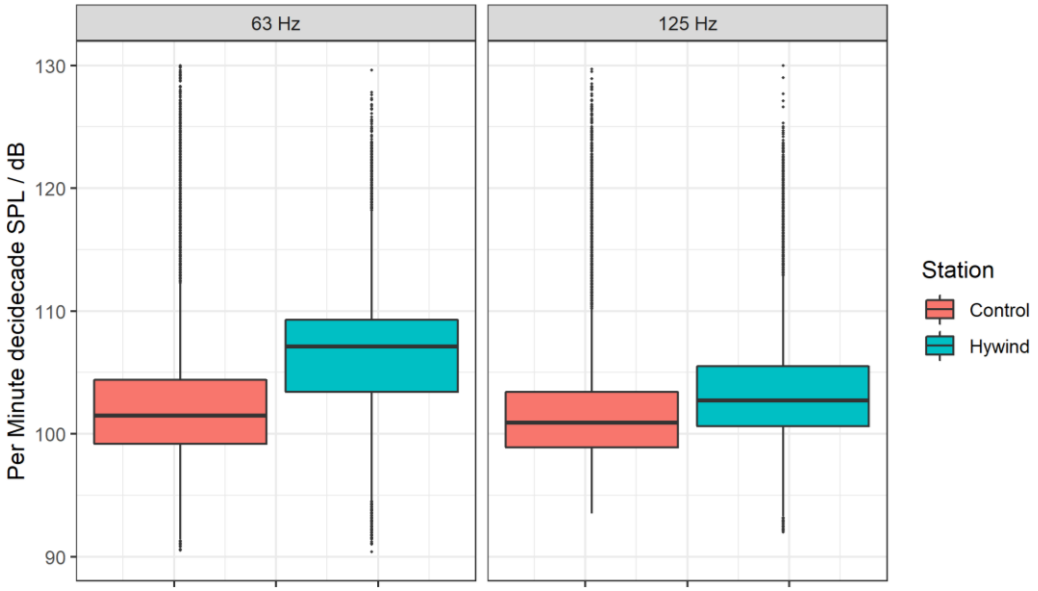

Figure 41. Distribution of 1 min decidecade sound pressure levels at the Control and Hywind sites at 63 and 125 Hz. The boxes represent the interquartile range of values, with the medians shown as the dark lines inside the boxes. The range of values above and below the quartiles are shown with the lines, and outliers beyond this span are shown as dots.

3.6. Marine Mammal Exposure Levels

The perception of underwater sound depends on the hearing sensitivity of the receiving animal in the frequency bands of the sound. Hearing sensitivity in animals varies with frequency, the hearing sensitivity curve (audiogram) usually follows a U-shaped curve (where there is a central frequency band of optimal hearing sensitivity and reduced hearing sensitivity at higher and lower frequencies). The hearing sensitivity frequency range differs between species, meaning that different species will perceive underwater sound differently, depending on the frequency content of the sound. Auditory frequency weighting functions for different functional hearing groups are applied to reflect an animal's ability to hear a sound and to de-emphasize frequencies animals do not hear well relative to the frequency band of best sensitivity. Figure 42 shows the difference between perceived daily sound exposure by low-, mid-, and high-frequency cetaceans and pinnipeds (otariid and phocid).

All daily sound exposure levels recorded during this study were found to lie below the thresholds for temporary or permanent hearing threshold shifts (i.e., hearing loss) from exposure to non-impulsive sounds for each functional hearing group (NMFS 2018). This suggests that there is no risk of auditory injury from the operational of the Hywind Scotland wind farm for any of the auditory groups for species potentially at the site. Section 3.7 provides an analysis of the impulsiveness of the Hywind soundscape.

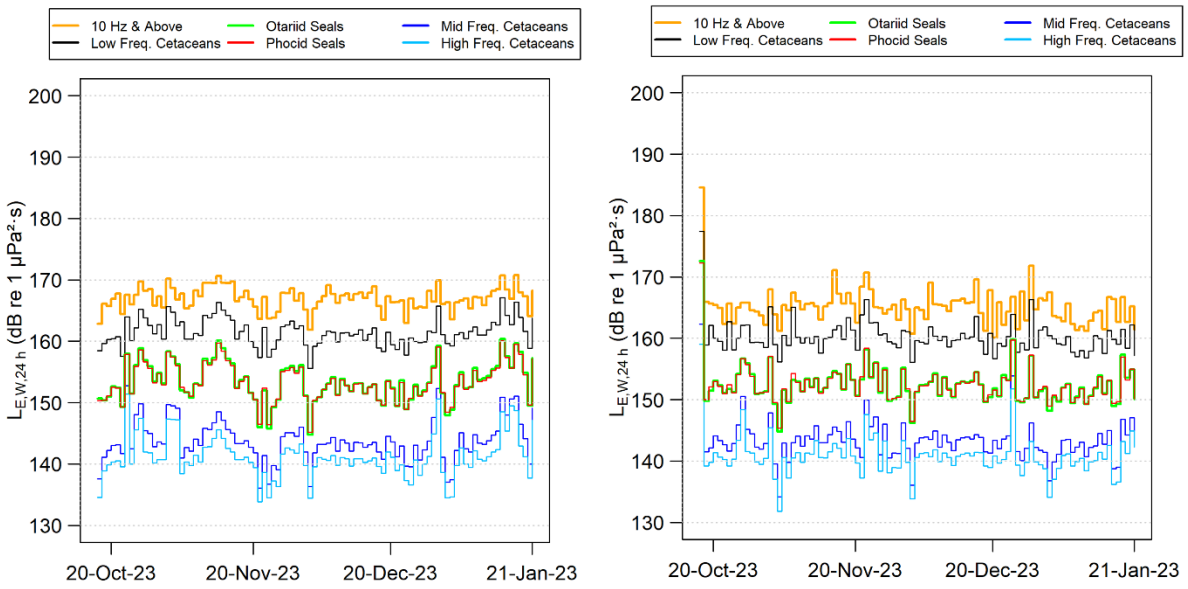

Figure 42. Control station (left) and Hywind station (right): NMFS (2018) auditory frequency weighted daily sound exposure levels (SEL). The 10 Hz & Above SEL is the unweighted daily SEL.

3.7. Impulsive Characterization of the Hywind Site

It is important to understand whether the sounds generated by the Hywind turbines are impulsive or non-impulsive to determine which hearing threshold shift regulatory criteria are appropriate to apply. Impulses are acoustic events that are broadband short duration (<1 s) with high peak sound pressures and short rise times (NIOSH 1998, NMFS 2018). The qualitative assessment of the impulses (Section 3.4.2), indicated that the impulses tended to be on the order of 1 s long, with multiple sub-pulses and/or tones buried inside the pulse. The peak pressures and rise times standout from the background, however, they do not compare to typical impulses such as pile driving or seismic airgun

surveys. Based on the qualitative assessment, the impulse detector was tuned for pulses on the order of 0.1–2.0 s duration (Section 2.2).

The impulse detector confirmed the manual analysis results. The interquartile duration of the detected impulses was 1.3–1.7, which is longer than the traditional definition of an impulse. As expected, the detector found a greater number of detections at higher wind speeds at Hywind, which was not replicated at Control (Figure 43). It was not surprising that the number of detections at Hywind decreased at the highest wind speeds since there is greater sound energy above 100 Hz from wind driven noise, which made it harder to detect the impulses. An output of the impulse detector is the per-impulse sound exposure level in decidecade bands. The mean, median, and 90th percentile of these is shown in Figure 44. The NMFS (2018) auditory frequency weightings were applied to the decidecade SEL that were summed to determine the daily SEL from impulses (Figure 45). By comparison to Figure 42, the high-frequency cetacean weighted impulsive SEL are generally 6 dB below the total daily SEL and often more than 10 dB below the total. A comparison of the kurtosis at Control and Hywind (Figure 46) supports the observation that there are more impulses at the Hywind site (e.g., Figure 43), however, the occurrence of highly impulsive minutes (β > 40) is exceptionally rare at both sites. This type of kurtosis distribution from a sound source is an excellent example of why a kurtosis-weighted SEL for predicting hearing threshold shifts would be valuable for regulatory applications (Zhao et al. 2010).

Due to the relatively infrequent high kurtosis minutes, the length of the impulses, as well as the impulsive SEL being 6 dB or more below the total SEL, use of the non-impulsive threshold from NMFS (2018) is recommended – i.e., the TTS threshold for high-frequency cetaceans (porpoise) is 153 dB re 1 µPa²s.

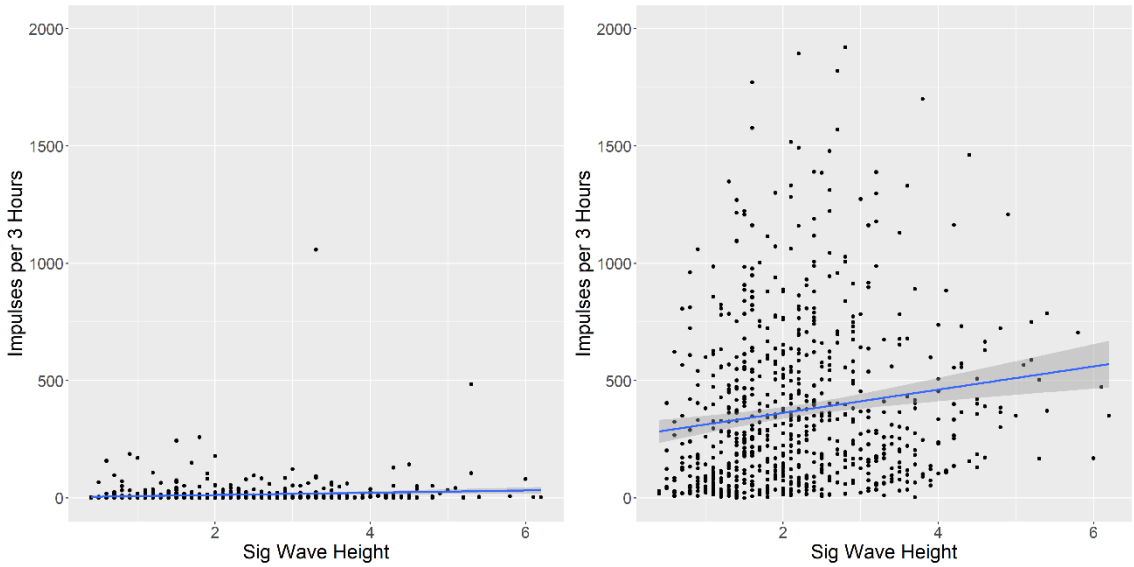

Figure 43. Scatterplot of the number of impulse detections per 3 h versus the significant wave heights at Control (left) and Hywind (right).

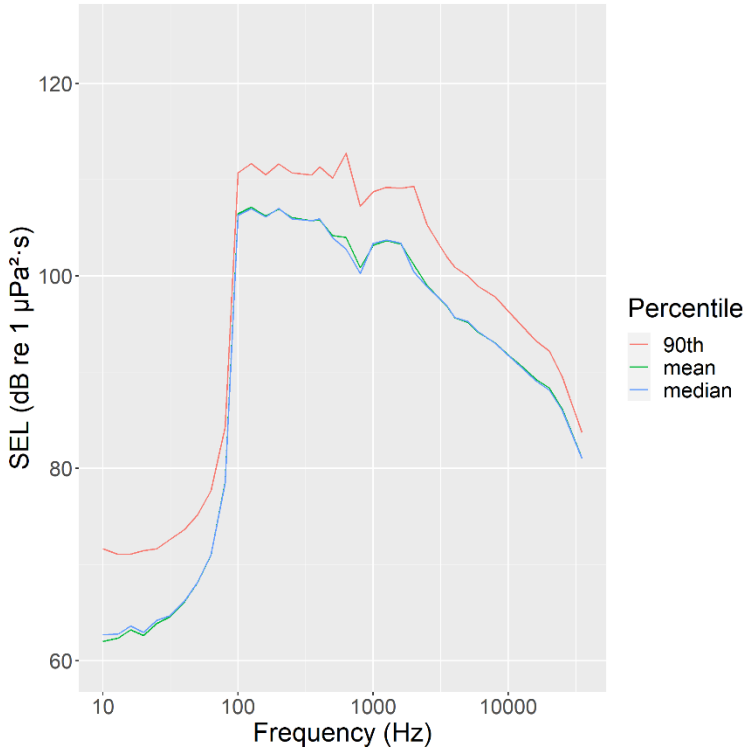

Figure 44. Mean, median, and 90th percentile decidecade sound exposure levels (SEL) of the impulses detected at Hywind.

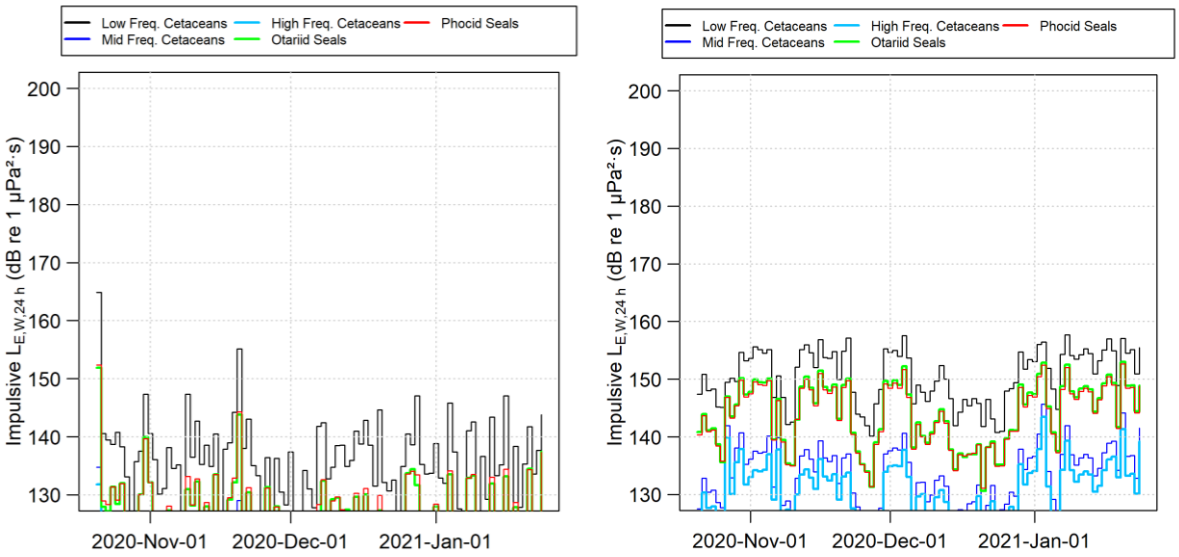

Figure 45. Daily auditory frequency weighted sound exposure level (SEL) for the impulsive events detected at the Control site (Left) and Hywind (right), which can be directly compared to the daily SEL for the full soundscape in Figure 42.

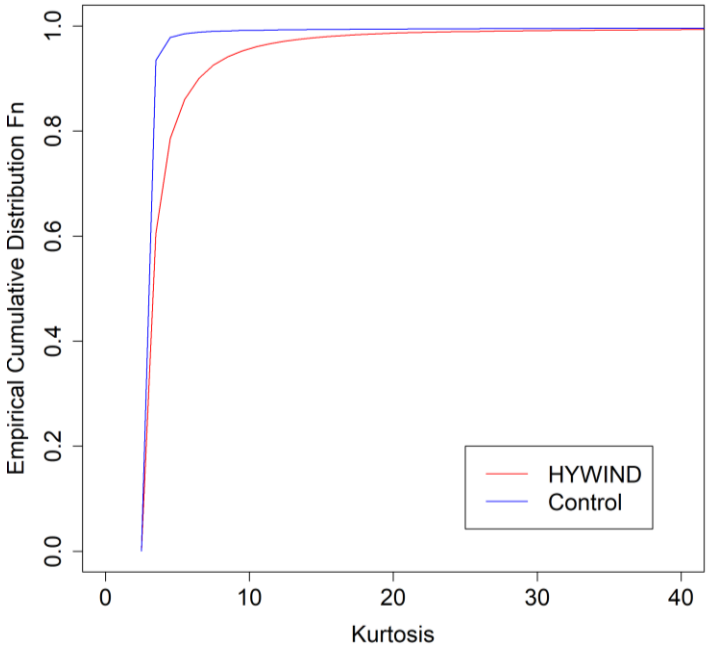

Figure 46. Empirical cumulative distribution functions for the 1 min kurtosis at the Hywind and Control sites.

4. Source Levels

This section describes the back-propagation methodology and results to determine an approximation for the sound source spectrum for varying operational conditions. Underwater propagation modelling is used to determine the propagation loss from a single point in the water column at the turbine location. Combined with the measured received levels, a sound source function can be determined.

It should be noted that the turbine spar exists as a line source covering a significant proportion of the water column. To determine the contribution to the sound field of multiple points down the spar length would require a much more detailed study. Back-propagating sound levels to a single point (rather than the submerged length of the spar) is a simplification of the source itself, and when repropagated may not represent the sound field particularly well, especially in the near field. Much of this is due to the initial propagation conditions of the two types of source considered (point and line sources); where a point source is considered, the initial sound radiation follows spherical spreading laws (i.e., sound pressure proportional to $20\log_{10}(r)$) and so rapid losses due to geometric spreading are realised close to the source; in the case of a line source, the propagation regime initially more closely follows that of cylindrical spreading (i.e., sound pressure proportional to $10\log_{10}(r)$), which has less rapid decay than for spherical spreading. Consequently, the values generated here provide an illustration of likely levels, but care should be taken when used as modelling source levels.

4.1. Metrics

The metrics used in this chapter are entirely based on those presented in ISO18405 and are summarised in Table 4.

Table 4. Metrics used in this section from or based on ISO 18405 as used in this section.

Metric	Abbr.	Symbol	Unit	Notes
Levels of acoustical power quantities				
sound pressure level	SPL	L_p	dB re 1 µPa²	May be written as 'field' quantity rather than 'power' quantity (i.e., dB re 1 µPa)
sound exposure level	SEL	$L_{E,p}$	dB re 1 µPa²s	
mean-square sound pressure spectral density level	PSD	$L_{p,f}$	dB re 1 µPa²/Hz	Referred to in text as 'power spectral density' (PSD)
Source levels				
source level	SL	L_S	dB re 1 µPa²m²	May use 'field' quantity (i.e., dB re 1 µPa m). Implies a statistically stationary sound source.
sound exposure source level/energy source level	ESL	$L_{S,E}$	dB re 1 µPa²m²s	
source power spectral density	—	$L_{S,f}$	dB re 1 µPa²m²/Hz	Not defined in ISO 18405
Propagation				
propagation loss	PL	N_{PL}	dB re 1 m²	Applies to a statistically stationary sound source

The mean-square pressure derived levels (i.e., received level: SPL; source level: SL) represent 'power' quantities which is presumed to be statistically stationary over time and remains static over time. The sound exposure levels (i.e., received level: SEL; source level: ESL) represent 'energy' quantities, in that they account for all received acoustic energy within a stated time window. Given the nature of the analysed source (i.e., mostly continuous) it is most appropriate to express the source levels using the mean-square property of SL in dB re 1 µPa²m² (equivalent to dB re 1 µPa m).

4.2. Modelled Environment

The back-propagation study requires a detailed descriptor of certain aspects of the environment. In the analysis performed for this study, these were the bathymetry, geology, temperature and salinity of the water (from which the sound speed profile can be generated), and wind speed.

The bathymetry for the back propagation requires only the direct path between the turbine (HS1) and the monitoring station (Hywind). This was sourced from EMODnet (2020) and shows a relatively flat bottom with little variability over distance, ranging from a minimum of 111 m and a maximum of 114 m (Figure 47). The sound speed profiles for the modelled sites were derived from temperature and salinity profiles from the US Naval Oceanographic Office's *Generalized Digital Environmental Model V 3.0* (GDEM; Teague et al. 1990, Carnes 2009). The sound speed profile was generated from extracted temperature and salinity profiles for December from 57.5°N, 358.75°E up to a depth of 100 m. Beyond this depth, the data were linearly extrapolated to the maximum water depth. The GDEM temperature-salinity profiles were converted to sound speed profiles according to Coppens (1981). The resulting sound speed profile is shown in Figure 48.

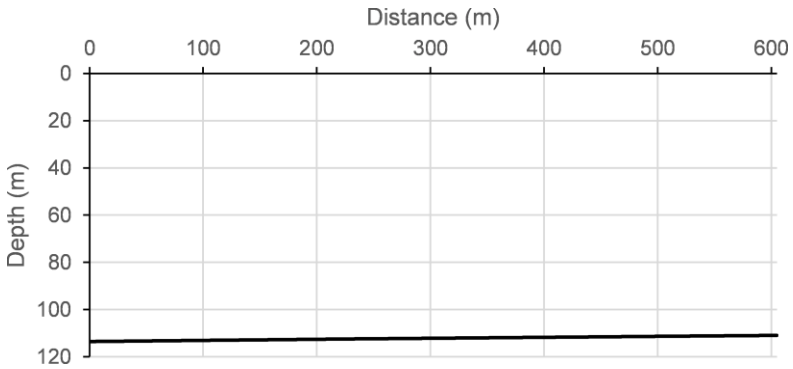

Figure 47. Bathymetric transect between HS1 and the monitoring station. Values taken from EMODnet Bathymetry Consortium (2020).

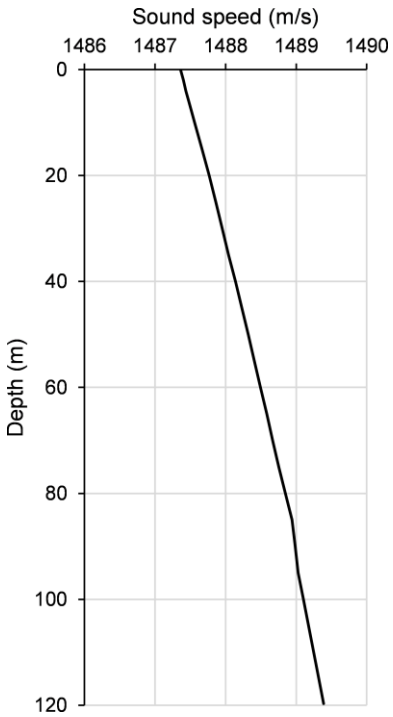

Figure 48. The sound speed profile used in the back propagation modelling. Values were calculated from salinity and temperature profiles taken for December at 57.5°N, 358.75°E from GDEM.

In shallow environments, interactions between the acoustic field and the seabed are important and accurate geoacoustic profiles are needed for proper acoustic modelling. A lithological description of the local geology was provided by Equinor that provided depths below the sea floor (up to 25.0 m) and a generalised soil description; beyond this depth, we have presumed increasingly consolidated gravelly clay. A geoacoustic profile was generated from this description using the sediment parameters by Hamilton (1980); shear wave properties at the seabed were based on values by Holzer et al. (2005) and Buckingham (2005). The geoacoustic profile used in the back propagation modelling is shown in Table 5.

Table 5. Geoacoustic model for Hywind. Within each depth range, each parameter varies linearly within the stated range. The compressional wave is the primary wave. The shear wave is the secondary wave.

Depth below seafloor (m)	Material	Density (g/cm^3)	Compressional wave		Shear wave	
			Speed (m/s)	Attenuation (dB/λ)	Speed (m/s)	Attenuation (dB/λ)
0–0.7	Fine sand	1.95–1.95	1715.9–1716.8	0.89–0.89	300	3.65
0.7–7.6	Sandy clay	1.38–1.39	1478.7–1487.7	0.08–0.08		
7.6–25	Gravelly clay	1.61–1.63	1548.3–1570.6	0.27–0.38		
25–50		1.63–1.66	1570.6–1601.8	0.38–0.54		
50–100		1.66–1.73	1601.8–1661.7	0.54–0.87		
100–200		1.73–1.85	1661.7–1771.6	0.87–1.24		
200–500		1.85–2.14	1771.6–2037.3	1.24–0.87		

4.3. Modelling Parameters

As stated, the back-propagation analysis has been performed presuming the turbine spar can be represented by a point source. The cylinder has a reported nominal draft of 78 m, with the modelled point source being positioned at the mid-point (i.e., source depth of 39 m).

The back-propagation modelling was performed with JASCO's Marine Operations Noise Model (MONM) for low-frequency propagation (less than 1 kHz) and MONM-BELLHOP for high-frequency propagation (1 kHz and greater).

MONM computes acoustic propagation via a wide-angle parabolic equation solution to the acoustic wave equation (Collins 1993) based on a version of the US Naval Research Laboratory's Range-dependent Acoustic Model (RAM), which has been modified to account for a solid seabed (Zhang and Tindle 1995). The parabolic equation method has been extensively benchmarked and is widely employed in the underwater acoustics community (Collins et al. 1996). MONM accounts for the additional reflection loss at the seabed, which results from partial conversion of incident compressional waves to shear waves at the seabed and sub-bottom interfaces, and it includes wave attenuations in all layers. MONM incorporates the following site-specific environmental properties: a bathymetric grid of the modelled area, underwater sound speed as a function of depth, and a geoacoustic profile based on the overall stratified composition of the seafloor.

MONM-BELLHOP is based on the BELLHOP Gaussian beam acoustic ray-trace model (Porter and Liu 1994). It accounts for sound attenuation due to energy absorption through ion relaxation and viscosity of water in addition to acoustic attenuation due to reflection at the medium boundaries and internal layers (Fisher and Simmons 1977). The former type of sound attenuation is important for higher frequencies and cannot be neglected without noticeably affecting the model results.

The propagation modelling was performed at the centre frequency of the decidecade bands from 10 Hz to 25 kHz. To account for sound in across the band rather than at the single frequency, the single-frequency sound fields were averaged in range using the algorithm developed by Harrison and Harrison (1995) that simulates a smearing in frequency by using a range-dependent smoothing factor – this avoids peaks and troughs in the sound field that are indicative of single-frequency analysis rather than for the frequency band.

4.4. Propagation Loss Results

The modelled decidecade-band propagation loss, between a point source at 39 m depth at the location of the spar and a receiver 1 m from the seabed at the location of the recorder is shown in Figure 49. As stated, propagation for bands below 1 kHz is calculated using the parabolic equation model which does not have sea surface roughness (i.e., variation with wind speed) included. The propagation loss for decidecade bands 1 kHz and above was calculated using the beam-tracing model and so takes the surface roughness due to the change in wind speed into account.

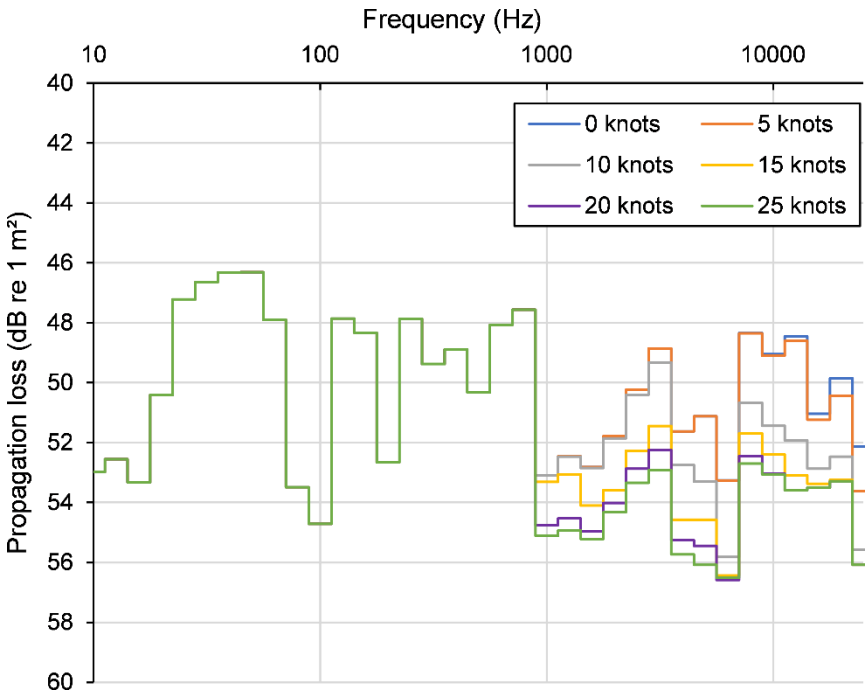

Figure 49. Propagation loss between the point source midway down the spar and the recorder for varying wind conditions.

4.5. Received Sound Levels

Received levels in decidecade bands were extracted from the recording at both the Hywind and Control AMARs for wind speed bins of the target speed ±1 kn (i.e., data for 5 kn comprises recorded levels for 4 to 6 kn). Directional analysis was used at the Hywind site recorder to ensure only the single turbine was being contributing to the signal. Median results of the received SPL in bands are shown in Figure 50.

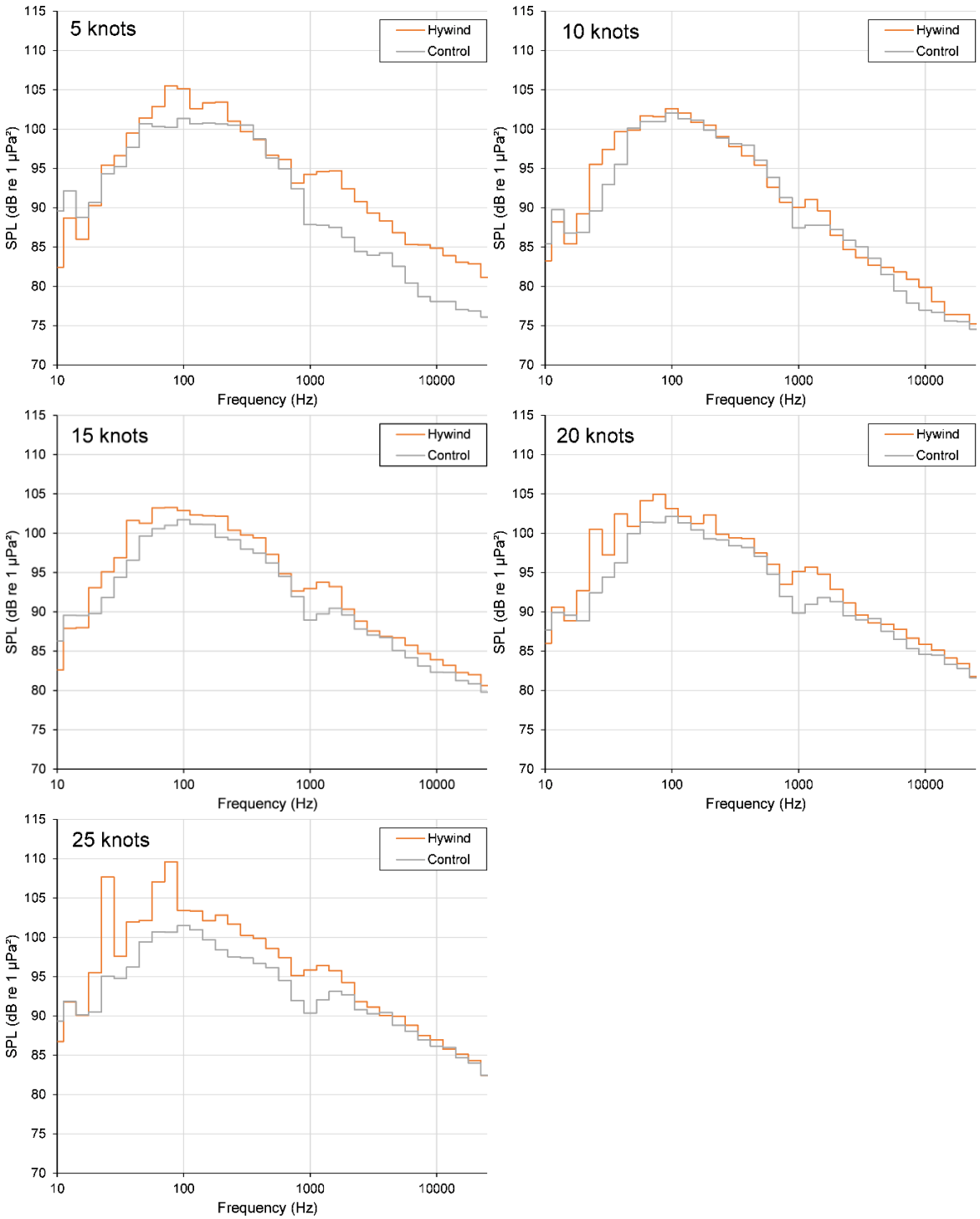

Figure 50. Received sound pressure levels (SPL) in decidecade bands at the Hywind and Control sites for periods where the wind speed was within 1 kn of the target value. Given the trends at other wind speeds, the elevated band levels recorded at 5 kn are likely to be a contamination of the data from nearby vessels rather than from the turbine.

The plots show that at the Control site, the sound comprises a broad peak from 50 to 400 Hz, with levels above 1 kHz being highly dependent on the wind speed. The broad peak at the Hywind site is typically at a slightly lower frequency than ambient with more energy between the 40 and 100 Hz bands. The Hywind result at 5 kn is likely to have been contaminated with local vessel noise as it features much more energy at higher frequencies that does not exist for analyses at the other wind speeds. At 10 kn, the turbine signal becomes prominent at 25–40 Hz, 1.0–1.6 kHz, and 6.3–10 kHz. At 15 kn, we see broadband sound with peaks at 400 Hz and at 1.0–1.25 kHz. At 20 kn, the peaks become more defined at 20–25, 40, 63–80, and 1.0–1.25 kHz. At 25 kn, there are increased levels over the ambient across all frequencies up to 2 kHz, with peaks occurring at the same frequencies as for 20 kn.

It should be noted that the received sound levels, processed in this way, include all aspects of the received sound averaged over the duration; this includes any transient signals as well as the continuous tonal noise.

4.6. Back-propagated Source Levels

Combining the received level at the Hywind site with the calculated propagation losses provided a source level spectrum for each wind speed in accordance with:

$$L_{\mathrm{S}} = L_p + N_{\mathrm{PL}}. \tag{2}$$

It is only possible to back-propagate the sound levels recorded at the monitoring station. If the radiated sound due to the source of interest is below that of ambient sound for a given frequency band, it is the ambient level that is back propagated and results in an artificially elevated source level at the affected frequencies. The analysis presented makes no allowance for this phenomenon, so it should be noted that the back-propagated source levels are likely to be overestimated where there is little difference between levels for a given frequency at the Control and Hywind sites (Figure 50).

The source levels calculated for the turbines at the different wind speeds are shown in Figure 51 for the median (50th percentile) sound levels and Figure 52 for the 95th percentile sound levels. The broadband back-propagated source levels for each analysed wind speed, shown in 5th, 25th, 50th, 75th, and 95th percentiles, are shown in Table 6 and graphically in Figure 53. Equivalent values for the sound exposure source level are shown in Table 7 and Figure 54.

While there is the trend of increased sound levels with increased wind speed, there is larger variation in the sound levels within a given wind speed bracket. There are definite spectral changes, however, as the wind speed increases. Most prominent are the peaks forming at 20 to 25, 40, and 63 to 80 Hz as well at 1.0 to 1.25 kHz most noticeable at 20 kn, with the addition of the peak at 200 to 250 Hz at 25 kn.

Back-propagated decidecade-band SLs for all studied percentiles and wind speeds are provided in tabulated format in Appendix E.1. Simulated decidecade-band sound exposure source levels over 24 h are provided in Appendix E.2.

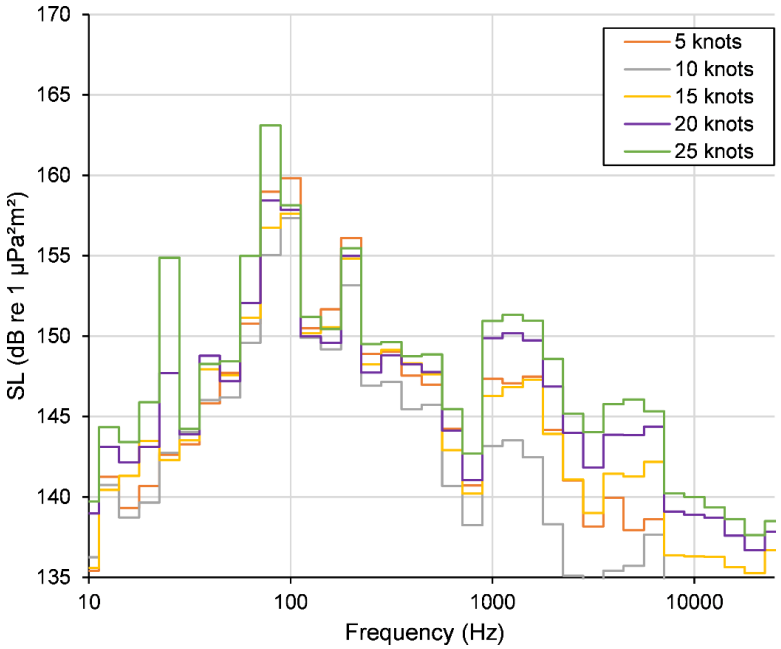

Figure 51. Back-propagated source levels for the turbines based on a point source assumption and median received sound levels.

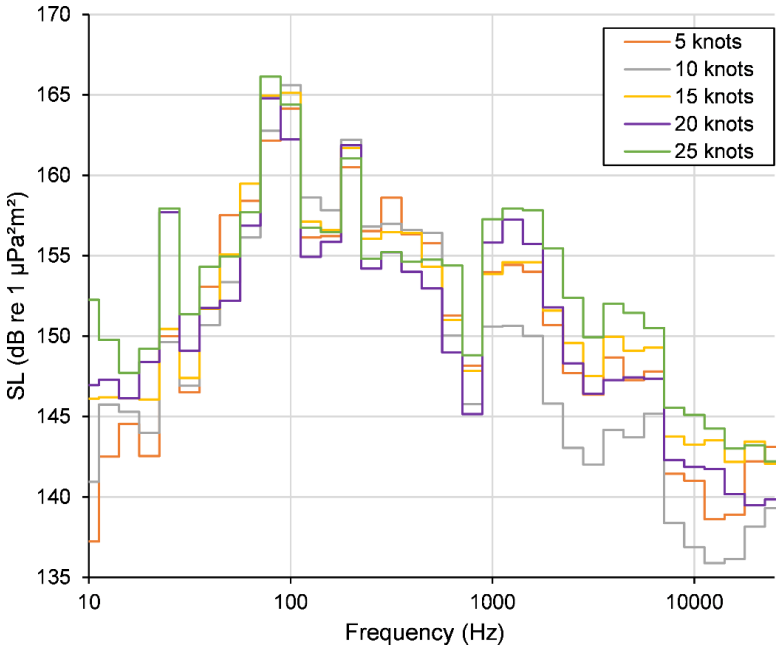

Figure 52. Back-propagated source levels for the turbines based on a point source assumption and 95th percentile received sound levels.

Table 6. Back-propagated broadband source levels for different percentiles.

Wind speed (kn)	Broadband source level (dB re 1 µPa²m²)				
	5th percentile	25th percentile	Median	75th percentile	95th percentile
5	158.9	161.5	165.1	167.2	170.5
10	156.7	160.1	162.5	165.6	170.8
15	159.6	162.0	163.9	166.5	171.4
20	160.4	162.8	164.8	167.2	170.6
25	162.1	164.9	167.2	169.3	172.0

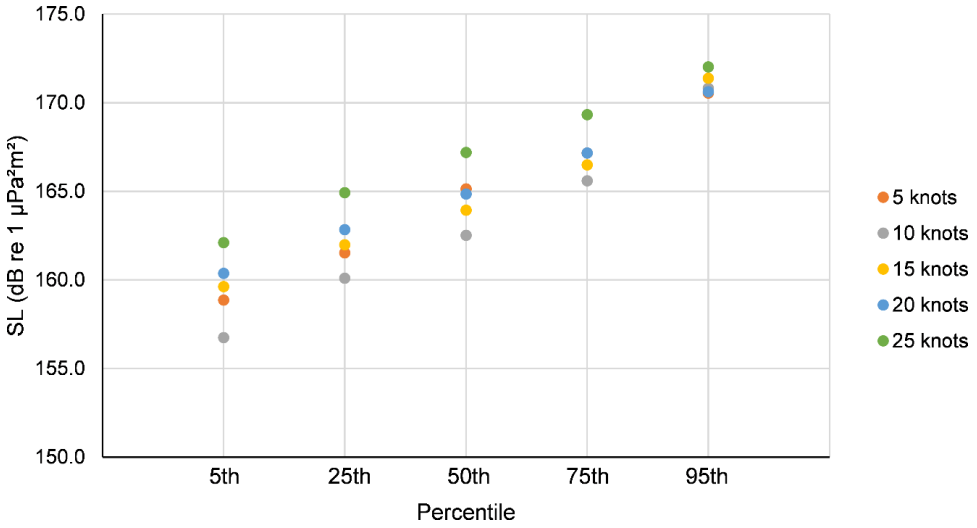

Figure 53. Broadband source levels as function of windspeed for 5th, 25th, 50th, 75th, and 95th percentile ranges.

Table 7. Back-propagated broadband sound exposure source levels for different percentiles.

Wind speed (kn)	Broadband energy source level over 24 h (dB re 1 µPa²m²s)				
	5th percentile	25th percentile	Median	75th percentile	95th percentile
5	208.2	210.9	214.5	216.5	219.9
10	206.1	209.5	211.9	215.0	220.2
15	209.0	211.4	213.3	215.9	220.8
20	209.7	212.2	214.2	216.5	220.0
25	211.5	214.3	216.6	218.7	221.4

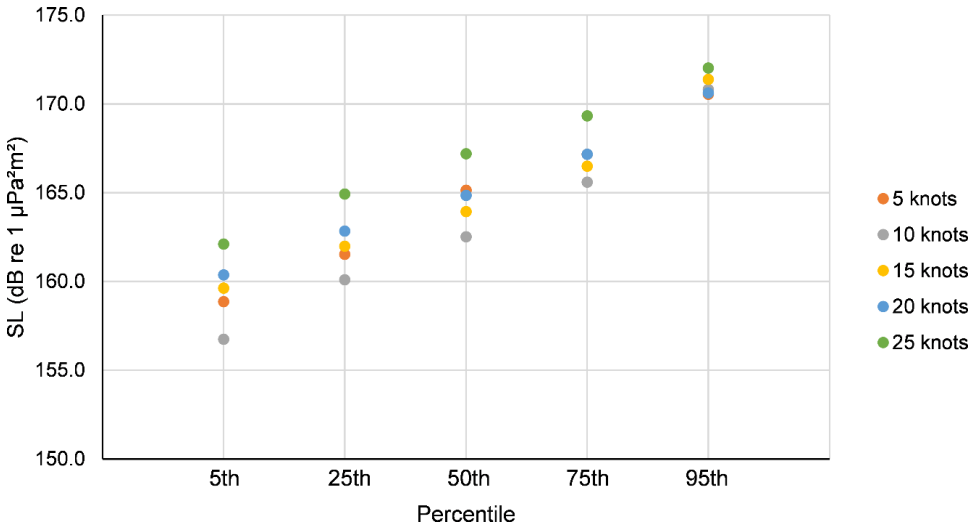

Figure 54. Broadband source levels as function of windspeed for 5th, 25th, 50th, 75th, and 95th percentile ranges.

4.7. Modelled Sound Fields

This section describes a basic sound propagation modelling study, using the generated source levels for the turbines, and the modelled propagation loss to determine the radiated sound fields.

4.7.1. Sound Pressure Level

Modelling was performed in the same way as for the back propagation, except that individual point sources representing all five turbines were modelled over 360° of radial transects to provide a full 3-D sound field. Sound field maps indicate the areas ensonified to certain sound levels. Two examples are shown that represent the SPL for the 10 kn, 50th percentile sound field (Figure 55), and the 25 kn, 95th percentile sound field (Figure 56).

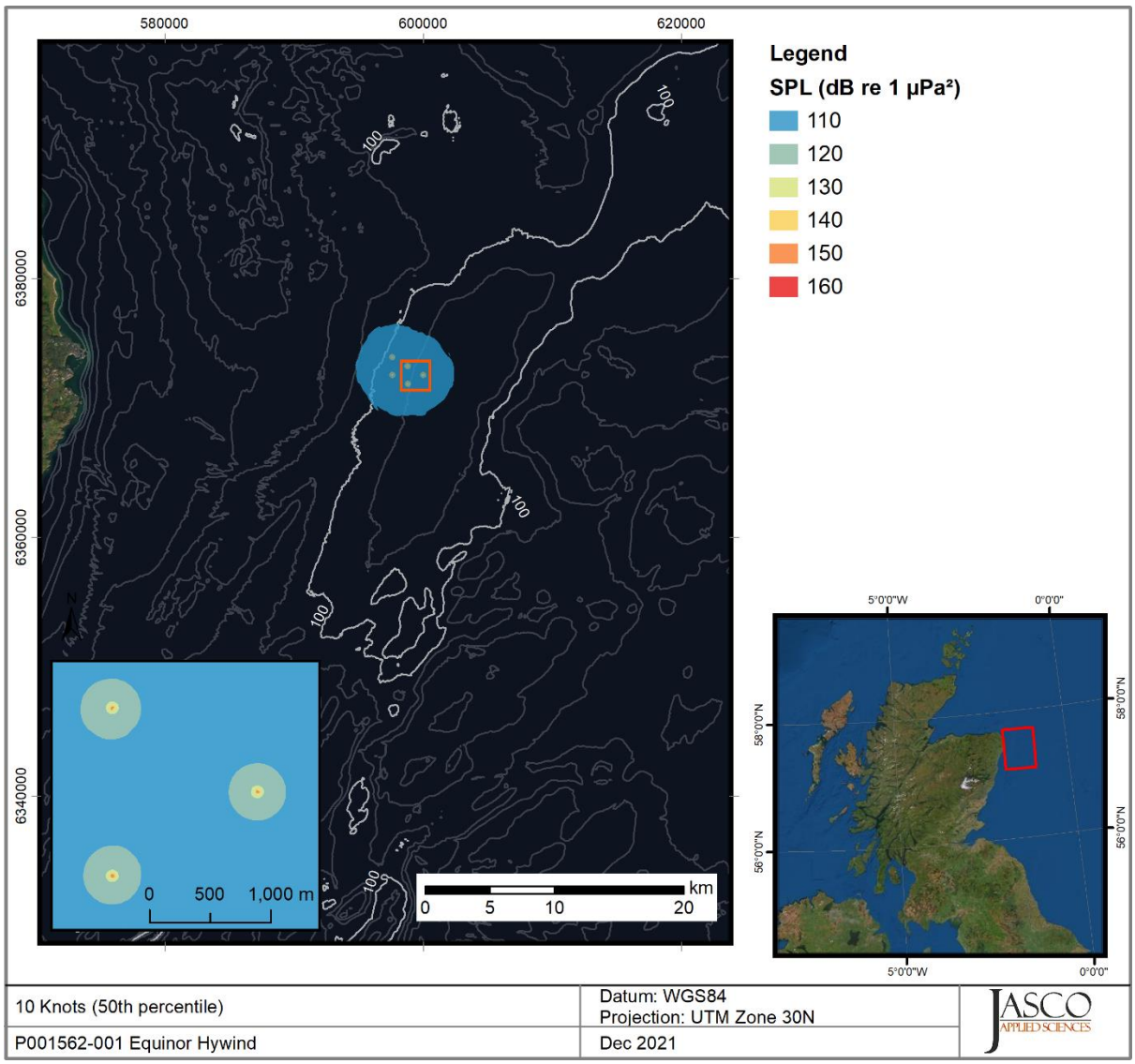

Figure 55. Modelled radiated sound field from the Hywind site presuming the 50th percentile source levels at a wind speed of 10 kn.

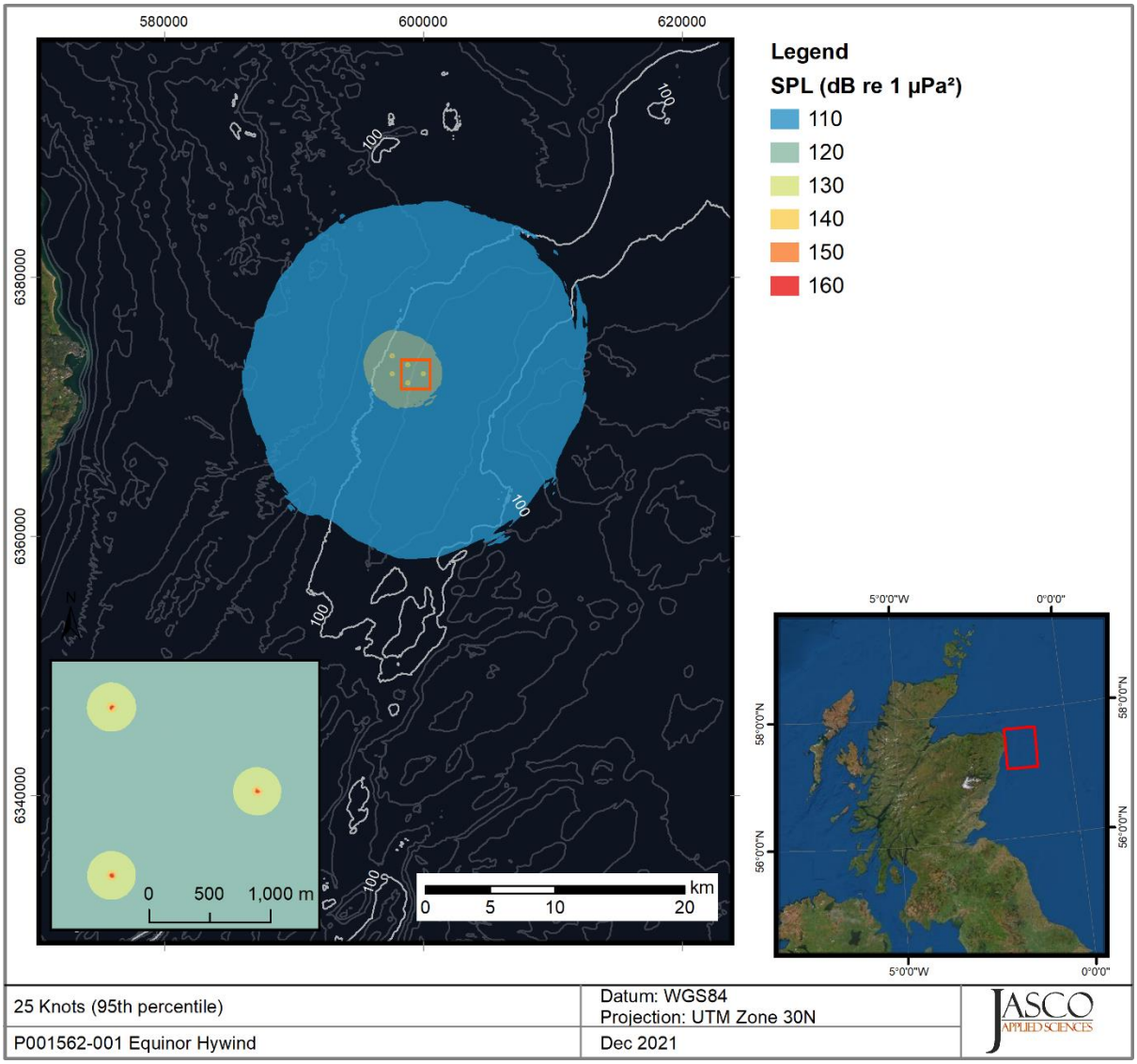

Figure 56. Modelled radiated sound field from the Hywind site presuming the 95th percentile source levels at a wind speed of 25 kn.

4.7.2. Weighted Sound Exposure Levels

Section 3.6 showed the recorded results of daily sound exposure for the considered auditory groups. The modelled outputs allows for an estimate of the predicted levels over the wider area for given conditions as well as the maximum distances to the impact thresholds recommended by Southall et al. (2019). This section provides modelled results pertinent to the frequency-weighted outputs for the cetacean and pinniped auditory groups.

Table 7 in Section 4.6 presented sound exposure source levels over 24 h for a broadband source with no frequency-weighting applied. Table 8 shows sound exposure source levels over 24 h for the 15 kn wind speed case for the different auditory groups. Table 9 shows the modelled weighted received SEL over 24 h for the considered auditory groups, again presuming a constant windspeed of 15 kn, for the median and 75th percentile cases; these values are directly comparable to those shown in Figure 42 for the different auditory groups.

Table 10 shows the maximum modelled distances from the closest turbine to calculated isopleths associated with auditory impacts presuming a 24 h period at 15 kn wind speed, and taking the median and 75th percentile sound levels, (i.e., constant sound level over 24 h).

Table 8. Back-propagated frequency-weighted sound exposure source levels for auditory groups for wind speeds of 15 kn. Auditory group frequency weightings from Southall et al. (2019).

Auditory group	Frequency-weighted energy source level over 24 h for 15 kn (dB re 1 µPa²m²s)				
	5th percentile	25th percentile	Median	75th percentile	95th percentile
Low-frequency cetaceans	204.8	207.1	209.0	211.5	216.4
High-frequency cetaceans	189.8	192.1	193.4	195.1	200.6
Very high-frequency cetaceans	187.7	189.8	191.1	192.7	198.1
Phocid pinnipeds	197.7	199.9	201.7	204.2	209.4
Otariid pinnipeds	197.9	200.1	201.9	204.5	209.6

Table 9. Modelled median and 75th percentile SEL_{24h} presuming 15 kn wind speed. Auditory group frequency weightings from Southall et al. (2019).

Auditory group	Modelled weighted received SEL_{24h} at monitoring site for 15 kn wind	
	50th percentile	75th percentile
Low-frequency cetaceans	157.9	158.3
High-frequency cetaceans	139.5	141.3
Very high-frequency cetaceans	137.2	138.8
Phocid pinnipeds	148.9	150.4
Otariid pinnipeds	148.8	150.5

Table 10. Modelled maximum distances to TTS threshold levels (Southall et al. 2019) for 15 kn wind speed.

Auditory group	TTS onset level (dB re 1 µPa²s)	Maximum distance to weighted SEL_{24h} TTS isopleth (m)	
		50th percentile	75th percentile
Low-frequency cetaceans	179	40	50
High-frequency cetaceans	178	10	20
Very high-frequency cetaceans	153	50	80
Phocid pinnipeds	181	20	30
Otariid pinnipeds	199	<10	<10

The results from Table 9, when compared to those in Figure 42, suggest that the sound levels over 24 h are dominated by the highest levels within the recorded period, i.e., the 75th percentile sound level modelled for 24 h more closely matches the recorded daily sound level than the 50th percentile level. It is also indicative of the variability of the sound level under the same conditions, as observed in Figure 53. When taking an average sound level over an extended period (e.g., 24 h), the average result is skewed towards the higher sound levels.

The maximum distances to the recommended TTS onset sound levels for the different auditory groups in Table 10 represent those for receivers that are stationary for the 24 h period, at the depth at which the sound level is at its greatest. Out of the analysed cases, the maximum distance to the TTS isopleth when considering the 75th percentile is for very high-frequency cetaceans, at a maximum distance of 80 m. Note, that the sound levels have been shown to be highly variable, so the exact distances will vary.

4.8. Source Levels of Tonal Features

The work detailed above investigates the total sound output in decidecade bands to provide the general overall noise levels. This approach involves a necessary reduction in the resolution of the data in terms of frequency and time; consequently, it does not account individually for either the audible tones (Figure 14) due to the smoothing of the data in frequency and the transient sounds from the moorings (Figure 19) due to the smoothing out of the data over time. This section, however, provides further analysis into source levels attributable to the tonal features of the overall signature.

Analysis of the recordings provided PSD levels across the entire deployment period; this indicated the presence of two primary low-frequency tones at ~24 and ~71 Hz. The received PSD levels for these two tones in percentile brackets are shown in Table 11.

Table 11. Received power spectral density levels of the two dominant low-frequency tones.

Frequency (Hz)	Power spectral density level (dB re 1 µPa²/Hz)							
	5%	10%	25%	50%	75%	90%	95%	Mean
24.0	81.6	83.7	90.9	103.2	105.6	106.8	107.4	103.4
71.0	85.1	87.2	93.7	103	107.6	109.1	109.8	105.2

A back-propagation modelling analysis was performed for the two tones, using the same methodology as the previous section, to provide the propagation losses listed in Table 12, but no smoothing was required due to the narrowband nature of the sources. Only one value is provided for the propagation loss as, at these low frequencies, there is no expected variation with wind speed.

Table 12. Propagation losses for the two tones: 24 and 71 Hz.

Frequency (Hz)	Propagation loss (dB re 1 m²)
24.0	47.8
71.0	51.2

Through addition of the modelled propagation losses to the received PSD levels, the source power spectral density levels were derived and are provided in Table 13.

Table 13. Back-propagated source power spectral density levels of the two dominant low-frequency tones.

Frequency (Hz)	Source power spectral density level (dB re 1 µPa²m²/Hz)							
	5%	10%	25%	50%	75%	90%	95%	Mean
24.0	129.4	131.5	138.7	151.0	153.4	154.6	155.2	151.2
71.0	136.3	138.4	144.9	154.2	158.8	160.3	161.0	156.4

5. Discussion and Conclusion

JASCO collected three months of underwater sound data from the Hywind site and a Control site, located approximately 14 km northeast of the wind farm, to investigate the operational noise of the floating wind turbine generators.

Ambient sound levels at both the Hywind and Control site are at or above the expected levels of prevailing noise described by Wenz (1962) across the full recorded spectrum. This is thought to be due to the relatively high level of commercial shipping in the North Sea, the fact that the recordings were made in winter when the sea state is generally elevated. There were occasional episodes where high sound levels in the 20–32 kHz frequency range were recorded at both locations, likely from survey, fish-finder, sub-bottom profilers, or other relatively loud anthropogenic vessel-mounted systems not related to the Hywind project.

The AMAR recording instrument placed within the Hywind site was almost equidistant from three of the turbines, HS-1, HS-2, and HS-4, and positioned specifically to isolate one turbine to the east to allow for uncontaminated directional analysis of a single Hywind system.

The dominant underwater noise of the operating wind turbines is thought to originate predominantly in the mechanical moving parts in the turbine nacelle and is dominated by low-frequency tonal elements (below 1 kHz) and a limited number of harmonics thought to correspond to the rotation rate of the generator. This noise propagates down through the turbine tower structure and into the surrounding water column through the walls of the submerged section of the pillar. Analysis suggests that there may be additional noise sources within the Hywind system that are not directly related to the generator – but this remains speculative.

The dominant noise from the Hywind system is tonal in nature with a set of primary tones around 24 Hz presumably related to rotational RPM. Further tones were evident but appeared unrelated directly to the rotational noise. They are thought to be derived from electrical transformer or other electrical system components and are increasingly important in the overall noise signature as wind speed increases.

The only other significant contributor to the overall noise field from the wind farm was a range of transient sounds that are thought to be associated with the mooring system. There was little evidence of the sharp and highly impulsive ‘snap’ noise that featured in the Hywind demonstration system recordings from 2011, but there was considerably more transient mooring noise that displayed relatively unique characteristics related to individual Hywind systems. HS-1 was found to produce a ‘bang’, HS-2 a ‘creak’, and HS-4 a ‘rattle’. These sounds could be clearly associated with each system through the directional processing of the AMAR array data. Occurrence was positively correlated to wave height and as this increased, the contribution of the transient sounds to the overall wind farm signature increased substantially. Unlike the Hywind Demo system, the Hywind Scotland mooring does not employ a ballast weight on the catenary chains to add tension. This may possibly explain the somewhat less impulsive mooring noises recorded ay Hywind Scotland.

A quantitative analysis of the impulsiveness of the soundscape at Hywind was undertaken using an impulse detector as well as studying the distribution of the per-minute kurtosis. The SEL of each detected impulse was summed, which showed that the impulsive SEL was generally 6 dB below the daily total SEL. The mean duration of the impulses was on the order of 1.5 s, longer than the 1.0 s typically used to identify impulses for the purposes of assessing the effects of sound on hearing. The soundscape at Hywind had a greater kurtosis than at the Control site; however, the kurtosis was not high enough to be considered impulsive. Based on these three measures, it is recommended that the non-impulsive TTS SEL thresholds be applied to the wind farm sounds.

The rate of impulses per hour was more positively correlated with wave height than wind speed. detector. Subjective aural interpretation of these noises suggests a somewhat lower rate of tension release in this mooring design but there is no quantifiable method to assert this. Directional analysis of

mooring noise from HS1, HS2, and HS4 indicates that it originates from mooring components at or very close to the pillar itself. There was no evidence of mooring noise being generated from the mooring system away from the bridle connection points on the Hywind spar. Given that the anchor chains fall through a catenary profile to the seabed and then submerge in the soil for some distance to the anchor, this finding is not wholly unexpected as the most significant movement in the mooring system is likely to be at the connection points of the chains around the pillar. Analysis of wind speed with mooring noise occurrence showed only a limited correlation, but comparison with wave height identified a more direct relationship. This suggests that wave height is the dominant environmental factor influencing movement and associated mooring component friction in the floating structure.

Back propagation of statistically derived received levels allowed for the calculation of a decidecade source levels for a single Hywind system at several different wind speeds. This level represents the combined tonal (turbine) and mooring transients. Unexpectedly, the noise levels in 5 kn of wind were higher than at 10 kn of wind. The cause of this feature in the signature pattern is unknown. The lowest derived broadband source level (5th percentile) was 156.7 dB re 1 μPa^2m^2 and occurred in 10 kn of wind and the highest (95th percentile) was 172.0 dB re 1 μPa^2m^2 in 25 kn of wind.

Analysis of the received levels of the dominant turbine-related tonal noise at 24 Hz and 71 Hz was also carried out and back-propagated to extract source levels, but deeper analysis for specific wind speeds was not carried out. The lowest source power spectral density levels (5th percentile) were 129.4 dB re 1 $\mu Pa^2m^2/Hz$ (24 Hz) and 136.3 dB re 1 $\mu Pa^2m^2/Hz$ (71 Hz) and the highest (95th percentile) were 155.2 dB re 1 $\mu Pa^2m^2/Hz$ (24 Hz) and 161.0 dB re 1 $\mu Pa^2m^2/Hz$ (71 Hz).

The non-impulsive NMFS (2018) thresholds for temporary hearing thresholds shifts were applied to assess the possible effects of Hywind on marine mammals. There was little difference in the daily marine mammal weighted SEL between the two sites, and no exceedances of the TTS threshold occurred. To estimate the cumulative footprint of the entire wind farm, the derived source levels were assigned to a turbine at HS1 system, then forward propagated to determine the sound field. The resulting sound maps indicate a significant difference in the spatial extent of the radiated noise between light winds and strong winds which, as described, is due to rising tonal noise from the turbine combined with a significant increase in mooring noise. However, even at a wind speed of 25 kn, the noise footprint is relatively benign and, in the quite noisy North Sea, does not present any threat of auditory injury to marine species. An estimate of the temporary hearing threshold shift exceedance distance for marine mammals exposed to the turbines was undertaken. It was found that a high-frequency cetacean such as a porpoise, would need to stay within 50 m of a turbine throughout a full 24 h period to accumulate sufficient energy for the onset of TTS (assuming 15 kn winds).

Literature Cited

[ISO] International Organization for Standardization. 2017. *ISO/DIS 18405.2:2017. Underwater acoustics—Terminology*. Geneva. https://www.iso.org/standard/62406.html.

[NIOSH] National Institute for Occupational Safety and Health. 1998. *Criteria for a recommended standard: Occupational noise exposure. Revised Criteria*. Document 98-126. US Department of Health and Human Services, NIOSH, Cincinnati, OH, USA. 122 p. https://www.cdc.gov/niosh/docs/98-126/pdfs/98-126.pdf.

[NMFS] National Marine Fisheries Service (US). 2018. *2018 Revision to: Technical Guidance for Assessing the Effects of Anthropogenic Sound on Marine Mammal Hearing (Version 2.0): Underwater Thresholds for Onset of Permanent and Temporary Threshold Shifts*. US Department of Commerce, NOAA. NOAA Technical Memorandum NMFS-OPR-59. 167 p. https://media.fisheries.noaa.gov/dam-migration/tech_memo_acoustic_guidance_(20)_(pdf)_508.pdf.

[NRC] National Research Council (US). 2003. *Ocean Noise and Marine Mammals*. National Research Council (US), Ocean Studies Board, Committee on Potential Impacts of Ambient Noise in the Ocean on Marine Mammals. The National Academies Press, Washington, DC, USA. https://doi.org/10.17226/10564.

Buckingham, M.J. 2005. Compressional and shear wave properties of marine sediments: Comparisons between theory and data. *Journal of the Acoustical Society of America* 117: 137-152. https://doi.org/10.1121/1.1810231.

Carnes, M.R. 2009. *Description and Evaluation of GDEM-V 3.0*. US Naval Research Laboratory, Stennis Space Center, MS. NRL Memorandum Report 7330-09-9165. 21 p. https://apps.dtic.mil/dtic/tr/fulltext/u2/a494306.pdf.

Collins, M.D. 1993. A split-step Padé solution for the parabolic equation method. *Journal of the Acoustical Society of America* 93(4): 1736-1742. https://doi.org/10.1121/1.406739.

Collins, M.D., R.J. Cederberg, D.B. King, and S. Chin-Bing. 1996. Comparison of algorithms for solving parabolic wave equations. *Journal of the Acoustical Society of America* 100(1): 178-182. https://doi.org/10.1121/1.415921.

Coppens, A.B. 1981. Simple equations for the speed of sound in Neptunian waters. *Journal of the Acoustical Society of America* 69(3): 862-863. https://doi.org/10.1121/1.382038.

EMODnet Bathymetry Consortium. 2020. *EMODnet Digital Bathymetry (DTM)* (webpage). EMODnet Bathymetry Consortium. https://doi.org/10.12770/18ff0d48-b203-4a65-94a9-5fd8b0ec35f6.

Fisher, F.H. and V.P. Simmons. 1977. Sound absorption in sea water. *Journal of the Acoustical Society of America* 62(3): 558-564. https://doi.org/10.1121/1.381574.

Hamilton, E.L. 1980. Geoacoustic modeling of the sea floor. *Journal of the Acoustical Society of America* 68(5): 1313-1340. https://doi.org/10.1121/1.385100.

Harrison, C.H. and J.A. Harrison. 1995. A simple relationship between frequency and range averages for broadband sonar. *Journal of the Acoustical Society of America* 97(2): 1314-1317. https://doi.org/10.1121/1.412172.

Holzer, T.L., M.J. Bennett, T.E. Noce, and J.C. Tinsley. 2005. Shear-Wave Velocity of Surficial Geologic Sediments in Northern California: Statistical Distributions and Depth Dependence. *Earthquake Spectra* 21(1): 161-177. https://doi.org/10.1193/1.1852561.

Kaiser, J.F. 1990. On a simple algorithm to calculate the 'energy' of a signal. *IEEE International Conference on Acoustics, Speech, and Signal Processing*. 3-6 Apr 1990, Albuquerque, NM, USA. pp. 381-384. https://doi.org/10.1109/ICASSP.1990.115702.

Kandia, V. and Y. Stylianou. 2006. Detection of sperm whale clicks based on the Teager-Kaiser energy operator. *Applied Acoustics* 67: 1144-1163. https://doi.org/10.1016/j.apacoust.2006.05.007.

Martin, B., J. MacDonnell, J. Vallarta, E. Lumsden, and R.D.J. Burns. 2011. *Hywind Acoustics Measurements Report. Ambient Levels and Hywind SIgnature. Ver 1.3*. Document 00229. JASCO Applied Sciences (UK) Ltd. https://static1.squarespace.com/static/52aa2773e4b0f29916f46675/t/5fda3a9324291a0a8b1d0a25/1608137377245/Equinor-Hywind-Acoustic-Measurement-Report-JASCO-00229-December-2011.pdf.

Martin, S.B., K. Lucke, and D.R. Barclay. 2020. Techniques for distinguishing between impulsive and non-impulsive sound in the context of regulating sound exposure for marine mammals. *Journal of the Acoustical Society of America* 147(4): 2159-2176. https://doi.org/10.1121/10.0000971.

Merchant, N.D., T.R. Barton, P.M. Thompson, E. Pirotta, D.T. Dakin, and J. Dorocicz. 2013. Spectral probability density as a tool for ambient noise analysis. *Journal of the Acoustical Society of America* 133(4): EL262-EL267. https://doi.org/10.1121/1.4794934.

Porter, M.B. and Y.C. Liu. 1994. Finite-element ray tracing. *In*: Lee, D. and M.H. Schultz (eds.). *International Conference on Theoretical and Computational Acoustics*. Volume 2. World Scientific Publishing Co. pp. 947-956.

Southall, B.L., J.J. Finneran, C.J. Reichmuth, P.E. Nachtigall, D.R. Ketten, A.E. Bowles, W.T. Ellison, D.P. Nowacek, and P.L. Tyack. 2019. Marine Mammal Noise Exposure Criteria: Updated Scientific Recommendations for Residual Hearing Effects. *Aquatic Mammals* 45(2): 125-232. https://doi.org/10.1578/AM.45.2.2019.125.

Teague, W.J., M.J. Carron, and P.J. Hogan. 1990. A comparison between the Generalized Digital Environmental Model and Levitus climatologies. *Journal of Geophysical Research* 95(C5): 7167-7183. https://doi.org/10.1029/JC095iC05p07167.

Thode, A.M., T. Sakai, J. Michalec, S. Rankin, M.S. Soldevilla, B. Martin, and K.H. Kim. 2019. Displaying bioacoustic directional information from sonobuoys using “azigrams”. *Journal of the Acoustical Society of America* 146(1): 95-102. https://doi.org/10.1121/1.5114810.

Urazghildiiev, I.R. and D.E. Hannay. 2017. Maximum likelihood estimators and Cramér–Rao bound for estimating azimuth and elevation angles using compact arrays. *Journal of the Acoustical Society of America* 141(4): 2548-2555. https://doi.org/10.1121/1.4979792.

Wenz, G.M. 1962. Acoustic Ambient Noise in the Ocean: Spectra and Sources. *Journal of the Acoustical Society of America* 34(12): 1936-1956. https://doi.org/10.1121/1.1909155.

Zhang, Z.Y. and C.T. Tindle. 1995. Improved equivalent fluid approximations for a low shear speed ocean bottom. *Journal of the Acoustical Society of America* 98(6): 3391-3396. https://doi.org/10.1121/1.413789.

Zhao, Y.-m., W. Qiu, L. Zeng, S.-s. Chen, X.-r. Cheng, R.I. Davis, and R.P. Hamernik. 2010. Application of the Kurtosis Statistic to the Evaluation of the Risk of Hearing Loss in Workers Exposed to High-Level Complex Noise. *Ear and Hearing* 31(4): 527-532. https://doi.org/10.1097/AUD.0b013e3181d94e68.

Appendix A. Acoustic Data Analysis Methods

A.1. Total Ambient Sound Levels

Underwater sound pressure amplitude is measured in decibels (dB) relative to a fixed reference pressure of p_0 = 1 µPa. Because the perceived loudness of sound, especially impulsive noise such as from seismic airguns, pile driving, and sonar, is not generally proportional to the instantaneous acoustic pressure, several sound level metrics are commonly used to evaluate noise and its effects on marine life. We provide specific definitions of relevant metrics used in this report. Where possible we follow the ANSI and ISO standard definitions and symbols for sound metrics, but these standards are not always consistent.

The zero-to-peak pressure level, or peak pressure level (PK or $L_{p,pk}$; dB re 1 µPa), is the decibel level of the maximum instantaneous sound pressure level in a stated frequency band attained by an acoustic pressure signal, $\mathrm{p(t)}$:

$$\mathrm{PK} = L_{p,\mathrm{pk}} = 10 \log_{10} \frac{\max|p^2(t)|}{p_0^2} \tag{A-3}$$

PK is often included as criterion for assessing whether a sound is potentially injurious; however, because it does not account for the duration of a noise event, it is generally a poor indicator of perceived loudness.

The sound pressure level (SPL or L_p; dB re 1 µPa) is the decibel level of the root-mean-square (rms) pressure in a stated frequency band over a specified time window (T; s) containing the acoustic event of interest. It is important to note that SPL always refers to an rms pressure level and therefore not instantaneous pressure:

$$\mathrm{SPL} = L_p = 10 \log_{10} \left[\frac{1}{T} \int_T p^2(t)\, dt \Big/ p_0^2 \right] \tag{A-4}$$

The SPL represents a nominal effective continuous sound over the duration of an acoustic event, such as the emission of one acoustic pulse, a marine mammal vocalization, the passage of a vessel, or over a fixed duration. Because the window length, T, is the divisor, events with similar sound exposure level (SEL), but more spread out in time have a lower SPL.

The sound exposure level (SEL or L_E, dB re 1 µPa^2 s) is a measure related to the acoustic energy contained in one or more acoustic events (N). The SEL for a single event is computed from the time-integral of the squared pressure over the full event duration (T):

$$\mathrm{SEL} = L_E = 10 \log_{10} \left[\int_T p^2(t)\, dt \Big/ T_0 p_0^2 \right] \tag{A-5}$$

where T_0 is a reference time interval of 1 s. The SEL continues to increase with time when non-zero pressure signals are present. It therefore can be construed as a dose-type measurement, so the integration time used must be carefully considered in terms of relevance for impact to the exposed recipients.

SEL can be calculated over periods with multiple events or over a fixed duration. For a fixed duration, the square pressure is integrated over the duration of interest. For multiple events, the SEL can be computed by summing (in linear units) the SEL of the N individual events:

$$L_{E,N} = 10\log_{10}\sum_{i=1}^{N} 10^{\frac{L_{E,i}}{10}} \quad \text{(A-6)}$$

To compute the SPL(T_{90}) and SEL of acoustic events in the presence of high levels of background noise, equations A-3 and A-4 are modified to subtract the background noise contribution:

$$\mathrm{SPL}(T_{90}) = L_{p90} = 10\log_{10}\left[\frac{1}{T_{90}}\int_{T_{90}}\left(p^2(t) - \overline{n^2}\right)dt \Big/ p_0^2\right] \quad \text{(A-7)}$$

$$L_E = 10\log_{10}\left[\int_{T}\left(p^2(t) - \overline{n^2}\right)dt \Big/ T_0 p_0^2\right] \quad \text{(A-8)}$$

where $\overline{n^2}$ is the mean square pressure of the background noise, generally computed by averaging the squared pressure of a temporally-proximal segment of the acoustic recording during which acoustic events are absent (e.g., between pulses).

Because the SPL(T_{90}) and SEL are both computed from the integral of square pressure, these metrics are related numerically by the following expression, which depends only on the duration of the time window T:

$$L_p = L_E - 10\log_{10}(T) \quad \text{(A-9)}$$

$$L_{p90} = L_E - 10\log_{10}(T_{90}) - 0.458 \quad \text{(A-10)}$$

where the 0.458 dB factor accounts for the 10% of SEL missing from the SPL(T_{90}) integration time window.

Energy equivalent SPL (dB re 1 µPa) denotes the SPL of a stationary (constant amplitude) sound that generates the same SEL as the signal being examined, $\mathrm{p(t)}$, over the same period of time, T:

$$L_{\mathrm{eq}} = 10\log_{10}\left[\frac{1}{T}\int_{T} p^2(t)\,dt \Big/ p_0^2\right] \quad \text{(A–11)}$$

The equations for SPL and the energy-equivalent SPL are numerically identical; conceptually, the difference between the two metrics is that the former is typically computed over short periods (typically of 1 s or less) and tracks the fluctuations of a non-steady acoustic signal, whereas the latter reflects the average SPL of an acoustic signal over times typically of 1 min to several hours.

A.2. Decidecade Band Analysis

The distribution of a sound's power with frequency is described by the sound's spectrum. The sound spectrum can be split into a series of adjacent frequency bands. Splitting a spectrum into 1 Hz wide bands, called passbands, yields the power spectral density of the sound. These values directly compare to the Wenz curves, which represent typical deep ocean sound levels (Figure 13) (Wenz 1962). This splitting of the spectrum into passbands of a constant width of 1 Hz, however, does not represent how animals perceive sound.

Because animals perceive exponential increases in frequency rather than linear increases, analysing a sound spectrum with passbands that increase exponentially in size better approximates real-world scenarios. In underwater acoustics, a spectrum is commonly split into decidecade bands, which are one tenth of a decade wide. A decidecade is sometimes referred to as a "1/3-octave" because one tenth of a decade is approximately equal to one third of an octave. Each decade represents a factor

10 in sound frequency. Each octave represents a factor 2 in sound frequency. The centre frequency of the *i*th band, $f_c(I)$, is defined as:

$$f_c(i) = 10^{\frac{i}{10}} \text{ kHz} \tag{A-1}$$

and the low (f_{lo}) and high (f_{hi}) frequency limits of the *i*th decade band are defined as:

$$f_{lo,i} = 10^{\frac{-1}{20}} f_c(i) \text{ and } f_{hi,i} = 10^{\frac{1}{20}} f_c(i) \tag{A-2}$$

The decidecade bands become wider with increasing frequency, and on a logarithmic scale the bands appear equally spaced (Figure A-1).

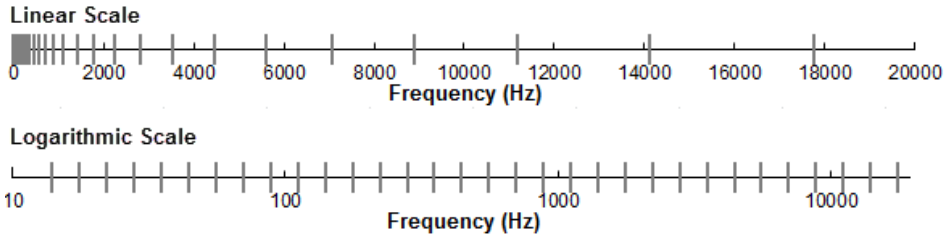

Figure A-1. Decidecade frequency bands (vertical lines) shown on a linear frequency scale and a logarithmic scale.

The sound pressure level in the *i*th band ($L_{p,i}$) is computed from the spectrum $S(f)$ between $f_{lo,I}$ and $f_{hi,i}$:

$$L_{p,i} = 10 \log_{10} \int_{f_{lo,i}}^{f_{hi,i}} S(f)\, df \text{ dB}, \tag{A-3}$$

summing the sound pressure level of all the bands yields the broadband sound pressure level:

$$\text{Broadband SPL} = 10 \log_{10} \sum_i 10^{\frac{L_{p,i}}{10}} \text{ dB}. \tag{A-4}$$

Figure A-2 shows an example of how the decidecade band sound pressure levels compare to the sound pressure spectral density levels of an ambient sound signal. Because the decidecade bands are wider than 1 Hz, the decidecade band SPL is higher than the spectral levels at higher frequencies. Decidecade band analysis is applied to continuous and impulsive noise sources. For impulsive sources, the decidecade band SEL is typically reported.

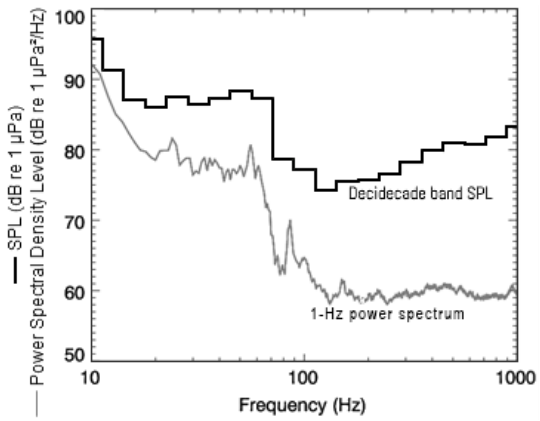

Figure A-2. Sound pressure spectral density levels and the corresponding decidecade band sound pressure levels of example ambient sound shown on a logarithmic frequency scale. Because the decidecade bands are wider with increasing frequency, the 1/3-octave-band SPL is higher than the power spectrum.

Table A-1. Decidecade-band frequencies (Hz).

Band	Lower frequency	Nominal centre frequency	Upper frequency
10	8.9	10.0	11.2
11	11.2	12.6	14.1
12	14.1	15.8	17.8
13	17.8	20.0	22.4
14	22.4	25.1	28.2
15	28.2	31.6	35.5
16	35.5	39.8	44.7
17	44.7	50.1	56.2
18	56.2	63.1	70.8
19	70.8	79.4	89.1
20	89.1	100.0	112.2
21	112	126	141
22	141	158	178
23	178	200	224
24	224	251	282
25	282	316	355
26	355	398	447
27	447	501	562
28	562	631	708
29	708	794	891
30	891	1000	1122
31	1122	1259	1413
32	1413	1585	1778
33	1778	1995	2239
34	2239	2512	2818
35	2818	3162	3548
36	3548	3981	4467
37	4467	5012	5623
38	5623	6310	7079
39	7079	7943	8913
40	8913	10000	11220
41	11220	12589	14125

Table A-2. Decade-band frequencies (Hz).

Decade band	Lower frequency	Nominal centre frequency	Upper frequency
1	8.9	50	89.1
2	89.1	500	891
3	891	5,000	8913
4	8913	50,000	N/A – above Nyquist

Appendix B. Ambient Noise Analysis Results

B.1. Data from the Remaining C-Lander Hydrophones

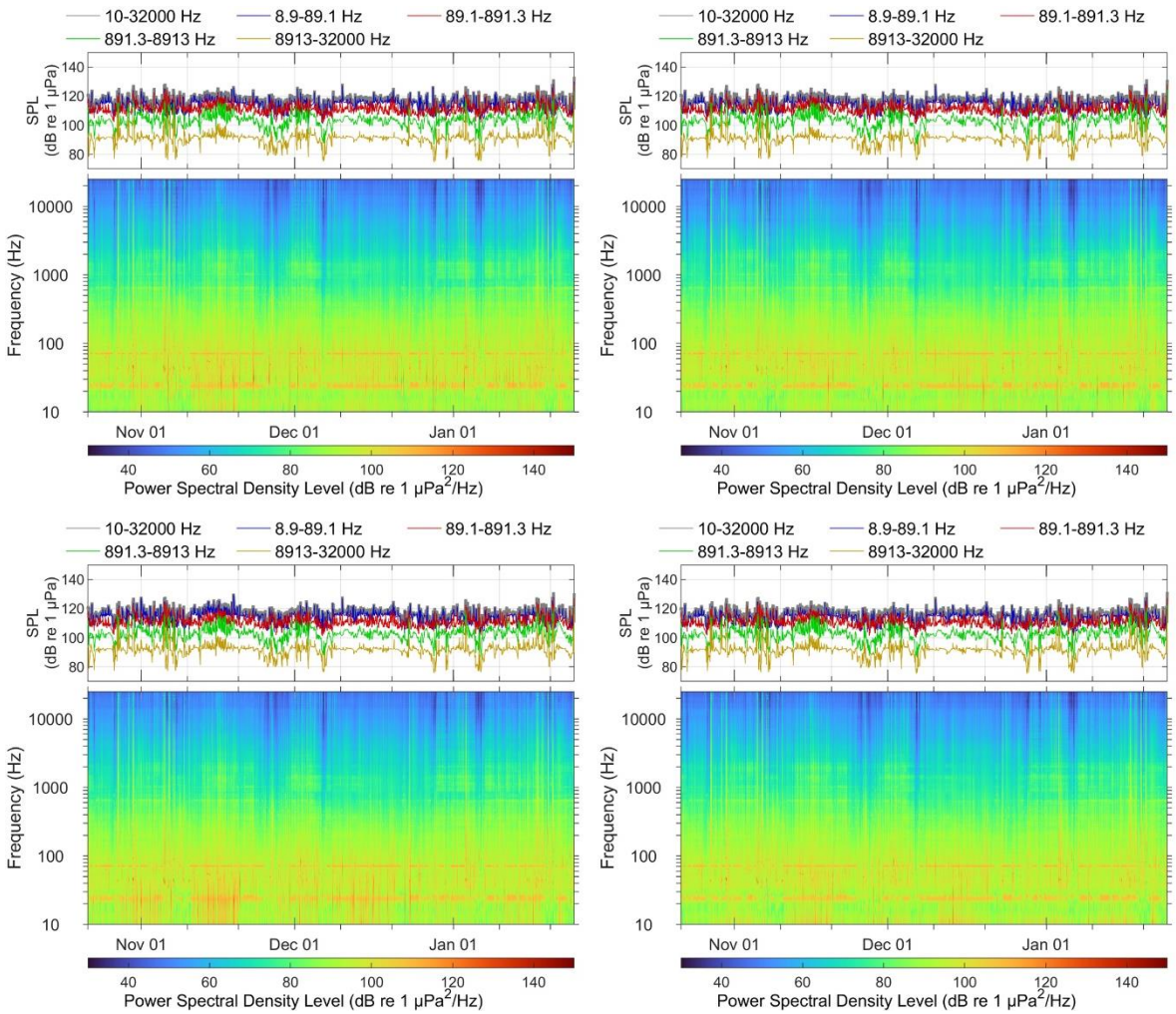

Figure B-1. Acoustic summary of the Hywind recorder for channels 0 (upper left), 1 (upper right), 2 (bottom left), and 3 (bottom right).

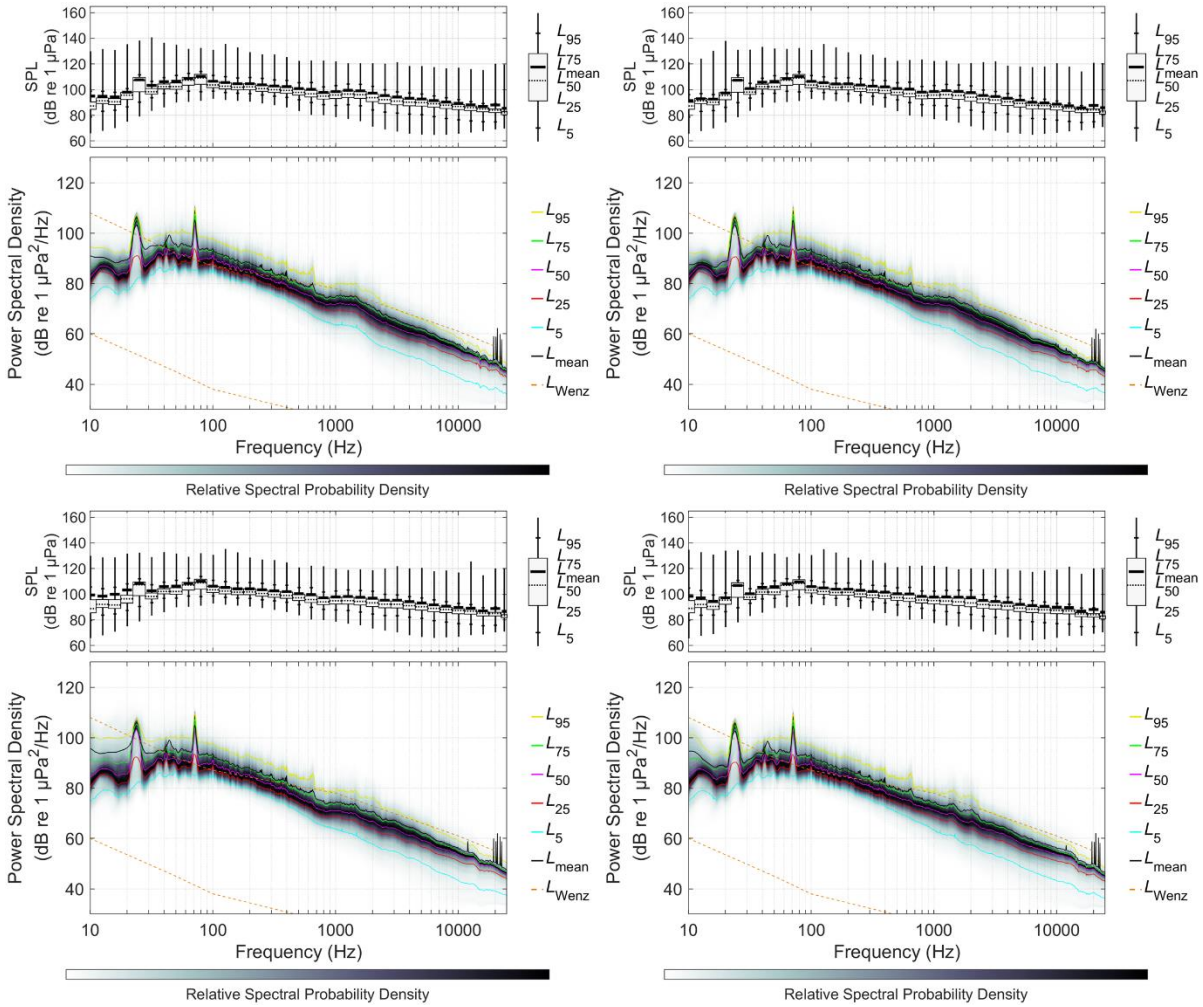

Figure B-2. Decidecade band SPL and power spectral densities with percentiles for the Hywind recorder for channels 0 (upper left), 1 (upper right), 2 (bottom left), and 3 (bottom right).

B.2. High-frequency Transient Signals

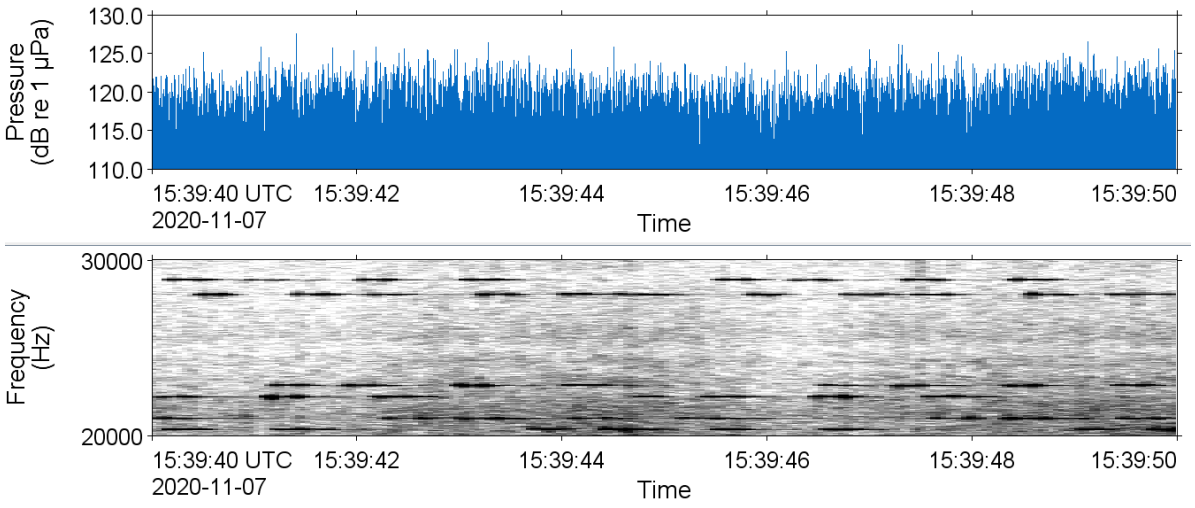

Figure B-3. Example of high-frequency transients above 20 kHz at Hywind station.

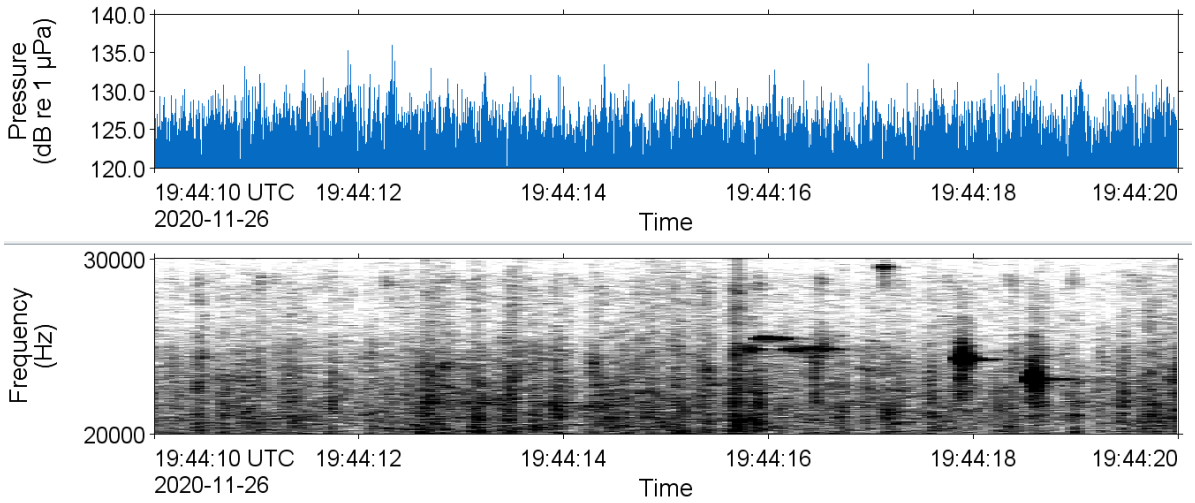

Figure B-4. Example of high-frequency transients above 20 kHz at the Control station.

Appendix C. Directional Analysis

C.1.1. Orthogonal Arrays of Omnidirectional Hydrophones

In acoustics, the particle velocity, u, and the acoustic pressure, p, are related by the linearized Euler's equation:

$$\rho_{0(\partial \mathrm{u}/\partial \mathrm{t})} = -\nabla p \,. \tag{C-1}$$

Here, ρ is the density of the medium, and ∇ is the spatial gradient function. The time derivative of velocity is acceleration. Therefore, the spatial gradient of pressure divided by the fluid density, yields the acceleration, which is the same quantity measured by M20-601 accelerometers. The spatial gradient of pressure is the difference between two closely spaced hydrophones. This operation only works for frequencies where the phase difference between the hydrophones is at most λ/4. For larger differences, the phase difference is not unique, and the results are ambiguous. For the array deployed near the Hywind turbines, the nominal hydrophone spacing was 0.5 m (Table C-1), and therefore the cut-off frequency at the speed of sound ~1450 Hz.

The relative locations of the hydrophones are essential for accurately analysing the direction of arrival. During deployment preparations the distances between the tips of each hydrophone pair were measured. These distances, along with the nominal hydrophone locations, were then used in a least-squares regression to find the precise hydrophone locations relative to the reference hydrophone. For simplicity and power savings, the landers with arrays of omnidirectional hydrophones did not include a compass sensor. Orientation of the arrays was determined by matching received tonals to known turbine bearings.

These arrays are formed from standard omni-directional hydrophones. The hydrophones are calibrated through normal processes before deployment and on retrieval, which provides assurance of system operations.

Table C-1. Locations (in meters) of the Hywind hydrophones. Hydrophone Channel 4 is the top hydrophone.

Location	AMAR Channel 1	AMAR Channel 2	AMAR Channel 3	AMAR Channel 4
X	0.481	0	0	0
Y	0	0	0.4820	0
Z	-0.5950	-0.5950	-0.5950	0

C.1.2. Determining the Direction of Arrival

The direction of arrival for the hydrophone arrays depends on the frequencies of interest. For frequencies below the 1450 Hz cut-off, analysis is performed by forming equally spaced beams in azimuth and elevation, then selecting the beam with the highest received signal level for each frequency and time. This method provides the Cramer-Rao lower bound estimate on the direction of arrival for a compact array (Urazghildiiev and Hannay 2017). This method does not rely on having a particular geometry for the compact array; the relative positions of each sensor must be known. A radial resolution of 10 degrees (36 beams) was employed. Vertical beams are important if the azimuthal direction for sources within ~3 water depths is desired.

For frequencies above the 1450 Hz cut-off, broadband direction of arrivals become ambiguous when applying a beamformer. Instead, the time delay of arrival of a transient signal on each of the hydrophones may be used to determine the direction.

C.1.3. Visualizing the Direction of Arrival of Broadband Data

Spectrograms that use an intensity gradient (e.g., grayscale) or a colour gradient (e.g., colour map) to communicate the differences in received sound levels as a function of frequency and time (Figure 10). However, it is also possible to use colour to represent direction. If intensity is not included in the mapping, then the result is an azigram (Thode et al. 2019). However, by including intensity the background noise is reduced, which improves a user's understanding of the data (e.g., Figure 14), which is referred to as a 'directogram'. This type of representation has also been used in airborne and naval sonar systems for several decades. The colour-direction-intensity was implemented using the HSV colour map for direction since it 'rotates' from red-to-red, and the 'alpha' channel used to encode intensity.

Appendix D. Hydrophone Technical Specifications

GeoSpectrum Technologies Inc.
Customizing Detection

M36-100

The M36-100 is a wide-band omni-directional hydrophone designed for marine observation. It comes with a pre-amplified output of 0 to 35 dB (selectable on order) with current or voltage signalling.

Characteristics	
Nominal Voltage Sensitivity (without preamp)	-200 dBV re 1 µPa @ 20°C
Size	7.8" length, 1.3" max OD
Depth Rating	2500 m
Storage and Operating Temperatures	-40 to +70°C
Acceleration Sensitivity	<1.5 mbar/g, in air, any axis
Labelling	Calibration parameters, serial number, date
Connector	MCBH-8M
Pre-Amplifier	
Preamp signalling	Current, single ended voltage or, differential voltage (selectable on order)
Gain	0 – 35 dB (selectable on order)
Input Voltage	6.8 VDC nominal 4.5 – 30 VDC operating range
Band Pass	5 Hz HPF, no LPF installed (unless otherwise specified)
IRN	<140 nV/√Hz @10 Hz <4 nV/√Hz @1 kHz
Current Draw	1.3 mA (at 6.8 VDC) 4.2 mA with current signalling preamp

ADDRESS:
10 Akerley Blvd., Unit 19
Dartmouth, NS
Canada B3B 1J4

Phone: 902.406.4111
Fax: 902.435.8987
website: www.geospectrum.ca
e-mail: sales@geospectrum.ca

M36-100-07-18-v4

GeoSpectrum Technologies Inc.
Customizing Detection

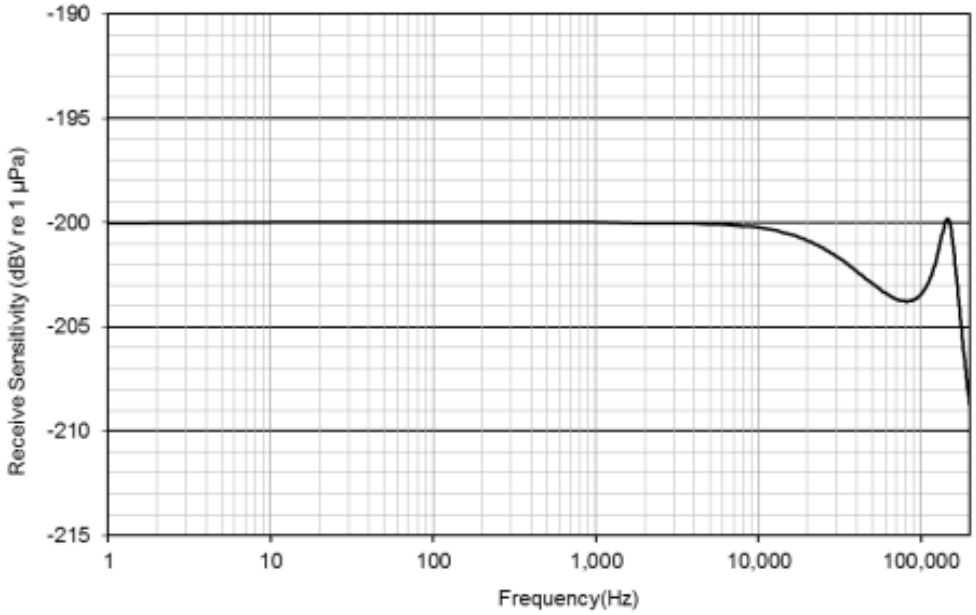

M36 Frequency Response (without preamp)

Appendix E. Back-propagated Source Levels and Energy Source Levels

E.1. Back-propagated Source Levels

This section presents back-propagated source levels (SL) in dB re 1 µPa²m² for the studied percentiles and wind speeds based on the analyses in Section 4.

Table E-1. Back-propagated decidecade-band source levels (SL; dB re 1 µPa²m²) for the turbine during periods of 5 kn windspeed.

Decidecade band centre frequency (Hz)	Percentile				
	5th	25th	50th	75th	95th
10.00	130.5	134.2	135.4	136.6	137.2
12.59	133.0	135.5	141.3	141.7	142.5
15.85	137.5	138.6	139.3	140.4	144.5
19.95	137.5	139.8	140.7	141.3	142.5
25.12	139.8	141.7	142.6	149.6	150.0
31.62	140.2	142.7	143.3	146.1	146.5
39.81	139.9	145.1	145.8	148.5	153.1
50.12	143.9	144.9	147.7	153.2	157.5
63.10	144.4	148.7	150.8	152.9	158.4
79.43	151.0	154.1	159.0	159.5	162.2
100.0	153.9	155.0	159.8	162.4	164.1
125.9	146.4	148.2	150.5	153.5	156.1
158.5	146.4	149.4	151.7	152.8	156.2
199.5	149.8	153.6	156.1	156.8	160.5
251.2	143.5	147.8	148.9	150.1	156.5
316.2	144.0	148.4	149.0	152.7	158.6
398.1	142.1	145.5	147.5	150.6	156.3
501.2	141.7	145.2	147.0	151.1	155.8
631.0	137.2	141.7	144.2	147.2	151.3
794.3	134.8	139.3	140.7	144.6	148.2
1000	138.6	140.7	147.3	149.8	154.0
1259	139.3	140.6	147.1	149.6	154.4
1585	138.6	140.2	147.5	149.2	154.0
1995	133.1	136.8	144.2	145.4	150.7
2512	130.2	132.9	141.0	142.8	147.7
3162	128.8	131.3	138.2	141.6	146.4
3981	130.7	133.6	140.0	143.2	148.7
5012	129.2	132.6	137.9	141.3	147.3
6310	128.2	133.2	138.6	141.9	147.8
7943	120.6	127.0	133.6	136.4	141.4
10000	119.4	125.5	133.9	136.7	141.0
12589	117.8	123.1	132.5	134.8	138.6
15849	120.7	125.5	134.3	136.1	138.9
19953	120.7	125.0	133.3	136.2	142.2
25119	124.2	127.7	134.7	138.3	143.1

Table E-2. Back-propagated decidecade-band source levels (SL; dB re 1 μPa²m²) for the turbine during periods of 10 kn windspeed.

Decidecade band centre frequency (Hz)	Percentile				
	5th	25th	50th	75th	95th
10.00	130.6	134.1	136.3	138.2	140.9
12.59	135.2	138.5	140.8	144.2	145.8
15.85	133.1	135.3	138.7	141.7	145.3
19.95	134.9	137.9	139.6	142.0	144.0
25.12	137.6	141.5	142.8	144.1	149.6
31.62	138.5	141.7	144.0	145.0	146.9
39.81	141.1	144.1	146.0	147.8	150.7
50.12	141.4	143.7	146.2	149.5	153.4
63.10	144.7	146.6	149.6	152.5	156.1
79.43	148.8	152.9	155.0	158.6	162.8
100.0	151.8	155.4	157.3	160.7	165.6
125.9	143.9	147.6	149.9	151.8	158.6
158.5	143.8	146.4	149.2	152.5	157.8
199.5	147.5	150.1	153.2	156.1	162.2
251.2	141.1	144.1	146.9	150.0	156.8
316.2	141.3	144.3	147.2	149.6	157.0
398.1	138.5	142.5	145.5	149.4	156.6
501.2	138.0	142.2	145.7	147.0	156.4
631.0	133.5	137.3	140.7	143.8	150.0
794.3	131.1	135.7	138.3	139.6	145.8
1000	136.6	139.8	143.2	145.6	150.6
1259	136.3	139.7	143.5	146.8	150.6
1585	135.7	139.3	142.5	145.7	150.0
1995	131.5	135.2	138.3	141.4	145.8
2512	128.8	132.0	135.1	138.2	143.1
3162	126.6	129.8	133.0	135.9	142.0
3981	128.9	132.2	135.4	138.6	144.2
5012	129.2	132.5	135.7	138.7	143.7
6310	131.0	133.8	137.7	140.0	145.2
7943	124.8	126.7	131.6	133.5	138.4
10000	124.7	126.3	131.3	132.9	136.9
12589	124.5	126.4	130.0	132.9	135.9
15849	124.4	126.8	129.3	132.6	136.2
19953	124.0	126.5	128.9	131.9	138.2
25119	126.9	128.9	130.8	133.8	139.3

Table E-3. Back-propagated decidecade-band source levels (SL; dB re 1 µPa²m²) for the turbine during periods of 15 kn windspeed.

Decidecade band centre frequency (Hz)	Percentile				
	5th	25th	50th	75th	95th
10.00	131.3	133.6	135.6	138.0	146.1
12.59	135.9	138.9	140.4	143.3	146.2
15.85	136.4	139.3	141.3	144.1	146.1
19.95	138.4	141.5	143.5	144.8	146.1
25.12	136.5	139.5	142.3	146.4	150.4
31.62	140.8	142.8	143.5	145.2	147.4
39.81	144.5	146.3	147.9	149.5	151.7
50.12	144.0	145.7	147.6	150.3	155.1
63.10	147.6	149.4	151.1	153.5	159.5
79.43	150.6	153.7	156.7	159.8	165.0
100.0	153.7	156.0	157.6	160.3	165.1
125.9	145.5	148.8	150.2	153.1	157.1
158.5	146.2	149.0	150.6	152.3	156.6
199.5	150.8	153.0	154.8	156.3	161.7
251.2	145.2	146.9	148.2	150.8	156.1
316.2	145.1	147.1	149.1	151.5	156.5
398.1	143.3	145.9	148.3	151.0	156.4
501.2	143.5	145.3	147.6	150.7	154.3
631.0	139.3	141.5	142.9	146.6	151.0
794.3	136.9	139.1	140.2	143.3	147.8
1000	142.7	144.3	146.3	150.0	153.9
1259	142.8	144.3	146.8	150.1	154.6
1585	143.2	144.9	147.3	150.1	154.6
1995	139.3	142.2	143.9	146.6	151.6
2512	136.4	139.5	141.1	144.5	149.6
3162	135.0	137.8	139.0	141.1	147.5
3981	137.9	140.0	141.4	143.0	150.0
5012	137.6	139.6	141.3	143.2	149.1
6310	138.1	140.7	142.2	143.9	149.3
7943	132.4	135.0	136.4	138.1	143.8
10000	132.6	135.1	136.3	137.8	143.3
12589	132.5	134.9	136.3	137.8	143.5
15849	132.3	134.5	135.7	137.2	142.2
19953	131.8	133.9	135.3	136.9	143.4
25119	133.7	135.4	136.7	138.1	142.1

Table E-4. Back-propagated decidecade-band source levels (SL; dB re 1 µPa²m²) for the turbine during periods of 20 kn windspeed.

Decidecade band centre frequency (Hz)	Percentile				
	5th	25th	50th	75th	95th
10.00	134.6	137.1	139.0	140.7	147.0
12.59	139.4	141.3	143.1	144.3	147.3
15.85	138.4	140.7	142.2	143.7	146.1
19.95	138.1	141.5	143.1	145.4	148.4
25.12	140.9	144.0	147.7	152.5	157.7
31.62	141.1	142.3	143.9	146.9	149.1
39.81	144.3	147.3	148.8	150.4	151.8
50.12	143.7	145.3	147.2	150.1	152.2
63.10	148.5	150.0	152.1	153.8	156.9
79.43	152.4	156.5	158.4	160.9	164.8
100.0	153.8	155.9	157.9	160.0	162.2
125.9	146.0	148.2	150.0	153.0	154.9
158.5	146.1	148.0	149.6	152.6	155.9
199.5	150.1	152.1	155.0	157.1	161.9
251.2	144.0	146.0	147.7	151.3	154.2
316.2	144.9	147.0	148.8	151.2	155.2
398.1	143.9	146.2	148.2	149.8	154.0
501.2	143.7	145.3	147.8	149.0	153.0
631.0	139.3	141.9	144.1	145.7	149.0
794.3	137.6	139.8	141.0	142.4	145.2
1000	145.5	147.9	149.9	152.1	155.8
1259	145.8	148.3	150.2	153.2	157.3
1585	145.7	147.7	149.7	152.2	155.7
1995	142.5	144.2	146.9	148.3	151.8
2512	140.1	141.8	144.0	145.5	148.3
3162	138.1	140.2	141.8	143.2	146.4
3981	140.1	142.9	143.9	145.4	147.3
5012	140.5	142.8	143.9	145.5	147.4
6310	141.2	142.5	144.4	145.8	147.3
7943	135.9	137.5	139.1	140.4	142.3
10000	135.6	137.5	138.9	139.8	141.9
12589	136.1	137.1	138.7	139.7	141.7
15849	135.1	136.3	137.6	138.5	140.2
19953	134.5	135.7	136.7	137.7	139.5
25119	136.0	137.0	137.8	138.7	139.8

Table E-5. Back-propagated decidecade-band source levels (SL; dB re 1 µPa²m²) for the turbine during periods of 25 kn windspeed.

Decidecade band centre frequency (Hz)	Percentile				
	5th	25th	50th	75th	95th
10.00	136.7	138.6	139.7	142.1	152.3
12.59	142.1	143.4	144.3	145.3	149.8
15.85	141.1	142.2	143.4	144.3	147.7
19.95	141.0	143.9	145.9	147.2	149.2
25.12	144.9	151.7	154.9	156.5	157.9
31.62	141.9	143.2	144.2	146.9	151.4
39.81	145.9	147.4	148.3	149.5	154.3
50.12	145.9	147.1	148.4	150.7	155.0
63.10	150.2	152.3	155.0	156.4	157.7
79.43	156.2	160.4	163.1	165.2	166.1
100.0	155.6	156.6	158.1	160.5	164.4
125.9	147.4	148.9	151.2	152.6	156.7
158.5	147.0	148.6	150.4	152.2	156.5
199.5	150.1	153.2	155.5	157.1	161.1
251.2	144.2	147.2	149.5	152.1	154.8
316.2	144.5	147.6	149.6	152.8	155.2
398.1	143.6	146.3	148.7	151.1	154.6
501.2	144.5	146.5	148.9	151.2	154.8
631.0	141.0	143.1	145.5	147.3	154.4
794.3	139.4	140.8	142.7	144.1	148.8
1000	146.1	149.0	150.9	154.6	157.3
1259	146.3	149.5	151.3	155.0	157.9
1585	146.4	149.0	151.0	154.2	157.8
1995	143.3	145.9	148.6	151.1	155.5
2512	140.9	143.5	145.2	148.2	152.4
3162	139.5	142.3	144.0	146.1	149.9
3981	141.8	144.5	145.8	147.3	152.0
5012	141.9	144.4	146.1	147.3	151.5
6310	141.1	143.9	145.3	146.8	150.5
7943	136.9	139.1	140.2	142.0	145.6
10000	136.6	138.5	140.0	141.6	145.1
12589	136.5	138.3	139.4	141.0	144.3
15849	135.7	137.4	138.6	139.7	143.0
19953	135.0	136.7	137.6	138.9	143.2
25119	136.4	137.9	138.5	139.6	142.2

E.2. Back-propagated Sound Exposure Source Levels

This section provides simulated sound exposure source levels (ESL; dB re 1 µPa²m²s) over 24 h of the turbine at different wind speeds. The values are not calculated from the raw recorded SEL taken over 24 h but are based on the SL results from Appendix E.1 (i.e., presuming a statistically stable source) and scaled up to provide a 24 h ESL for each of the percentiles presented.

The conversion from SL to ESL over 24 h is calculated using the following equation (where t_0 is 1 s):

$$L_{S,E,24\text{h}} = L_S + 10\log_{10}((24 \times 60 \times 60)/t_0)$$
$$L_{S,E,24\text{h}} = L_S + 49.37\,. \quad \text{(E-1)}$$

Table E-6. Simulated back-propagated decidecade-band 24 h sound exposure source levels (ESL; dB re 1 µPa²m²s) for the turbine during periods of 5 kn windspeed.

Decidecade band centre frequency (Hz)	Percentile				
	5th	25th	50th	75th	95th
10.00	179.9	183.5	184.8	186.0	186.6
12.59	182.4	184.9	190.6	191.1	191.9
15.85	186.9	188.0	188.7	189.8	193.9
19.95	186.9	189.1	190.0	190.7	191.9
25.12	189.2	191.1	192.0	198.9	199.4
31.62	189.6	192.1	192.6	195.5	195.9
39.81	189.3	194.4	195.2	197.8	202.4
50.12	193.3	194.3	197.1	202.6	206.9
63.10	193.7	198.0	200.2	202.3	207.8
79.43	200.4	203.4	208.3	208.8	211.5
100.0	203.3	204.4	209.2	211.8	213.5
125.9	195.7	197.5	199.8	202.8	205.5
158.5	195.8	198.8	201.0	202.2	205.6
199.5	199.2	203.0	205.5	206.1	209.9
251.2	192.9	197.2	198.2	199.5	205.9
316.2	193.4	197.8	198.4	202.1	208.0
398.1	191.5	194.9	196.9	199.9	205.7
501.2	191.1	194.6	196.3	200.5	205.2
631.0	186.6	191.0	193.6	196.6	200.7
794.3	184.1	188.7	190.1	193.9	197.5
1000	188.0	190.1	196.7	199.2	203.3
1259	188.7	189.9	196.4	199.0	203.8
1585	187.9	189.6	196.9	198.6	203.4
1995	182.4	186.2	193.6	194.8	200.1
2512	179.6	182.3	190.4	192.2	197.1
3162	178.2	180.7	187.5	191.0	195.7
3981	180.0	183.0	189.3	192.5	198.0
5012	178.6	182.0	187.3	190.7	196.6
6310	177.5	182.5	188.0	191.3	197.2
7943	169.9	176.3	183.0	185.7	190.8
10000	168.7	174.9	183.3	186.0	190.4
12589	167.2	172.4	181.9	184.1	188.0
15849	170.1	174.9	183.7	185.5	188.3
19953	170.1	174.4	182.6	185.6	191.6
25119	173.6	177.0	184.1	187.7	192.5

Table E-7. Simulated back-propagated decidecade-band 24 h sound exposure source levels (ESL; dB re 1 µPa²m²s) for the turbine during periods of 10 kn windspeed.

Decidecade band centre frequency (Hz)	Percentile				
	5th	25th	50th	75th	95th
10.00	180.0	183.5	185.6	187.5	190.3
12.59	184.6	187.8	190.1	193.6	195.1
15.85	182.4	184.7	188.1	191.0	194.7
19.95	184.2	187.3	189.0	191.4	193.4
25.12	186.9	190.9	192.1	193.5	199.0
31.62	187.8	191.1	193.4	194.3	196.3
39.81	190.5	193.4	195.4	197.1	200.0
50.12	190.7	193.1	195.6	198.9	202.7
63.10	194.0	196.0	199.0	201.8	205.5
79.43	198.1	202.3	204.4	208.0	212.1
100.0	201.2	204.7	206.7	210.1	215.0
125.9	193.3	197.0	199.3	201.2	208.0
158.5	193.1	195.8	198.5	201.9	207.2
199.5	196.8	199.4	202.5	205.5	211.6
251.2	190.5	193.5	196.3	199.4	206.2
316.2	190.7	193.7	196.5	199.0	206.4
398.1	187.9	191.8	194.8	198.8	206.0
501.2	187.3	191.5	195.1	196.3	205.8
631.0	182.9	186.7	190.1	193.1	199.4
794.3	180.4	185.1	187.6	189.0	195.1
1000	185.9	189.2	192.5	195.0	200.0
1259	185.7	189.0	192.9	196.2	200.0
1585	185.1	188.7	191.8	195.0	199.4
1995	180.9	184.6	187.7	190.8	195.2
2512	178.1	181.4	184.5	187.6	192.4
3162	176.0	179.2	182.3	185.3	191.4
3981	178.3	181.6	184.8	188.0	193.5
5012	178.6	181.9	185.1	188.1	193.1
6310	180.3	183.2	187.0	189.4	194.5
7943	174.2	176.0	181.0	182.9	187.7
10000	174.0	175.7	180.7	182.3	186.2
12589	173.9	175.7	179.3	182.3	185.3
15849	173.8	176.1	178.7	182.0	185.5
19953	173.4	175.8	178.2	181.3	187.5
25119	176.3	178.3	180.1	183.1	188.7

Table E-8. Simulated back-propagated decidecade-band 24 h sound exposure source levels (ESL; dB re 1 µPa²m²s) for the turbine during periods of 15 kn windspeed.

Decidecade band centre frequency (Hz)	Percentile				
	5th	25th	50th	75th	95th
10.00	180.7	183.0	185.0	187.4	195.5
12.59	185.3	188.3	189.8	192.6	195.6
15.85	185.8	188.6	190.7	193.4	195.5
19.95	187.8	190.9	192.9	194.1	195.4
25.12	185.9	188.9	191.7	195.7	199.8
31.62	190.2	192.1	192.9	194.6	196.8
39.81	193.8	195.6	197.3	198.9	201.1
50.12	193.3	195.1	196.9	199.6	204.4
63.10	197.0	198.7	200.5	202.9	208.8
79.43	199.9	203.1	206.1	209.1	214.3
100.0	203.1	205.4	207.0	209.6	214.5
125.9	194.9	198.1	199.6	202.5	206.5
158.5	195.5	198.3	199.9	201.7	206.0
199.5	200.1	202.4	204.2	205.7	211.0
251.2	194.5	196.2	197.6	200.1	205.4
316.2	194.5	196.5	198.5	200.9	205.8
398.1	192.6	195.3	197.7	200.3	205.8
501.2	192.8	194.7	197.0	200.1	203.7
631.0	188.7	190.9	192.3	196.0	200.4
794.3	186.3	188.4	189.6	192.7	197.2
1000	192.1	193.6	195.6	199.3	203.2
1259	192.1	193.7	196.2	199.4	204.0
1585	192.6	194.3	196.7	199.5	204.0
1995	188.7	191.6	193.3	196.0	200.9
2512	185.8	188.8	190.5	193.8	198.9
3162	184.4	187.2	188.4	190.5	196.9
3981	187.3	189.4	190.8	192.4	199.3
5012	186.9	189.0	190.6	192.5	198.5
6310	187.5	190.0	191.6	193.3	198.6
7943	181.8	184.4	185.7	187.5	193.1
10000	182.0	184.5	185.7	187.2	192.6
12589	181.8	184.2	185.6	187.1	192.9
15849	181.6	183.9	185.0	186.6	191.5
19953	181.2	183.3	184.6	186.3	192.8
25119	183.0	184.8	186.1	187.4	191.4

Table E-9. Simulated back-propagated decidecade-band 24 h sound exposure source levels (ESL; dB re 1 µPa²m²s) for the turbine during periods of 20 kn windspeed.

Decidecade band centre frequency (Hz)	Percentile				
	5th	25th	50th	75th	95th
10.00	184.0	186.5	188.3	190.1	196.3
12.59	188.8	190.7	192.5	193.7	196.6
15.85	187.8	190.1	191.5	193.1	195.5
19.95	187.5	190.9	192.5	194.8	197.8
25.12	190.3	193.4	197.1	201.9	207.1
31.62	190.4	191.7	193.3	196.3	198.5
39.81	193.7	196.6	198.2	199.7	201.1
50.12	193.1	194.7	196.6	199.5	201.6
63.10	197.9	199.3	201.4	203.2	206.2
79.43	201.8	205.9	207.8	210.2	214.1
100.0	203.2	205.3	207.2	209.4	211.6
125.9	195.3	197.6	199.4	202.3	204.3
158.5	195.4	197.3	199.0	202.0	205.2
199.5	199.5	201.5	204.4	206.5	211.2
251.2	193.4	195.4	197.1	200.7	203.6
316.2	194.3	196.3	198.2	200.6	204.6
398.1	193.2	195.5	197.6	199.1	203.4
501.2	193.0	194.6	197.1	198.3	202.3
631.0	188.7	191.3	193.5	195.1	198.4
794.3	186.9	189.2	190.4	191.8	194.5
1000	194.8	197.3	199.2	201.4	205.2
1259	195.2	197.7	199.6	202.5	206.6
1585	195.1	197.1	199.1	201.6	205.1
1995	191.9	193.6	196.2	197.7	201.2
2512	189.4	191.2	193.4	194.8	197.7
3162	187.5	189.5	191.2	192.6	195.8
3981	189.5	192.3	193.2	194.8	196.6
5012	189.9	192.1	193.2	194.9	196.8
6310	190.6	191.8	193.7	195.2	196.7
7943	185.3	186.9	188.5	189.8	191.7
10000	184.9	186.9	188.3	189.2	191.2
12589	185.5	186.5	188.1	189.1	191.1
15849	184.5	185.7	187.0	187.9	189.5
19953	183.9	185.0	186.1	187.0	188.8
25119	185.3	186.4	187.2	188.1	189.2

Table E-10. Simulated back-propagated decidecade-band 24 h sound exposure source levels (ESL; dB re 1 µPa²m²s) for the turbine during periods of 25 kn windspeed.

Decidecade band centre frequency (Hz)	Percentile				
	5th	25th	50th	75th	95th
10.00	186.0	188.0	189.1	191.4	201.6
12.59	191.5	192.7	193.7	194.7	199.1
15.85	190.5	191.5	192.8	193.7	197.1
19.95	190.4	193.3	195.3	196.5	198.6
25.12	194.3	201.0	204.2	205.8	207.3
31.62	191.3	192.6	193.6	196.2	200.7
39.81	195.2	196.8	197.6	198.9	203.7
50.12	195.3	196.4	197.8	200.1	204.3
63.10	199.6	201.6	204.3	205.8	207.1
79.43	205.5	209.8	212.5	214.6	215.5
100.0	204.9	206.0	207.5	209.8	213.8
125.9	196.7	198.2	200.6	202.0	206.1
158.5	196.3	198.0	199.8	201.6	205.8
199.5	199.5	202.6	204.8	206.4	210.4
251.2	193.6	196.6	198.9	201.4	204.2
316.2	193.9	197.0	199.0	202.1	204.6
398.1	193.0	195.7	198.1	200.5	204.0
501.2	193.9	195.9	198.2	200.6	204.1
631.0	190.4	192.5	194.8	196.7	203.8
794.3	188.8	190.2	192.1	193.5	198.2
1000	195.5	198.3	200.3	203.9	206.6
1259	195.7	198.8	200.7	204.3	207.3
1585	195.7	198.4	200.3	203.6	207.2
1995	192.7	195.3	197.9	200.5	204.8
2512	190.2	192.9	194.5	197.6	201.7
3162	188.9	191.7	193.4	195.5	199.3
3981	191.2	193.9	195.1	196.7	201.4
5012	191.3	193.8	195.4	196.7	200.8
6310	190.5	193.3	194.7	196.2	199.9
7943	186.3	188.5	189.6	191.4	194.9
10000	186.0	187.9	189.4	191.0	194.5
12589	185.8	187.6	188.7	190.3	193.6
15849	185.0	186.7	188.0	189.1	192.4
19953	184.4	186.1	187.0	188.3	192.6
25119	185.8	187.2	187.9	188.9	191.6

Appendix F. Decidecade Percentile Values

Table F-1. Values used for decidecade percentiles in Figure 9 for the Hywind station.

Decidecade band (Hz)	Percentile						
	5th	10th	25th	50th	75th	90th	95th
1	96.27	97.94	100.72	102.99	104.94	107.29	109.44
1.3	97.27	98.94	101.72	103.99	105.94	108.29	110.44
1.6	94.83	96.63	99.62	102.19	105.89	109.93	111.89
2	93.39	95.34	98.48	101.19	106.47	111.1	113.14
2.5	92.04	94.01	97.36	100.27	105.66	110.26	112.3
3.2	88.6	90.78	94.89	98.63	104.01	108.56	110.66
4	88.66	91.11	95.34	98.29	100.84	104.56	107.75
5	86.2	88.78	93.09	95.92	98.59	102.67	106.23
6.3	81.51	84.82	89.53	92.53	95.5	100.18	104.16
7.9	78.78	81.62	86.39	89.48	92.6	97.69	101.8
10	78.71	81.22	84.65	87.23	90.39	95.06	98.7
12.6	83.14	85.33	89.15	91.31	93.52	96.56	98.67
15.8	83.96	85.75	88.29	90.53	93.06	96.04	97.98
20	86.54	88.84	92.36	95.69	97.91	99.68	100.84
25.1	90.23	92.33	98.32	107.3	109.52	110.74	111.51
31.6	93.64	94.77	96.48	98.37	100.86	104.03	106.47
39.8	97.01	98.6	100.58	102.39	104.38	107.08	109.35
50.1	97.28	98.47	100.28	102.34	105.23	108.68	111.1
63.1	98.82	100.77	103.5	107.43	109.56	111.22	112.69
79.4	98.36	100.13	104.15	109.12	111.94	113.21	114.08
100	98.83	99.87	101.57	103.69	106.4	109.34	111.08
125.9	97.75	98.77	100.52	102.7	105.46	108.29	110.11
158.5	97.23	98.19	99.89	101.9	104.41	107.25	109.13
199.5	96.88	98.04	99.92	102.13	104.58	107.43	109.42
251.2	95.81	96.91	98.65	100.81	103.32	106.48	108.73
316.2	94.93	96.15	97.82	99.96	102.35	105.43	107.55
398.1	93.9	95.22	97.16	99.37	101.94	105.12	107.2
501.2	92.12	93.69	95.73	97.88	100.27	103.36	105.43
631	89.95	91.8	94.26	96.68	99.48	103.2	105.57
794.3	88.27	90.15	92.64	94.96	97.21	99.95	102.09
1000	87.69	90.05	93.09	95.77	98.27	101.1	103.09
1258.9	88.2	90.59	93.8	96.55	99.03	101.99	104.4
1584.9	87.38	89.93	93.24	96.07	98.57	101.56	104.09
1995.3	84.19	86.99	90.66	93.72	96.48	99.94	102.61
2511.9	82.46	85.42	89.16	92.17	94.7	97.59	99.88
3162.3	81.62	84.56	88.14	91.02	93.41	96.08	98.28
3981.1	80.91	83.88	87.4	90.2	92.58	95.25	97.34
5011.9	80.46	83.52	87.21	89.92	92.09	94.6	96.53
6309.6	78.95	82.35	86.34	89	90.91	93.21	95.12
7943.3	77.55	81.3	85.28	87.87	89.54	91.67	93.67
10000	76.48	80.38	84.42	86.96	88.4	90.3	92.21
12589.3	75.62	79.61	83.68	86.04	87.2	88.7	90.62
15848.9	74.99	78.78	82.72	84.91	85.92	87.28	89.12
19952.6	74.85	78.43	82.15	84.05	84.98	86.68	89.03
25118.9	73.94	77.01	80.48	82.08	82.89	84.37	86.38

Table F-2. Values used for decidecade percentiles in Figure 9 for the Control station.

Decidecade band (Hz)	Percentile						
	5th	10th	25th	50th	75th	90th	95th
1	74.9	76.9	81	86.2	92.2	97.4	100.5
1.3	75	77.1	81.1	86.3	92.3	97.5	100.5
1.6	75.1	77.2	81.2	86.3	92.3	97.5	100.5
2	75.2	77.3	81.3	86.4	92.3	97.5	100.5
2.5	75.3	77.4	81.3	86.5	92.4	97.5	100.5
3.2	75.5	77.5	81.4	86.5	92.4	97.6	100.5
4	75.5	77.6	81.5	86.5	92.4	97.6	100.6
5	75.6	77.7	81.5	86.6	92.5	97.6	100.6
6.3	75.7	77.7	81.6	86.6	92.5	97.6	100.6
7.9	75.8	77.8	81.6	86.7	92.5	97.6	100.6
10	75.9	77.9	81.7	86.7	92.5	97.7	100.6
12.6	75.9	77.9	81.7	86.8	92.6	97.7	100.6
15.8	76	78	81.8	86.8	92.6	97.7	100.6
20	76.1	78.1	81.9	86.8	92.6	97.7	100.6
25.1	76.1	78.1	81.9	86.9	92.6	97.7	100.6
31.6	76.2	78.2	81.9	86.9	92.6	97.7	100.7
39.8	76.3	78.2	82	86.9	92.7	97.7	100.7
50.1	76.3	78.3	82	87	92.7	97.7	100.7
63.1	76.4	78.3	82.1	87	92.7	97.8	100.7
79.4	76.4	78.4	82.1	87	92.7	97.8	100.7
100	76.5	78.4	82.2	87	92.7	97.8	100.7
125.9	76.5	78.5	82.2	87.1	92.7	97.8	100.7
158.5	76.6	78.5	82.3	87.1	92.7	97.8	100.7
199.5	76.6	78.6	82.3	87.1	92.7	97.8	100.7
251.2	76.7	78.6	82.3	87.1	92.7	97.8	100.7
316.2	76.7	78.6	82.4	87.1	92.7	97.8	100.8
398.1	76.7	78.7	82.4	87.2	92.7	97.8	100.8
501.2	76.8	78.7	82.4	87.2	92.7	97.8	100.8
631	76.8	78.8	82.5	87.2	92.7	97.8	100.8
794.3	76.9	78.8	82.5	87.2	92.8	97.8	100.8
1000	76.9	78.9	82.6	87.3	92.8	97.9	100.8
1258.9	77	79	82.7	87.3	92.8	97.9	100.8
1584.9	77.1	79	82.7	87.4	92.8	97.9	100.8
1995.3	77.1	79.1	82.8	87.4	92.8	97.9	100.8
2511.9	77.1	79.1	82.9	87.4	92.8	97.9	100.8
3162.3	77.2	79.2	82.9	87.5	92.9	97.9	100.8
3981.1	77.2	79.2	83	87.5	92.9	97.9	100.8
5011.9	77.3	79.3	83	87.5	92.9	97.9	100.8
6309.6	77.3	79.3	83.1	87.5	92.9	97.9	100.8
7943.3	77.4	79.4	83.1	87.6	92.9	97.9	100.8
10000	77.4	79.4	83.2	87.6	92.9	97.9	100.8
12589.3	77.5	79.5	83.2	87.6	92.9	97.9	100.8
15848.9	77.5	79.5	83.3	87.6	92.9	97.9	100.8
19952.6	77.5	79.5	83.3	87.7	93	97.9	100.8
25118.9	77.6	79.6	83.4	87.7	93	97.9	100.8